2-2-2022 1:00 PM

Effects of Modulating the Culture Microenvironment on the Growth and Secretome of Human Adipose-Derived Stromal Cells

Zhiyu Liang, *The University of Western Ontario*

Supervisor: Flynn, Lauren, *The University of Western Ontario*

A thesis submitted in partial fulfillment of the requirements for the Master of Engineering Science degree in Biomedical Engineering

Abstract

The cell microenvironment plays a critical role in modulating adipose-derived stromal cell (ASC) proliferation and paracrine function. The current study investigated the effects of decellularized adipose tissue (DAT) coatings, low-level oscillatory shear stress (~0.04-0.3 dyn/cm^2), hypoxia (2% O_2), and pro-inflammatory cytokine priming with IFN-γ and TNF-α on human ASC proliferation and paracrine factor secretion in the context of a rocking bioreactor. Culturing under 20% O_2 resulted in a higher cell density after 7 days of culture. Without cytokine priming, the varying culture conditions significantly impacted the levels of the pro-angiogenic factors VEGF, HGF, and angiogenin detected in conditioned media samples. In contrast, when the cells were primed, the levels of the immunomodulatory factors IL-6 and IL-8 were most affected by the varying microenvironmental factors. Overall, a novel bioreactor system was developed for ASC expansion and preconditioning, demonstrating that the cell microenvironment could be tuned to modulate ASC paracrine factor secretion.

Keywords

Adipose-derived stromal cells; Rocking bioreactor; Microenvironment; Decellularized adipose tissue; Dynamic culture; Mechanical stimulation; Hypoxia; Cytokine priming; Paracrine secretion; Regenerative Medicine.

Summary for Lay Audience

Adipose tissue or fat is found throughout the body and has important structural and functional roles, including defining the normal body contours. Adipose tissue loss due to disease, trauma, or resection of tumors can lead to contour defects, impaired function, and decreased emotional well-being of the patient. Therefore, adipose tissue reconstruction is usually considered in cases of large adipose tissue defects. However, conventional reconstruction therapies used to restore adipose tissue after damage generally only provide temporary solutions that lack long-term stability. To support functional regeneration, tissue engineering strategies utilizing pro-regenerative cells that can be isolated from fat, termed adipose-derived stromal cells (ASCs), have gained significant interest. Promisingly, ASCs are abundant within fat and have the ability to secrete therapeutic signalling molecules that can promote blood vessel growth and modulate the inflammatory response to stimulate healing. With the goal of developing a clinically-applicable strategy for ASC expansion that augments their therapeutic properties, efforts have been made to assess how the environment in which the ASCs are cultured in the lab influences their pro-regenerative functionality. One strategy is to culture the cells on decellularized adipose tissue (DAT) scaffolds that mimic the composition of their native environment within the body. Other factors, such as mechanical stimulation, low oxygen concentration, and the addition of inflammation-triggering molecules, have also been shown to regulate ASC therapeutic properties. This study aimed to develop a rocking bioreactor system that enabled the systematic investigation of these factors and evaluated their effects on human ASC expansion and therapeutic signalling molecule secretion. In general, cell growth was well supported under all conditions studied, with a higher cell density observed at 7 days in the samples cultured under 20% O_2. Without the addition of inflammation triggering molecules, the different culture environmental factors had the greatest effects on the secretion of signalling molecules that can promote blood vessel growth. In contrast, with the addition of inflammation-triggering molecules, the different culture environmental factors had the greatest effects on the secretion of signalling molecules that can modulate inflammation. Overall, this study showcases the complex relationships between the culture environment and the therapeutic properties of ASCs, and developed a novel rocking bioreactor system that may hold potential for augmenting the pro-regenerative functionality of ASCs for future clinical applications in cell-based therapies.

Acknowledgments

First and foremost, I would like to express my heartfelt gratitude to my supervisor, Dr. Lauren Flynn, for her ongoing support and guidance throughout my graduate study. I am so grateful to have had the opportunity to join her lab and learn from such an incredible mentor for the last two years.

I would like to extend my appreciation to my advisory committee, Drs. Cheryle Seguin and Gregory Dekaban for their continuous advice, help and encouragement. I would also like to thank Drs. Tamie Poepping and Olga Trichtchenko for helping me with the computational model.

I would like to thank all of the past and present Flynn Lab members. Special thanks to Dr. Tim Han and Courtney Brooks for teaching me the techniques and preparing me for the adventure, Dr. John Walker for the stats help and office chats, Dr. Anna Kornmuller for career advice, Fiona Serack for organizing all the fun events, and Dr. Tyler Cooper for helping with the PCA analysis. I'm incredibly grateful to have had all of your company for the past two years.

Last but not least, I would like to thank my parents for their never-ending love and support and for always being there when I need them the most.

Table of Contents

List of Tables

List of Figures

List of Appendices

List of Abbreviations

2D	2-dimentional
3D	3-dimentional
α-MEM	α-minimal essential medium
AMPK	Adenosine monophosphate activated-protein kinase
ANOVA	Analysis of variance
Arg-1	Arginase-1
ASC	Adipose-derived stromal cell
BM-MSC	Bone marrow derived stromal cell
BSA	Bovine serum albumin
CM	Conditioned media
COX-2	Cyclooxygenase-2
DAT	Decellularized adipose tissue
DC	Dendritic cell
ddH2O	Double-distilled water
DFU	Diabetic foot ulcer
DMEM	Dulbecco's modified Eagle's medium
DMEM/F-12	Dulbecco's modified Eagle's medium/Ham's F12
dsDNA	Double stranded DNA
ECM	Extracellular matrix
EDTA	Ethylenediaminetetraacetic acid
EGF	Epidermal growth factor
ELISA	Enzyme-linked immunosorbent assay
EV	Extracellular vesicle
FAL	Femoral artery ligation
FBS	Fetal bovine serum
FGF2	Fibroblast growth factor-2
G-CSF	Granulocyte colony-stimulating factor
HGF	Hepatocyte growth factor
HIF-1	Hypoxia inducible factor-1
HLA-G5	Human leukocyte antigen-G5

HMEC-1	Immortalized human dermal microvascular endothelial cells
HMVEC	Human microvascular endothelial cell
hPL	Human platelet lysate
HUVEC	Human umbilical vein endothelial cell
IDO	Indolamine 2, 3 dioxygenase
IF	Immunofluorescence
IFN-γ	Interferon gamma
IGF	Insulin-like growth factor
IHD	Ischemic heart disease
IL-10	Interleukin 10
IL-1β	Interleukin 1 beta
IL-4	Interleukin 4
IL-6	Interleukin 6
IL-8	Interleukin 8
iNOS	Inducible nitric oxide synthase
KGF	Keratinocyte growth factor
L-NAME	N-nitro-L-arginine methyl ester
LILRB1	Leukocyte immunoglobulin-like receptor subfamily B1
LPS	Lipopolysaccharide
MCP-1	Monocyte chemoattractant protein-1
miRNA	MicroRNA
MMP-2	Metalloproteinase-2
MSC	Mesenchymal stromal cell
NF-κB	Nuclear factor kappa-light-chain-enhancer of activated B cells
NK	Natural killer
NO	Nitric oxide
PBMC	Peripheral blood mononuclear cell
PBS	Phosphate buffered saline
PDGF	Platelet-derived growth factor
PGE2	Prostaglandin E2
PIGF	Placental growth factor
ROS	Reactive oxygen species

SF	Serum-free
SIRT1	Silent information regulator type 1
STAT3	Signal transducer and activator of transcription 3
SV40	Simian virus 40
SVF	Stromal vascular fraction
TCPS	Tissue culture polystyrene
TGF-β	Transforming growth factor-β
TNF-α	Tumor necrosis factor alpha
UC	Uncoated
UC-MSC	Umbilical cord derived stromal cell
VEGF	Vascular endothelial growth factor
XF	Xeno-free

Chapter 1

1 Introduction

1.1 Adipose tissue reconstruction

Adipose tissue (fat) is ubiquitous throughout the human body, primarily localized under the skin (subcutaneous) and around the internal organs (visceral) [1]. Although originally thought to be an inert tissue with only energy storage functions, it was later found that adipose tissue also plays critical roles in regulating energy homeostasis and the immune response through endocrine and paracrine signalling [1]–[3]. In addition, adipose tissue provides biomechanical support and cushioning for skeletal structures [4]. Following damage or loss as a result of disease, trauma, burns, or congenital defects, subcutaneous adipose tissue has a very limited capacity for self-repair [5]. Moreover, contour deformities resulting from adipose tissue loss can have significant psychological impacts on patients [5], and adipose tissue reconstruction can have a very positive impact on patient quality of life [6].

1.1.1 Conventional reconstruction therapies and new directions

Synthetic implants and autologous fat grafting are two common clinical strategies used for adipose tissue reconstruction, in particular following breast cancer treatment such as mastectomy [7]. Synthetic implants are a common choice for patients undergoing reconstruction of an entire breast, and are available in a variety of shapes and sizes. Through decades of development, the safety and efficacy of saline- or silicone-filled implants have considerably improved [8]. However, these implant-based treatments have inherent limitations due to the nature of the procedure and the structure of the implants [8], [9]. Whenever an implant is introduced to the body, the risk associated with infection arises and the formation of a biofilm on the implant can be challenging to treat using antibiotics [8], [10]. It has been reported that up to 2.9% of patients receiving breast implants experience implant-related infections [8]. In addition, due to body's immune response to the foreign object and/or the formation of a biofilm, a fibrous capsule often

forms around the implant [11]. The contraction of the fibrous capsule can lead to severe pain, deformities, implant migration, and possibly rupture, resulting in the need for an implant removal procedure [8], [10], [12]. In addition to these complications, implant-based treatments are also considered short-term solutions due to the lack of long-term structural stability of the implant, with implant replacement ultimately required [8].

As an alternative approach, autologous fat grafting has been used for various reconstructive and cosmetic purposes, ranging from small volume for facial rejuvenation to large volume for breast and buttock augmentation [13]. Fat grafts can be easily harvested using liposuction from various depots including the abdomen, back, and hips [14]. The isolated graft is composed primarily of adipocytes, which are mature fat cells, and a small amount of stromal vascular fraction (SVF), which includes adipose progenitor cells such as preadipocytes and adipose-derived stromal cells (ASCs), along with other cell types including endothelial cells, erythrocytes, fibroblasts, lymphocytes, monocytes/macrophages, and pericytes [15], [16]. However, fat grafting has some notable limitations. For the harvesting method, liposuction can cause donor site contour deformity [14]. In addition, depending on the fat processing and grafting technique, as well as the volume used, graft resorption and necrosis are observed, with up to 70% resorption of the initial grafting volume observed [17]. The unpredictable volume loss is attributed in part to the lack of revascularization of the graft, which can dramatically impact the survival of the mature adipocytes [13], [17].

More recent evidence suggests that the long-term success of fat grafting may be more dependent on tissue remodelling and replacement rather than tissue survival [13]. More specifically, adipose progenitor cells from the graft can differentiate into adipocytes and/or facilitate the regeneration and revascularization of the adipose tissue, thus improving the overall outcome of the fat grafting therapy [13]. In particular, ASCs have been demonstrated to support graft retention by modulating the inflammatory response, reducing apoptosis, and promoting vascularization and preadipocyte differentiation [13], [18], [19]. With this knowledge, ASC-enriched fat grafting has become a new research interest and appears to hold great potential as a means to improve the outcome of fat grafting procedures. However, additional research is needed to characterize and harness

the regenerative potential of ASCs, as well as to more fully evaluate the efficacy of ASC enrichment.

1.2 Adipose-derived stromal cells

Adipose-derived stromal cells (ASCs) are a type of multipotent mesenchymal stromal cell (MSC) derived from adipose tissue. Similar to other MSCs, such as bone marrow derived stromal cells (BM-MSC) and umbilical cord derived stromal cells (UC-MSC), ASCs are capable of differentiation towards osteogenic, chondrogenic, and adipogenic lineages in culture [20]. However, a growing body of evidence supports that the therapeutic capacity of MSCs is primarily mediated by their paracrine activities, specifically through the secretion of immunomodulatory and pro-angiogenic paracrine factors [21]. Compared to BM-MSCs, ASCs have been reported to have higher proliferative, immunomodulatory, and pro-angiogenic capacities [22]–[25]. In addition, the less-invasive procedures associated with ASC extraction and their higher relative abundance also make ASCs a promising resource for cell-based therapies [26]. In addition to the previously mentioned clinical implications in adipose reconstruction therapies, ASCs are a promising cell source for the development of pro-angiogenic cell-based therapies targeting other conditions including wound healing [27], [28] and cardiovascular diseases [29]–[31].

1.2.1 Isolation, culture, and characterization of human ASCs

Human ASCs can be found throughout the body within two types of adipose tissue: brown adipose tissue, responsible for heat generation at early ages, and white adipose tissue, responsible for energy storage and metabolic activities [4]. As the human body matures, white adipose tissue becomes the predominant type of adipose tissue in the body within both the subcutaneous and intraabdominal depots [32], [33]. Due to its ease of access and relative abundance, subcutaneous white adipose tissue is the most common source for ASC isolation.

1.2.1.1 Isolation and culture of human ASCs

Adipose tissue is typically harvested as a form of surgical waste from procedures such as liposuction, resection, and biopsy. ASCs can then be obtained from these tissue samples through mechanical processing and/or enzymatic digestions. The mechanical dissociation processes generally involve mincing of the tissue, filtration, and centrifugation, whereas enzymatic processing usually involves collagenase, trypsin, and/or dispase digestions [33]. A general workflow of ASC isolation begins with fine mincing of the tissue, followed by collagenase digestion and centrifugation to collect the SVF [34]. To remove erythrocytes, a sodium chloride and ammonium chloride lysis buffer can be used, followed by filtration to remove cellular debris [33]. Finally, the adherent spindle-like ASC population can be isolated from the rest of the SVF through *in vitro* culture on tissue culture plastic. Although commonly used, one limitation of these conventional ASC isolation methods is that the separation of ASCs from the other SVF cell populations relies on ASC adhesion to tissue culture plastic, which does not necessary ensure a homogenous cell population [15]. To allow for a more precise isolation and purification of ASCs, Rada *et al.* developed a novel isolation method utilizing immunomagnetic beads coated with specific antibodies targeting ASCs or subpopulations of ASCs with different differentiation potential [35]. For clinical applications and large-scale usage, many automated closed ASC isolation systems have been developed and made available commercially [26]. These systems, as summarized by Oberbauer *et al.*, allow standardization of the process in a sterile environment, which could be beneficial for immediate usage as an autologous fat graft supplement [16].

For clinical applications and research purposes, *in vitro* culture and expansion of ASCs is usually needed to obtain enough cells. The culture media is one of the key factors in ASC culture that can affect cell yield, as well as the clinical utility of the cells [36]. ASC culture media usually includes a basal media, such as α-minimal essential medium (α-MEM), Dulbecco's modified Eagle's medium (DMEM), or Dulbecco's modified Eagle's medium/Ham's F12 (DMEM/F-12), supplemented with serum and antibiotics [33]. Fetal bovine serum (FBS) is the mostly commonly used serum for this purpose as it contains high concentrations of growth factors and nutrients necessary for cell growth

and proliferation [34]. However, using a supplement of animal origin can introduce the risk of xeno-pathogen transmission and allergic response in patients [37]. Furthermore, the high batch-to-batch variability of FBS can impact cell phenotype and function [36].

To avoid the use of animal serums, human blood derived supplements, such as human platelet lysate (hPL) and autologous/allogeneic human serum, have been used as alternatives and have been shown to improve the proliferation rate of MSCs as compared to FBS [34], [36], [38], [39]. Though promising, the effects of these xeno-free (XF) medium formulations on MSC immunomodulatory capacities are not well understood. Kandoi *et al.* reported improved immunomodulation of human UC-MSC cultured with hPL as compared to FBS supplemented media, assessed based on their ability to suppress lymphocyte proliferation [40]. In contrast, Oikonomopoulos *et al.* reported that hPL supplemented medium diminished the ability of human BM-MSC and ASC to suppress lymphocyte proliferation as compared to those cultured in FBS supplemented media [41]. Moreover, as human blood derived supplements are also not well defined, batch-to-batch variability is still a relevant limitation, rendering them non-ideal for clinical applications.

To overcome these problems and to standardize the formulation of ASC culture media, chemically-defined XF and serum-free (SF) media have been developed. Depending on the brand and the formulation, this type of media can significantly increase the proliferation rate of ASCs compared to media supplemented with FBS or human serum [36], [42]. Since the introduction of XF/SF media, numerous studies have been conducted to screen various commercially-available options mainly for expansion and differentiation purposes. Depending on the MSC source and applications, the performance of different commercial options may vary and can lead to varying levels of change in cell characteristics [36], [39], [43]. The specific components within the media formulations are often not fully disclosed, and extensive screening and characterization studies are required before selecting a XF/SF media formulation for a given application [34], [36].

1.2.1.2 Characterization of human ASCs

Due to the heterogeneity of the SVF cell populations, cell characterization by immunophenotyping using flow cytometry is typically performed to verify the identity of the ASC population. ASCs are expected to express MSC-specific markers, including CD44, CD73, CD90, and CD105, while lacking the expression of hematopoietic markers, such as CD14, CD31, CD45 [44], [45]. In addition to these classic markers for ASCs, many other variable markers also exist, making it difficult to establish a complete expression profile of ASCs. The expression of these variable markers depends on many factors, such as donor variability, passage number, and confluency of the culture [45], [46]. In particular, CD34 is a marker that was traditionally believed to be a hematopoietic marker, but it is now recognized that it can be expressed by ASCs at early passages [47]. When comparing the $CD34^+$ and $CD34^-$ ASC subpopulations, Suga *et al.* reported differences in proliferative and differentiative capacities, as well as angiogenesis-related gene expression, suggesting the presence of ASC subpopulations with distinct properties [48]. A comprehensive list of ASC surface markers is shown in **Table 1.1**. In addition to their unique immunophenotype, ASCs can also be identified based on their multilineage differentiation capacities (adipogenesis, chondrogenesis, and osteogenesis), which can be achieved *in vitro* with the use of lineage-specific induction media. Through a combination of histological analysis and gene expression analysis, as summarized by Bourin *et al.*, the differentiation potential of ASCs can be evaluated [15].

Table 1.1 The immunophenotypic profile of human ASCs [15], [26].

Marker type	Antigen
Primary stable positive	CD13 (Aminopeptidase N)
	CD29 (β-1 integrin)
	CD44 (Hyaluronan receptor)
	CD73 (Ecto-5'-nucleotidase)
	CD90 (Thymocyte differentiation antigen 1)
	CD105 (Endoglin)
Primary unstable positive	CD34 (Transmembrane glycoprotein)
Secondary positive	CD10 (Neutral endopeptidase)
	CD26 (Dipeptidyl peptidase 4)
	CD36 (platelet glycoprotein 4)
	CD49d (α-4 integrin)
	CD49e (α-5 integrin)
Primary negative marker	CD31 (Platelet endothelial cell adhesion molecule)
	CD45 (lymphocyte common antigen)
	CD235a (Glycophorin A)
Secondary low or negative	CD3 (T-cell co-receptor)
	CD11b (α-M integrin)
	CD49f (α-6 integrin)
	CD106 (Vascular cell adhesion protein 1)
	PODXL (Podocalyxin-like protein)

1.2.2 ASC paracrine function

Since the discovery of MSCs, their multilineage differentiation potential was long considered their key mechanism of action in tissue regeneration [49]. Only recently, researchers have started to shift their focus towards MSC paracrine activities, which may be a more important therapeutic property of MSCs compared to their differentiation capacities [50]. ASCs in particular secrete a wide range of growth factors, cytokines, pro-angiogenic factors, adipokines, and neurotrophic factors, in the form of soluble proteins or enclosed in extracellular vesicles (EVs), all of which enable ASCs to promote tissue regeneration [51]–[53]. The two major therapeutic potentials that lie within the ASC secretome are their pro-angiogenic and immunomodulatory properties.

1.2.2.1 Pro-angiogenic properties

ASCs have been reported to secrete a diverse range of pro-angiogenic factors including vascular endothelial growth factor (VEGF), hepatocyte growth factor (HGF), fibroblast growth factor-2 (FGF2), platelet-derived growth factor (PDGF), transforming growth factor-β (TGF-β), angiopoietin-1, and many others [51], [54]–[56]. VEGF and HGF are two key pro-angiogenic factors secreted by ASCs that have been shown to act directly on endothelial cells. More specifically, VEGF and HGF function synergistically to promote endothelial cell growth, while inhibiting apoptosis [57]. Nakagami *et al.* demonstrated that by neutralizing VEGF and HGF in ASC-conditioned media (CM) used for endothelial cell culture, endothelial cell viability and migration were significantly impaired [58]. Other factors secreted by ASCs have also been shown to play critical roles in angiogenesis, which is the process of blood vessel formation from pre-existing vasculature [59]. In particular, FGF2 mediates endothelial cell migration, while PDGF is involved in endothelial cell proliferation and tubule formation [60], [61]. TGF-β and angiopoietin-1 are critical to blood vessel remodelling and maturation [62], [63].

In addition to soluble factors, the EVs released by ASCs have also been shown to promote angiogenesis *in vitro* and *in vivo*. In addition to the pro-angiogenic factors mentioned above, EVs also contain microRNAs (miRNAs), which have been shown to act on specific signaling pathways that are critical in angiogenesis [64]. In particular, miRNA-31 was shown to target the hypoxia inducible factor-1 (HIF-1) inhibiting factor, thus positively contributing to endothelial cell migration and tubule formation [65]. The mechanisms of action of other miRNAs produced by ASCs that have been reported to regulate angiogenesis, such as miRNA-125a, miRNA-126, and miRNA-181b [54]. In particular, Yang *et al.* demonstrated that miRNA-181b present in the exosomes derived from rat ASC is capable of promoting brain microvascular endothelial cell migration and tube formation following oxygen–glucose deprivation [66].

1.2.2.2 Immunomodulatory properties

The immunomodulatory and immunosuppressive properties of ASCs are another key aspect of their therapeutic potential. ASCs are capable of modulating both the adaptive and innate immune response, by secreting a wide range of soluble factors, including indolamine 2, 3 dioxygenases (IDO), nitric oxide (NO), interleukin 10 (IL-10), prostaglandin E2 (PGE2), and human leukocyte antigen-G5 (HLA-G5) [64].

IDO plays a key role in MSC-mediated immunosuppression, particularly in response to the presence of pro-inflammatory cytokines such as interferon gamma (IFN-γ) or tumor necrosis factor alpha (TNF-α) and interleukin 1 beta (IL-1β) [67]. IDO is an intracellular enzyme that supports the catabolism of tryptophan into kynurenine, which in turn suppresses T cell responses [68]. IDO also supports the proliferation of $CD5^+$ B cells, which induce the differentiation of immunosuppressive regulatory T cells (Tregs) by secreting IL-10 [50]. As for the innate immune cells, IDO activity also supports monocyte differentiation into alternatively-activated “M2-like” macrophages, which are an IL-10 secreting subpopulation of macrophages that are anti-inflammatory [69]. NO has been reported to have a very similar role as IDO in the immunomodulatory effects of MSCs sourced from mice, rats, and rabbits [67]. In humans, NO has been reported to inhibit TNF-α and prevent dendritic cell (DC) maturation [68].

PGE2 is a homeostatic factor that is cyclooxygenase-2 (COX-2)-dependent and can be upregulated by the pro-inflammatory factors IFN-γ and TNF-α [70], [71]. PGE2 works alongside IDO to inhibit natural killer (NK) cell proliferation, while promoting Treg cell differentiation. PGE2 has also been reported to modulate DC maturation and prevent the differentiation of naive T cells into pro-inflammatory T helper 17 cells [71], [72].

Soluble HLA-G5 is an isoform of the nonclassic HLA-G molecules that can be secreted by MSCs depending on IL-10 expression. HLA-G5 targets leukocytes and inhibits the activation of T, B, and NK cells through the leukocyte immunoglobulin-like receptor subfamily B1 (LILRB1) receptors [68].

When comparing the immunomodulatory properties of MSCs from different sources, studies suggest that ASCs are superior to BM-MSCs [73]. For example, Melief *et al.* demonstrated that, compared to human BM-MSCs, human ASCs are better at suppressing peripheral blood mononuclear cell (PBMC) proliferation, as well as inhibiting the differentiation of blood monocytes towards DCs [25]. Furthermore, another group reported significantly higher levels of secretion of the anti-inflammatory cytokine IL-10 by monocyte-derived DC when cultured with human ASCs as compared to human BM-MSCs [74]. Besides the differences present between ASCs and BM-MSCs, the immunomodulatory properties of ASCs may also differ depending on the location of the tissue source. A recent study by Abu-Shahba *et al.* reported that ASCs isolated from breast tissue exhibited elevated expression of the immunosuppressive genes IL-10 and IDO, as well as a number of antioxidative genes, as compared to those isolated from abdominal adipose tissue [75].

1.2.3 ASCs in clinical applications

Due to their pro-angiogenic, immunomodulatory and anti-apoptotic properties, ASCs have been proposed for many clinical applications. Reported in 2004, ASCs were first used in the clinical setting as a supplement to a bone graft to treat a large bone deficit in the skull [76]. Since then, autologous or allogeneic ASCs have been investigated in a growing number of clinical trials. According to the ClinicalTrials.gov database (https://clinicaltrials.gov/, Dec 2, 2020, search term: adipose derived stem cells and adipose derived stromal cells), there have been 504 studies registered using adipose derived stromal or stem cells as treatments for a wide range of conditions, including limb ischemia, diabetes, osteoarthritis, ischemic heart disease, Crohn's disease, skin ulcer, and many others [77]. The following sections will focus on two common areas of application of ASCs as pro-angiogenic treatments for wound healing and ischemic heart diseases, followed by an analysis of the limitations and future directions of ASC treatment.

1.2.3.1 Wound healing

Wound healing is a natural process of the skin regenerating itself, however in the case of deep burns or in patients with diabetes or cancer, the process can be compromised. For chronic wounds or large skin defects, current treatments such as autologous skin grafting can result in complications such as donor site morbidity [28], [78]. As a result, ASC-based treatments have been proposed to accelerate and improve the wound healing process. In particular, the paracrine activities of ASCs can help promote a pro-regenerative microenvironment within the wound bed. As discussed, ASCs secrete a wide range of growth factors, including VEGF, HGF, and FGF2, that can promote new blood vessel formation [79]. Other growth factors secreted by ASCs, such as PDGF, insulin-like growth factor (IGF), and keratinocyte growth factor (KGF), can also promote fibroblast proliferation, migration, and collagen secretion [80].

ASC treatments have been shown to be effective for treating diabetic foot ulcers (DFUs) and irradiation-induced lesions in clinical trials [81]. In a phase II clinical trial in Korea, the use of allogeneic ASC hydrogel sheets as treatment for DFU has shown promising results, with 82% of patients achieving complete wound closure at 12 weeks as compared to 53% in the polyurethane film control group [82]. Another study by Rigotti *et al.* demonstrated neovascularization and improved tissue structure, remission of tissue necrosis and wound healing following repeated injections of ASC-containing autologous lipoaspirates [83]. Many other clinical studies have also shown effectiveness in improving wound healing [78], however more randomized controlled trials with a greater sample size are needed to further demonstrate the efficacy of ASC treatments.

1.2.3.2 Ischemic heart disease

Ischemic heart disease (IHD) is the leading cause of death and disability worldwide [84]. Despite technical advancements, IHD remains a medical challenge as most treatments are only capable of delaying the progressive disease process [85]. The use of ASCs has emerged as a promising regenerative approach for heart disease due to their beneficial secretome profile. In addition to the pro-angiogenic and immunomodulatory properties

described above, rat ASCs have also be shown to inhibit scar fibrosis and reduce cardiac hypertrophy in a rat model [86].

In addition to the promising results reported in animal studies, clinical studies conducted have also shown the efficacy of adipose-derived SVF in treating acute and chronic heart diseases [64].The APOLLO trial demonstrated that SVF infusion after acute myocardial infarction improved cardiac function, with a 50% reduction in scar formation and improvement of perfusion [87]. For treating chronic ischemic cardiomyopathy in the PERCISE trial, although SVF treatment did not reduce the scar size, it was able to stabilize the scar while improving perfusion and left ventricle contractility [88]. Besides direct infusion, ASCs can also be administrated in the form of a cell sheet, which has been shown to improve cell survival. However, clinical studies have yet to be performed to demonstrate the efficacy of ASC sheets for treating IHD [31].

1.2.3.3 Limitations and future directions

Although many promising benefits have been reported in preclinical studies using ASCs, the effectiveness of ASC treatments in clinical studies has been less satisfactory, which has hindered the continuation of clinical trials into more advanced phases [85], [89]. For example, in treating ischemic heart disease, ASCs have a low cardiac retention rate while not producing sufficient paracrine factors to yield a therapeutic effect [56]. The inadequate performance of ASC treatments may also be related to donor variability and the *in vitro* expansion process [90]. The therapeutic properties of ASCs are dependent on donor characteristics such as age, sex, obesity, and chronic diseases [91]. For elderly patients, autologous cell therapy may not always provide positive outcomes. Similarly, obesity is linked to reduced angiogenic and immunosuppressive properties [28]. A recent study by Harrison *et al.* demonstrated that ASCs isolated from donors with obesity can promote pro-inflammatory activation of innate immune cells, specifically inducing polarization of macrophages towards classically-activated pro-inflammatory M1-like phenotypes [92]. In addition, *in vitro* culture of ASCs generally involves 2-dimensional (2D) culture on tissue culture plastic, which fails to recapitulate their native

microenvironment, and can affect their affecting their differentiation and immunomodulatory potentials [93], [94].

To enhance ASC survival and overall effectiveness in clinical applications, a variety of preconditioning strategies have been explored in an attempt to improve the *in vitro* expansion process while augmenting their therapeutic properties [89]. A common strategy in ASC preconditioning is to tune the cell microenvironment in culture as it plays a critical role in modulating the regenerative potential of ASCs [95]. In recent years, efforts have focused on modulating factors including oxygen tension and the culture substrate, as well as stimulating cells mechanically or with growth factors and cytokines. The following sections will focus on these preconditioning strategies and their effects on ASC or MSC proliferation, differentiation, and paracrine function.

1.3 Preconditioning effects of hypoxia

Although the oxygen concentration in the ambient air is ~ 21%, the oxygen concentration in the human body is significantly lower, ranging from 0% to 14% depending on the cell type and the physiological and pathological states of the tissue [96], [97]. For MSCs in general, the oxygen level of their native microenvironment is in the range of 2-8% [98]. In subcutaneous adipose tissue, an oxygen concentration of 7.5% has been reported in lean patients [99]. Like many other cell types, ASCs are usually cultured *in vitro* under ~20% O_2, which fails to mimic their native microenvironment. With the goal of improving the *in vitro* expansion process, extensive research has been performed with results demonstrating benefits of culturing ASCs under physiologically relevant oxygen levels.

1.3.1 Proliferation and differentiation potential

Several studies have shown maintenance or improvement of a progenitor-like phenotype in human or murine ASCs after culturing for 7 days under oxygen levels ranging from 1-3% [100]–[102]. In these studies, gene expression of the stem cell markers Oct4, Nanog, Sox2, and Rex-1 were enhanced under hypoxic conditions. Other studies have evaluated changes in the ASC immunophenotype following hypoxic culture. For

example, Weijers *et al.* demonstrated maintenance of human ASC phenotype in terms of levels of CD34 expression, which is present in freshly-isolated ASCs but declines rapidly in culture, over 21 days of culture under 1% O_2 compared to 20% O_2 [103].

It is well known that the proliferative capacity of MSCs decreases as the passage number increases due to *in vitro* aging and senescence [104]. By incorporating a hypoxic culture environment, the overall proliferative potential of ASCs can be improved. For a culture period of 10 days to up to 6 weeks, the proliferation of human and murine ASCs cultured under 1-2% O_2 was reported to be 1.5-1.7 fold higher than those cultured under 20% O_2 [100], [101], [103].

The effect of hypoxia on ASC differentiation has also been studied extensively. Multiple studies have demonstrated that low oxygen levels (1-5% O_2) enhance the chondrogenic differentiation of ASCs [100], [101], [105], [106]. However, for adipogenic and osteogenic differentiation, contradictory results exist in the literature. Weijers *et al.* [103] and Choi *et al.* demonstrated reduced adipogenic and osteogenic differentiation of human ASCs cultured under 1 or 2% O_2, possibly due to the upregulated expression of HIF-1α under low oxygen tension [100]. However, another group demonstrated higher adipogenic differentiation and a sustained osteogenic differentiation ability of murine ASCs under 2% O_2 [101]. These discrepancies may be due to different passage numbers of ASCs used, as extended *in vitro* culture can also affect the differentiation capacity of ASCs. In addition to the three major differentiation lineages, researchers have also demonstrated that hypoxia can upregulate markers of endothelial cells [105], smooth muscle cells [107], and neuron-like cells [108] in cultured ASCs. Overall, it has been hypothesized that the positive effects of hypoxia on ASC phenotype are regulated by the Notch signalling pathway. Lower oxygen tension leads to a higher level of glycolytic metabolism, which in turn improves cell proliferation, prevents senescence, and maintains the differentiation capacities of ASCs [109].

1.3.2 Paracrine functions

The positive effects of hypoxia on the pro-angiogenic paracrine functions of ASCs have been well studied and demonstrated in various *in vitro* and *in vivo* models. In response to

hypoxia, ASCs generate reactive oxygen species (ROS), which activate a series of signalling pathways that in turn inhibit the degradation of HIF-1α [110]. Accumulated HIF-1α can modulate a number target genes, including the pro-angiogenic factor VEGF [110]. At the protein level, hypoxic preconditioning upregulate a number of pro-angiogenic factors, including VEGF, FGF2, and angiogenin [57], [111], [112]. The conditioned medium of human ASCs cultured under 1% O_2 for 72 h has been shown to promote endothelial cell proliferation while preventing apoptosis [57].

An *in vivo* study utilizing a murine subcutaneous implant model has demonstrated improved cell infiltration and blood vessel formation in response to treatment with hypoxia-preconditioned human ASC conditioned media relative to normoxic cultured controls [112]. The upregulated secretion of VEGF and FGF2 by hypoxia-preconditioned ASCs can also help with wound healing by improving human dermal fibroblast migration [111]. In addition to the soluble factors, the EVs secreted by ASCs under hypoxia have also been shown to promote angiogenesis. Xue *et al.* reported that the exosomes secreted by human ASCs cultured under 1% O_2 were taken up by human umbilical vein endothelial cells (HUVECs) at a faster rate compared to those secreted by ASCs cultured under 20% O_2 [113]. In addition, the EVs secreted by hypoxia-preconditioned human ASCs increase tube formation of HUVECs, with the effects potentially mediated through activation of the protein kinase A signaling pathway and VEGF upregulation in HUVECs [113], [114].

Compared to the pro-angiogenic paracrine functions, the effects of hypoxia on the immunomodulatory paracrine functions of ASCs are not as extensively studied. Gornostaeva *et al.* demonstrated that at 5% O_2, the anti-proliferative effects of human ASCs on T cells were enhanced, likely due to transcriptional change in the T cells, with upregulation of immune suppression genes and downregulation of pro-inflammatory markers observed [115]. Similarly at 1% O_2, the ability of human ASCs to inhibit $CD4^+$ and $CD8^+$ T cell proliferation was enhanced [116]. Regarding the ability of ASCs to modulate macrophage polarization, Liu *et al.* demonstrated that murine ASCs cultured under 1% O_2 induced RAW264.7 macrophages towards a more anti-inflammatory M2-like phenotype [117]. These effects were mediated by the HIF-1α-dependent secretion of

IL-10 by the ASCs, acting on the signal transducer and activator of transcription 3 (STAT3)/Arginase-1 (Arg-1) signaling pathway [117].

It is evident that oxygen tension is a critical factor of the cell microenvironment and low oxygen tension favours ASC proliferation, differentiation and maintenance of a progenitor-like phenotype. With the altered secretome, ASCs preconditioned under hypoxia may be better able to promote angiogenesis, as well as modulating the immune response in cell therapy. This preconditioning method could easily be applied to a wide range of clinical applications, such as for pro-angiogenic cell-based treatments for ischemic diseases, or as a way to augment the general therapeutic potential of ASCs.

1.4 Preconditioning effects of pro-inflammatory cytokines and growth factors

Studies suggest that the immunomodulatory properties of MSCs can be enhanced through stimulation with pro-inflammatory cytokines such as IFN-γ, IL-1β, and/or TNF-α [118], [119]. IFN-γ is the most commonly used cytokine for MSC priming as it is capable of stimulating MSCs to increase secretion of a number of important immunomodulatory factors, including IDO, PGE2, HGF, and TGF-β [120], which in turn can modulate the response of various immune cells, as discussed in previous section. Ragni *et al.* reported that IFN-γ priming can mediate changes in miRNA expression in human ASC-secreted EVs, including reducing macrophage M1-related miRNAs and augmenting M2-related miRNAs [121]. They also performed functional assays that demonstrated that the secretome of IFN-γ primed ASCs can prevent macrophage polarization towards an M1-like phenotype [121]. In addition, IFN-γ priming has also been demonstrated to enhance the ability of human ASCs to inhibit activated T cell proliferation [122].

IL-1β is another pro-inflammatory cytokine commonly used for MSC priming. IL-1β priming can enhance the secretion of anti-inflammatory miRNA-147b by human BM-MSCs [123]. Along with other secreted factors, exosomes secreted by IL-1β-primed human BM-MSCs were shown to reduce the expression of the pro-inflammatory cytokines IL-1β, IL-6, and monocyte chemoattractant protein-1 (MCP-1) secreted by the

human synovial SW982 cell line [123]. Aussel *et al.* also demonstrated improved immunomodulatory effects of IL-1β-primed rat BM-MSCs in a rat hemorrhagic shock-induced kidney and liver injury model [124].

TNF-α is another pro-inflammatory cytokine that has been used in conjunction with IFN-γ for MSC priming [118]. François *et al.* demonstrated that the combination of IFN-γ and TNF-α priming can inhibit T cell proliferation by IDO upregulation in MSCs, and that the primed human BM-MSCs also induced M2 macrophage differentiation [125]. It is noteworthy that IL-1β and TNF-α can be used to enhance the responsiveness of human nasal mucosa MSCs to IFN-γ priming through the nuclear factor kappa-light-chain-enhancer of activated B cells (NF-κB) signalling pathway [126].

In addition to the pro-inflammatory cytokines, pre-treatment with other growth factors such as TGF-β and FGF2 has been also explored to improve MSC migration and survival, as well as their pro-angiogenic potential [118]. Overall, pro-inflammatory cytokine and growth factor priming have been shown to be effective in improving the immunomodulatory and immunosuppressive properties of MSCs, however the priming process can increase the immunogenicity of MSCs, which may be less desirable for cell-based therapies [118].

1.5 Preconditioning effects of culture substrates

The extracellular matrix (ECM) is a complex network consisting of various proteins and polysaccharides that surrounds cells within tissues and plays a critical role in supporting and regulating normal cell functions [127]. In the context of ASCs, the native ECM may also be important in directing their paracrine activities [95]. Therefore, for the *in vitro* expansion of ASCs, the selection of the culture substrate is an important factor in regulating cell function.

In terms of culture substrates, there are many factors that can affect the cell response, including dimensionality, stiffness, and the biochemical composition of the material [128]. Conventional *in vitro* expansion of MSCs generally involves culturing cells as monolayers on a 2D surface, such as tissue culture polystyrene (TCPS), which fails to

recapitulate the complex 3-dimentional (3D) structure of the native ECM [129]. The potential benefits of 3D culture substrates on improving the therapeutic potential of MSCs have been demonstrated by multiple research studies [129]. In particular, culturing MSCs as 3D spheroids is a promising approach to augment their immunomodulatory capacity [95]. Compared to 2D culture, human BM-MSCs cultured as 3D aggregates were reported to have improved anti-inflammatory properties, evident in the more effective suppression of the inflammatory response of lipopolysaccharide (LPS) activated-macrophages [130]. Miceli *et al.* also demonstrated increased capillary maturation and inhibition of PBMC proliferation in the presence of conditioned media derived from human amnion-derived MSC spheroid as compared to 2D cultured controls [131].

Substrate stiffness is an intrinsic mechanical cue that can affect MSC differentiation and secretome by modulating cell morphology controlled by integrin binding [132]. Huebsch *et al.* demonstrated that in a 3D culture system, a stiffer culture substrate (11-30 kPa) favours osteogenic differentiation, whereas a softer culture substrate (2.5-5 kPa) favours adipogenic differentiation of murine and human MSCs [133]. Substrate stiffness has also been shown to affect the pro-angiogenic paracrine functionalities of human MSCs, with the conditioned media of MSCs cultured on fibronectin with higher stiffness (40 kPa) promoting greater human microvascular endothelial cell (HMVEC) tube formation as compared to conditioned media of MSCs cultured on fibronectin with lower stiffness (0.5 kPa) [134].

Material composition is another key factor that can instruct MSC differentiation as well as paracrine factor secretion. Proteins that are present in the native ECM of MSCs, such as collagen, elastin, and fibrin, are potential candidates as culture substrates. A recent study by Sawadkar *et al.* compared the performance of collagen, elastin, and fibrin as 3D scaffolds for adipose regeneration with human ASCs [135]. The three materials each had specific properties that contributed to adipose regeneration. More specifically, collagen supported cellular activities *in vivo* and adipogenesis *in vitro*, elastin contributed to maintaining the balance between scaffold degradation and tissue formation, and fibrin supported angiogenesis *in vivo*. To better make use of the properties of each material,

composites such as collagen/fibrin have been developed and have shown promising results in supporting angiogenesis [136] and articular cartilage repair [137].

In addition to developing protein composites, decellularized ECM scaffolds are a promising alternative that takes advantage of the inherent structural and compositional characteristics of the native tissue. With the goal of recapitulating the native cell niche of the ASCs, the Flynn lab has pioneered the development of decellularized adipose tissue (DAT) as a biomimetic and cell-instructive scaffold for ASC culture and delivery [138], [139]. Adipose tissue, otherwise discarded as surgical waste, can be rendered useful as a biomaterial after a detergent-free decellularization process that removes cells, cellular content and lipids [139]. Depending on the application, the DAT can be further processed into various forms, such as microcarriers, foams, bead foams [139], or coatings [140]. Several studies from our group have demonstrated the efficacy of DAT in facilitating ASC proliferation [140], [141], adipogenic differentiation [138], [140], [142], and *in vivo* angiogenesis [142]. Furthermore, previous work from the Flynn lab demonstrated enhanced angiogenic factor secretion by human fibroblasts cultured on DAT scaffolds as compared to collagen scaffolds, further supporting the potential advantages of using DAT as a cell culture substrate [143].

1.6 Preconditioning effects of mechanical stimulation

Within the body, biomechanical forces are extrinsic mechanical cues present in the native MSC niche, introduced by blood flow and body movements [144]. Similar to how cells sense mechanical stimulations from the ECM, extrinsic mechanical forces are also sensed by the cells through a range of mechanotransduction pathways [145], [146], as well as mechanosensitive ion channels [147] and primary cilium [148], [149]. Various means of mechanical stimulation, namely shear stress (fluid flow) [6], [7], tensile stress (stretching) [150]–[153], compression (pressure, including hydrostatic pressure) [154]–[157], and vibrations [158], [159], have been studied extensively in dynamic loading systems to guide the lineage commitment of MSCs, specifically towards the chondrogenic, osteogenic, or endothelial lineages [160]. In recent years, the use of mechanical stimulation to enhance MSC paracrine functions has emerged as a promising direction as

more evidence is present to show that it has the potential to enhance immunomodulatory and angiogenic functionalities.

1.6.1 Differentiation capacities

All cells in their native environment experience some level of mechanical forces, and depending on the physiological state of the tissue, the type and magnitude of the forces can be different [161]. Similar physiological forces can be applied to precondition MSCs to induce their differentiation towards a specific lineage. In articular cartilage, compressive mechanical loading is a key mechanical force experienced by chondrocytes. Similarly, compression is also capable of modulating the chondrogenic differentiation of MSCs [162]–[164]. Studies have reported that cyclic compression can upregulate chondrogenic gene expression in human BM-MSCs [162], [164]. At the protein level, joint-mimicking mechanical load is capable of inducing the secretion of TGF-β, which can in turn can induce the chondrogenic differentiation of human BM-MSCs [162], [163].

In terms of the osteogenic differentiation of MSCs, the effects of cyclic tensile strain are the most studied. Different levels of strain (5%-10%) have been shown to improve the osteogenesis of human and rat BM-MSC, as well as human ASCs and UC-MSC, in the presence of ostegenic differentiation media [165]–[169]. Interestingly, in a mechanical stimulated environment where osteogenic differentiation is favoured, adipogenesis of BM-MSCs can be impeded [169]. A possible mechanism behind the mechanical strain induced osteogenesis of human BM-MSC was suggested by Chen *et al.* as involving the activation of the adenosine monophosphate activated-protein kinase (AMPK)-silent information regulator type 1 (SIRT1) signalling pathway, which also involves MSC antioxidant functions [168].

1.6.2 Paracrine functions

Various forms of mechanical stimulation have been reported to modulate MSC paracrine factor secretion, of which fluid shear stress has been reported by several research groups to enhance both the pro-angiogenic and immunomodulatory paracrine functionalities of MSCs [150], [170]–[176]. Both short term (10 min) and long term (up to 4 days)

exposure to shear stress (10 dyn/cm^2) were able to upregulate pro-angiogenic factor VEGF secretion by human ASCs [172], [173]. Further, short-term intermittent exposure to shear stress also resulted in increased secretion of granulocyte colony-stimulating factor (G-CSF), HGF, Leptin, IL-8, PDGF-BB, Angiopoietin-2, and follistatin, which were believed to be COX-2 dependent [172]. Another research group also demonstrated the effects of short-term exposure (3-8 h) of unidirectional shear stress (10 dyn/cm^2) on the immunoregulatory function of human BM-MSC [174], [175]. More specifically, they reported suppressed TNF-α production by activated immune cells when co-cultured with the mechanically stimulated BM-MSCs. The focal adhesion kinase signalling pathway and NFκB-COX-2-PGE2 signalling pathway were reported as the key mechanisms behind the effects of shear stress [174], [175].

In addition to shear stress, other research groups have explored the effects of mechanical strain on MSC pro-angiogenic properties. Two groups have demonstrated upregulated VEGF secretion by human and murine BM-MSCs that were cultured under cyclic 10% strain [150], [170]. One group also demonstrated upregulation of angiogenic related genes FGF2 and matrix metalloproteinase-2 (MMP-2) in human ASCs cultured under 10% strain in osteogenic differentiation media [150]. Similarly, human BM-MSCs that were cultured under 30% strain also showed enhanced pro-angiogenic properties in terms of their capacity to stimulate *in vitro* tube formation and spheroid sprouting of Simian virus 40 (SV40)-immortalized human dermal microvascular endothelial cells (HMEC-1) [171].

Taken together, mechanical stimulation can have significant effects on the pro-angiogenic and immunomodulatory paracrine functions of MSCs. However, the different types and levels of mechanical stimulation, as well as the frequency or duration of their administration, can make it challenging to compare the results to inform the design of future studies. Standardized mechanical loading systems may be helpful in this case for research and clinical purposes.

1.7 Bioreactors for MSC expansion and preconditioning

Building upon the understanding of mechanical cues and other previously discussed stimuli, bioreactors have been explored for MSC expansion and preconditioning. In addition to improving oxygen diffusion and nutrient transportation [177], these complex dynamic culture systems are also capable of introducing multiple stimuli that can modulate cell phenotype and function while expanding the MSC population. Two common types of bioreactors used for MSC preconditioning are perfusion bioreactors and spinner flask bioreactors.

Hollow-fiber bioreactors are small-scale perfusion systems that can house a large number of cells due their structural design and have been used for EV production by MSCs [178]. Interestingly, the bioreactor system was reported to improve exosome production by 19.4-fold compared to a conventional 2D culture system [179]. The produced exosomes also contained high levels of the immunomodulatory and pro-angiogenic factors VEGF-A and IL-8 [180]. In a mouse acute kidney injury model, treatment with exosomes produced by hollow-fiber bioreactor cultured human UC-MSC modulated the inflammatory response in cisplatin-treated mice, evident in the reduced gene expression of pro-inflammatory markers, diminished kidney interstitial infiltration of inflammatory cells, and reduced levels of IL-6 and TNF-α in mouse serum as compared to exosomes produced by human UC-MSC cultured on TCPS [179]. Allen *et al.* also demonstrated that human BM-MSCs cultured in a hollow-fiber bioreactor were capable of suppressing activated human PBMC when co-cultured in the system [181]. In addition to the immunomodulatory effects, culturing within a perfusion bioreactor has also been reported to enhance the osteogenic differentiation of MSCs when seeded on an amine-functionalized scaffold [182].

Spinner flasks integrating microcarriers that have a high surface area to volume ratio are a versatile system for larger-scale expansion of MSCs [183]. Many off-the-shelf options are available for both the bioreactors and the microcarriers [178]. Culturing within spinner flask systems has also been reported to improve the therapeutic properties of MSCs. Compared to conventional 2D culture, human ASC spheroids cultured in a

spinner flask system produced significantly higher levels of the pro-angiogenic factors VEGF, FGF2, and HGF [184]. When applied in a wound healing mouse model, direct administration of dynamically-cultured ASC spheroids significantly improved the wound healing speed and vascularization [184].

In addition to the two common types of bioreactors introduced above, many other bioreactor systems, such as vertical-wheel and rotating wall systems, are also being investigated for MSC expansion or EV production [185]–[187]. In many of these systems, the use of biomaterials alongside mechanical stimulation in the form of seeding scaffolds and microcarriers can provide critical structural support to the cells in a loaded and dynamic culture environment. However, the effects of the individual factors can be hard to characterize in a complex dynamic system, making system modifications hard to implement without comprehensive testing in an already established system.

1.8 Project rationale and overview

As introduced in previous sections, ASCs can be preconditioned by hypoxia, pro-inflammatory cytokines, biomaterials, and/or mechanical stimulation to improve their therapeutic potentials. An ASC culture system capable of incorporating and probing for the above-mentioned factors could potentially serve as a mean of preconditioning ASCs to enhance their proliferation and/or pro-angiogenic and immunomodulatory properties for future clinical usage. In exploring this possible research direction, Dr. Tim Han from the Flynn lab utilized a DAT scaffold-based perfusion bioreactor to study the effects of dynamic culture and oxygen tension on ASC phenotype and paracrine function [188], [189]. *In vitro* studies over a 14-day period demonstrated increased cell expansion under hypoxia (2% O_2) as compared to normoxia (~20% O_2) [188], as well as an altered ASC phenotype in terms of angiogenic and immunomodulatory cytokine production under dynamic culture as compared to static culture [189]. Specifically, the preconditioning effects were more prominent on the periphery of the scaffold, suggesting that shear forces generated by the fluid flow may be a key factor in modulating the properties of the ASCs expanded within this system.

Interestingly, *in vivo* studies comparing dynamically-preconditioned ASC-seeded DAT scaffolds to a range of controls in athymic nude mice demonstrated enhanced angiogenesis in the hypoxic dynamic group at 1, 4, and 8 weeks post-implantation (measured based on histological density of blood vessels) [188]. Macrophage phenotype within the implants was also explored by immunostaining for the pro-regenerative macrophage marker CD163, and results suggested that dynamic preconditioning of the ASCs on the DAT may help promote a more pro-regenerative response at later timepoints [189]. These results taken together demonstrated that dynamic culture, specifically under the influence of shear stress, along with hypoxia could potentially be an effective ASC preconditioning strategy.

Notably, the previous bioreactor system had two main limitations: 1) the perfusion bioreactor had a complex setup and would be difficult to scale up, and 2) the preconditioning effects were limited to the periphery of the scaffolds, indicating limited perfusion and mechanical stimulus towards the centre of each scaffold. In search of a more translatable and scalable system, the current project focused on developing a new rocking bed bioreactor as an alternative platform for introducing mechanical stimulus in the form of shear stress, with the goal of enhancing the pro-regenerative capacity of human ASCs through controlled expansion within this system.

1.9 Hypothesis

Human ASC expansion and paracrine factor secretion can be modulated by culturing the cells on DAT coatings under shear stress on a rocking bioreactor, and will also be affected by oxygen tension and the addition of pro-inflammatory cytokines to the culture medium.

1.10 Specific aims

This Master's thesis focused on investigating the collective effects of DAT substrates, oxygen tension, shear stress, and cytokine priming on ASC proliferation and paracrine factor secretion in the context of a new rocking bioreactor system. Specifically, this was divided into three aims:

1) To establish the rocking bioreactor platform and explore the effects of culture substrate, various rocking conditions and oxygen tension on ASC expansion within the system relative to static culture controls.
2) To evaluate the effects of modulating the cellular microenvironment through bioreactor preconditioning on human ASC pro-angiogenic and immunomodulatory paracrine factor secretion.
3) To characterize the effects of stimulating ASCs cultured within the rocking bioreactor system with the pro-inflammatory cytokines IFN-γ and TNF-α as a priming strategy to alter pro-angiogenic and immunomodulatory paracrine factor secretion.

Chapter 2

2 Materials and methods

2.1 Materials

Unless otherwise stated, all chemicals and reagents were purchased from Sigma Aldrich Canada Ltd. (Oakville, Canada), and all antibodies were purchased from Abcam (Cambridge, UK).

2.2 Bioreactor design and computational modelling of fluid shear stress

The bioreactor was comprised of 8-well rectangular plates (Nunc, ThermoFisher) as cell culture vessels, a compact digital rocker (Ohaus) to introduce shear stress, and a HypOxystation H35 system (HypOxygen) to maintain the hypoxic environment (2% O_2). The setup of the system, including the placement of the cell culture plates on the rocker, is demonstrated in **Figure 2.1**. A standard cell culture incubator (37°C, 95% air/5% CO_2) was used for the normoxic (~20% O_2) culture conditions.

Figure 2.1 Rocking bioreactor system setup. Left: The rocking bioreactor system placed in the HypOxystation H35 system. Right: The operating rocking bioreactor system under the 11° 50 rpm rocking condition. The placement of the culture plate ensured that the centre of the wells in use were aligned with the rotating axis of the rocker.

A computational model of shear stress within the bioreactor culture vessels was developed using MATLAB to aid in the selection of the rocking conditions (i.e., fluid height, rocking angle, and rocking frequency). The model was adapted from Zhou *et al.* [190], with modifications to the modeling parameters to match the current rocking bioreactor system design. The calculation of fluid shear stress in the mathematical model developed by Zhou *et al.* is based on two parameters, the rocking angle at a given time (θ) and the fluid height when the plate is horizontal (h_o). The rocking angle at a given time (t) can be determined using equation (1) with the set rocking angle (θ_{max}) and rocking frequency ($\frac{1}{T}$) given.

$$\theta = \theta_{max} \sin \frac{2\pi t}{T} \qquad (1)$$

Based on the rocking angle (θ) and the fluid height (h_o), the fluid flux (q) and fluid height at a given time and location (h_f) can be determined. Finally using equation (2), the fluid shear stress can be determined based on the velocity profile (u) along the vertical cross section (z) at a given location, with the medium viscosity (μ) and culture well width (b) given.

$$Fluid\ shear\ stress = \mu \frac{\partial u}{\partial z}\Big|_{z=0}, \text{ where } u = \frac{3q}{2bh_f^3} z(2h_f - z) \qquad (2)$$

The analysis was also expanded to include presentation of the modeling results using 3-dimentional (3D) plots and coloured heatmaps to aid in data visualization and interpretation. Fluid shear stress and time derivatives of fluid shear stress were calculated and displayed as 3D plots across the length of the culture well over one rocking cycle. The maximum fluid shear stress was calculated across all possible combinations of rocking angle (1-13°, in increments of 1°) and rocking frequency (5-60 rpm, in increments of 5 rpm), and displayed in coloured heatmaps. Two representative locations in the culture well were used for calculations: 1) at the centre of the well (x = 0), and 2) at the edge of the coverslip used for the cell density/immunofluorescence staining studies (x = 11 mm).

2.3 Adipose tissue collection and processing

Subcutaneous adipose tissue samples were collected with informed consent from female patients undergoing elective breast or abdomen reduction surgeries at the London Health Sciences Centre (London, ON) with human research ethics board approval from Western University (HSREB 105426). Patient information including sex, age, weight, height, and excision site was collected and recorded. The samples were transported to the lab on ice in sterile phosphate buffered saline (PBS) with 2% bovine serum albumin (BSA).

2.3.1 Human ASC isolation

For human adipose-derived stromal cell (ASC) isolation, the adipose tissue samples were processed within 2 h following published protocols [191]. Isolated ASCs were cultured on tissue culture polystyrene (TCPS; Corning, NY, USA) at 37°C, 5% CO_2 in complete proliferation media comprised of Dulbecco's Modified Eagle Medium and Ham's F12 nutrient mixture (DMEM/F12) supplemented with 10% fetal bovine serum (FBS), 100 U/mL penicillin, and 0.1 mg/mL streptomycin. The complete media was changed every 2–3 days. Cells were frozen at passage 0 or passage 1, stored in liquid nitrogen, and thawed when needed. Appendix A Table 1 includes the donor information for all cells used and the specific studies in which they were applied.

2.3.2 Adipose tissue decellularization and DAT coating fabrication

For generation of the decellularized adipose tissue (DAT), the freshly isolated adipose tissue samples were transferred into hypotonic cell lysis buffer (Solution A:10 mM Tris base and 5 mM ethylenediaminetetraacetic acid (EDTA), pH 8.0) and frozen at -80°C. The tissues were then processed following published detergent-free decellularization protocols established by the Flynn lab that involve freeze-thaw cell lysis, enzymatic digestion with trypsin-EDTA and DNAse/RNAse, and lipid extraction with isopropanol [192]. For DAT coating fabrication, decellularized tissue samples from 5-6 donors were pooled and processed following published protocols to generate DAT suspensions [140]. Briefly, lyophilized DAT was minced, cryomilled, and digested for 3 days under agitation using α-amylase (0.3% w/w of dry tissue) dissolved in 0.22 M NaH_2PO_4 (pH 5.4). Following digestion, the suspension was centrifuged and the digested ECM pellet

was washed with 5% (w/v) NaCl solution and double-distilled water (ddH_2O). Finally, the digested DAT was centrifuged and resuspended in acetic acid (0.2 M) to achieve a concentration of 25 mg/mL based on the starting dry mass of milled tissue. The DAT suspension was homogenized using a PowerGen Model 125 homogenizer (Fisher Scientific) and stored at 4°C until use.

To produce the coatings, the DAT suspension was applied to the rectangular culture plates at 125 $\mu L/cm^2$. For immunohistochemical analyses, square glass coverslips were placed in the centre of the wells prior to applying the coatings. The coatings were then left in a biological safety cabinet to dry overnight. To disinfect the coatings in preparation for culture, an ethanol gradient wash method was used. In brief, the DAT coatings underwent three 30 min incubations in sterile 70% ethanol, followed by one 30 min incubation in sterile 35% ethanol. The coatings were then rinsed three times using sterile PBS before seeding. Uncoated (UC) wells were also included as controls.

2.4 ASC seeding and culture

Human ASCs at passage 3-4 were used for all studies. ASCs were seeded at a density of 5000 cells/cm^2 on the DAT coatings or uncoated controls and cultured in complete DMEM/F12 proliferation media. The plates were incubated statically overnight under normoxic conditions to promote cell attachment (37 °C, 5% CO_2). On day 0, the plates were moved to their assigned culture environment. The samples were then dynamically or statically cultured under 2% or 20% O_2 for up to 7 days. The specific dynamic culture conditions investigated included rocking angles and frequencies of: 1) 11° 50 rpm, 2) 11° 25 rpm, and 3) 5° 50 rpm, selected based on the shear stress modeling results.

For studies analyzing the effects of the culture microenvironment on ASC paracrine factor production using Human Magnetic Luminex® Assays or enzyme-linked immunosorbent assay (ELISA), the ASCs were cultured in complete proliferation media for 5 days and then transferred into low-serum media (DMEM/F12 supplemented with 2% FBS, 100U/mL penicillin, and 0.1 mg/mL streptomycin) and cultured for an additional 48 h. For subsequent studies focused on analyzing the additional effects of priming with the pro-inflammatory cytokines tumor necrosis factor alpha (TNF-α) and

interferon gamma (IFN-γ) on ASC paracrine factor secretion, ASCs were cultured in complete proliferation media for 5 days and then transferred into priming media comprised of low-serum media supplemented with 10 ng/mL TNF-α and 100 ng/mL IFN-γ [193] or low-serum media as controls and cultured for an additional 48 h.

2.5 Immunohistochemical analysis of ASC density and expression of iNOS and IDO

To evaluate the effects of the culture microenvironment on ASC growth and phenotype, nuclear staining with Hoechst 33258 was used to quantify the cell density and immunofluorescence staining was performed to examine the expression of inducible nitric oxide synthase (iNOS), as a potential indicator of ASCs with a more pro-regenerative secretory phenotype [189], in combination with phalloidin to visualize cell morphology. Samples (11° 50 rpm: n=2 replicate wells/trial, N=4 trials with different ASC donors; 11° 25 rpm: n=2 replicate wells/trial, N=4 trials with different ASC donors; 5° 50 rpm: n=2 replicate wells/trial, N=2 trials with different ASC donors) were collected after 3 and 7 days of culture, fixed in 10% phosphate buffered formalin for 10 min, permeabilized for 10 min (PBS, 0.1% Triton X-100), and blocked for 30 min (PBS, 0.1% Tween 20, 1% BSA). Next, the samples were incubated overnight at 4 °C with rabbit anti-iNOS antibody (PA1-036, ThermoFisher, 1:250). The samples were then stained with an Alexa Fluor 594 conjugated goat anti-rabbit IgG secondary antibody (ab150080, Abcam, 1:500), phalloidin (ab176760, Abcam, 1:2000), and Hoechst 33258 (ThermoFisher, 1:1000) for 1 h at room temperature. Finally, the samples were mounted in Fluoroshield mounting medium (Abcam). Ten non-overlapping images were captured for each sample using an EVOS® FL fluorescence imaging system (Thermo Fisher Scientific) under 20X magnification. Nuclei per mm^2 were quantified using ImageJ software.

Pilot immunofluorescence staining studies were conducted to confirm that cytokine priming induced the expression of indoleamine 2,3-dioxygenase (IDO) as expected, which has been suggested to be a potential marker associated with the immunomodulatory function of ASCs [69], with phalloidin to visualize cell morphology

and Hoechst 33258 to visualize cell nuclei. ASC samples (11° 50 rpm: n=1 replicate wells/trial, N=2 trials with different ASC donors) were collected after 7 days of culture, and then stained and imaged following the methods described above with rabbit anti-IDO antibody (ab211017, Abcam, 1:2000) as the primary antibody.

2.6 ASC pro-angiogenic and immunomodulatory paracrine factor production

To quantify the secretion levels of a range of pro-angiogenic and immunomodulatory paracrine factors by the ASCs, the concentration of angiogenin, vascular endothelial growth factor (VEGF), hepatocyte growth factor (HGF), monocyte chemoattractant protein-1 (MCP-1), and interleukin 8 (IL-8) were quantified by Human Magnetic Luminex® Assay (R&D Systems), and the concentration of secreted IDO and interleukin 6 (IL-6) were quantified by ELISA (DuoSet ELISA, R&D Systems) within the conditioned media (CM) samples collected at 7 days, following the methods described in detail below. IL-6 was analyzed by ELISA instead of Luminex because it was much more highly expressed than the other factors included in the panel. Initial testing also included screening for angiopoietin-1, interleukin 1 beta (IL-1β), interleukin 4 (IL-4), interleukin 10 (IL-10), TNF-α, epidermal growth factor (EGF), fibroblast growth factor-2 (FGF2), leptin, platelet-derived growth factor-AA (PDGF-AA), and placental growth factor (PIGF), but findings indicated that they were below the range of the standard curve under the conditions included in the current study (Appendix A Table 2). Protein concentrations were normalized to the double stranded DNA (dsDNA) content in each sample as determined by the PicoGreen Assay, as described below.

2.6.1 Human Magnetic Luminex® Assay

To evaluate the effects of the culture microenvironment on ASC paracrine factor secretion, the ASCs were cultured as previously described (11° 50 rpm: n=2 replicate wells/trial, N=4 trials with different ASC donors; 11° 25 rpm: n=2 replicate wells/trial, N=4 trials with different ASC donors). On day 7, the supernatant media from each sample was collected, centrifuged at 1200 × g for 10 min to remove particulates, and frozen at -80 °C. All CM samples were diluted 2-fold with the calibrator buffer RD6-52

provided with the kit immediately prior to analysis using a 5-plex Luminex assay (angiogenin, VEGF, HGF, MCP-1, IL-8). For the studies evaluating the effects of cytokine priming, ASC samples (11° 50 rpm: n=2 replicate wells/trial, N=3-4 trials with different ASC donors) were cultured and processed as previously described. For the analysis of IL-8 and MCP-1 in a duplex Luminex assay, the primed samples were diluted 200-fold (donor ID: 1, 2, and 4) or 300-fold (donor ID: 3) (Appendix A Table 1) to accommodate the high expression levels of these analytes, and the non-primed samples were diluted 2-fold as previously described. A triplex assay was performed for the analysis of angiogenin, VEGF, and HGF, with all samples diluted 2-fold as previously described.

The Luminex Assays were performed in accordance with the manufacturer's protocols. In brief, the CM samples were first diluted as described above and loaded into a 96-well plate along with the provided standards in duplicates. Pre-mixed magnetic beads were then added and incubated for 2 h at room temperature with shaking (500 rpm). The diluted biotin-antibody cocktail was then added to each sample and incubated for 1 h at room temperature with shaking before the Streptavidin-PE cocktail was added and incubated for 30 min. The 96-well plate was then read using a MAGPIX® System (Millipore). The results were analyzed using the xPONENT program with a five-parameter logistic curve-fit. Protein concentrations were determined based on comparison to the standard curves and normalized to the dsDNA content measured in each sample using a PicoGreen® dsDNA Assay, described below.

2.6.2 ELISA

For the studies investigating the effects of the varying culture microenvironments, the ASCs were cultured as previously described (11° 50 rpm: n=2 replicate wells/trial, N=5 trials with different ASC donors; 11° 25 rpm: n=2 replicate wells/trial, N=4 trials with different ASC donors; 5° 50 rpm: n=2 replicate wells/trial, N=2 trials with different ASC donors) and ELISA was performed to measure the levels of secreted IL-6. The collected CM samples were processed and stored as previously described, and diluted 30-fold with reagent diluent provided with the kit immediately prior to analysis. For the cytokine

priming studies, ELISA was performed to measure the levels of both secreted IL-6 and IDO in the CM samples. The ASCs were cultured and CM samples were collected as previously described (11° 50 rpm: n=2 replicate wells/trial, N=3-4 trials with different ASC donors). For the IL-6 ELISA, all primed samples were diluted 60-fold based on the high expression levels in these samples, and the non-primed samples were diluted 30-fold. For the IDO ELISA, the samples were not diluted.

ELISA was performed in accordance with the manufacturer's protocols. Briefly, a 96-well plate was coated with diluted capture antibody overnight and blocked for 1 h before sample addition. The samples were diluted with the provided reagent diluent, loaded into the prepared plate along with the provided standards in duplicates, and incubated for 2 h at room temperature. The diluted detection antibody was then added with a 2 h incubation at room temperature. The diluted Streptavidin-HRP was added with a 20 min incubation at room temperature, protected from light. Substrate solution was then added and incubated for 20 min before the addition of the stop solution. The 96-well plate was then read using a CLARIOstar® microplate reader (BMG Labtech, Guelph, Canada) at 450 nm and 540 nm. The results were analyzed using the MARS analysis program with a four-parameter logistic curve-fit. Protein concentrations were determined based on comparison to the standard curves and normalized to the dsDNA content measured in each sample using a PicoGreen® dsDNA Assay.

2.6.3 Picogreen® dsDNA assay

PicoGreen® dsDNA assays were performed following the manufacturer's instructions, to normalize the secreted proteins levels in the CM samples based on the total number of cells in each corresponding well at 7 days. In brief, cell samples from the uncoated and DAT-coated conditions were collected using trypsin release or cell scraping, respectively. Sample digestion and total DNA extraction were then performed using the DNeasy Blood & Tissue kit (Qiagen). Briefly, samples were digested overnight in 1 mL of buffer ATL supplemented with 32.5 μL of proteinase K. The dsDNA was then extracted from the digested samples and analyzed using the Quant-iT™ PicoGreen® Assay kit (Invitrogen) according to the manufacturer's instructions with a CLARIOstar® microplate reader

(BMG Labtech, Guelph, Canada). The standard curve was generated using the Lambda DNA standard provided in the kit. Unseeded DAT coating samples were also included for background adjustment.

2.7 Statistical analysis

For analysis of ASC density and paracrine factor production, a mixed effects model was used to first evaluate the main effect of oxygen tension. The data were then divided into two groups based on the oxygen level and analyzed separately. To evaluate the effects of the culture microenvironment on ASC density and paracrine factor production, a two-way analysis of variance (ANOVA) test was performed, followed by a Tukey's post hoc multiple comparisons test. To evaluate the effects of cytokine priming on ASC paracrine factor production, due to the additional variable (i.e., priming or non-priming media), a repeated-measures two-way ANOVA was performed, followed by a Tukey's post hoc multiple comparisons test (comparing primed and non-primed under the same culture condition) and a Sidak's post hoc multiple comparisons test (comparing between culture conditions under the same priming condition). All statistical analyses were performed using the GraphPad Prism 8 software. All numerical values are represented as the mean ± standard deviation, and differences were considered statistically significant at $p<0.05$.

Chapter 3

3 Results

3.1 Computational modelling of fluid shear stress

To characterize the fluid shear stress introduced by the system under different rocking conditions, a computational model was developed to calculate the shear stress across the length of the culture well for a single rocking cycle. The results indicated that the fluid shear stress varied greatly depending on the rocking angle and rocking frequency. Under a specific rocking condition, the fluid shear stress also varied depending on the location in the culture well and time, and a notable non-uniformity was introduced along the edges of the plate when the rocking angle was greater than the critical angle (=7° in the current system). The critical angle is defined as the maximum angle where the entire bottom of the culture plate would still be covered by fluid. In other words, if the rocking angle was greater than the critical angle, the bottom of the plate would no longer be fully covered by fluid throughout the rocking cycle, resulting in a "dry area" near the edge of the wells. This region could not be modelled (resulted in infinite values), as in the absence of fluid, shear stress would no longer be applied. In reality, there will always be at least a thin layer of fluid covering the bottom of the plate due to the presence of the coatings or the hydrophilicity of the TCPS. However, attempting to incorporate these features into the model would be extremely challenging and was beyond the scope of the current work. Based on the model results, a media volume of 2.5 mL (height = 2.38 mm) was selected. Changing the media volume introduced a lot of variability to the system, which was difficult to model, so it was decided to use this volume for all studies. The selected volume also ensured that there would be adequate media for the cells and avoided potential issues with spillover during rocking.

The rocking conditions investigated in this study were determined based on 1) the maximum shear stress achievable, 2) the shear stress profile, which indicates how the shear stress changes over time at each location in the well, and 3) the profile of the time derivative of shear stress, which indicates how quickly the shear stress changes over time at each location in the well. To select rocking conditions for subsequent studies, the area

of the coverslip used for the cell density study was considered as the primary area of interest. The model also analyzed the shear stress profile over the entire well, which was relevant for the conditioned media studies. The heatmaps generated by the model (**Figure 3.1**) summarize the maximum shear stress at the centre of the well and at the edge of the area of interest (i.e., the coverslip) under every rocking condition achievable by the rocker. The analysis suggested that the maximum rocking angle that was practical to use in the system was 11°, above which there was significant non-uniformity in the shear stress in the area of interest within the well, as reflected by a much higher maximum shear stress level near the edge (**Figure 3.1B)**. Within these constraints on the rocking conditions, 11° 50 rpm introduced the highest shear stress (0.094 dyn/cm^2 at x=0 and 0.294 dyn/cm^2 at x=0.29 L =11 mm) and was therefore selected as the starting point for the culture studies. To evaluate the effects of different magnitudes of shear stress on the ASCs, the rocking condition 11° 25 rpm was also selected, which would apply approximately half of the maximum shear stress of the 11° 50 rpm condition (0.047 dyn/cm^2 at x=0 and 0.147 dyn/cm^2 at x=0.29 L).

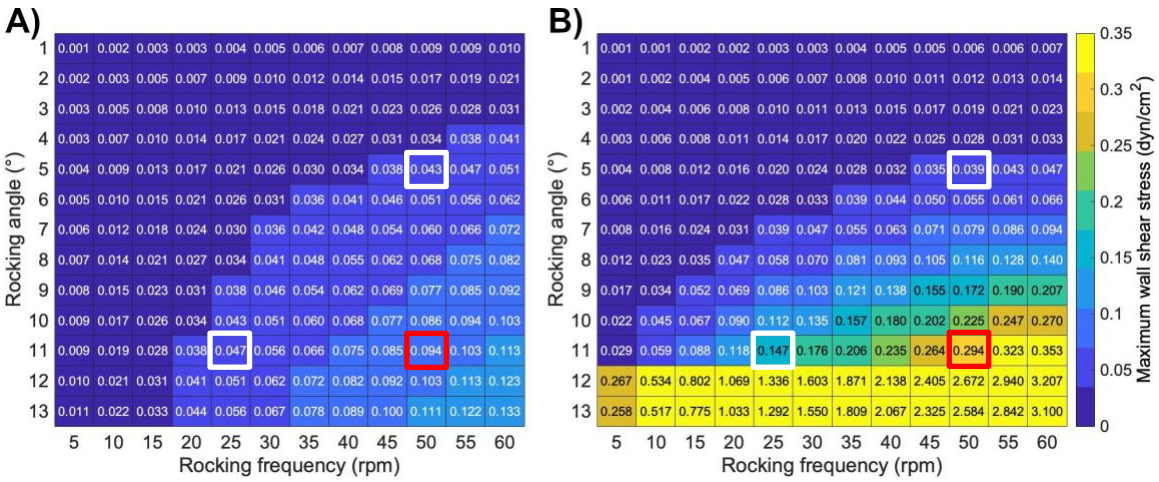

Figure 3.1 Maximum fluid shear stress under different rocking conditions. A) At the centre of the well (x = 0) and B) at the edge of the coverslip in the well (x = 11 mm) as a function of rocking angle and frequency. The colour gradient from blue to yellow shows an increase in the value of the maximum shear stress, which increases at both locations as the rocking angle and frequency increase. Selected rocking conditions highlighted: red boxes: 11° 50 rpm, white boxes: 11° 25 rpm and 5° 50 rpm.

As effects of shear stress on ASCs have not been well studied in the literature, little is known regarding how different aspects of shear stress, such as magnitude, change over time, and how fast it changes, would impact the cellular response. Therefore, an additional rocking condition was included for preliminary testing to evaluate if and how different shear stress profiles could influence the cellular response. More specifically, 5° 50 rpm was selected for this purpose as under this rocking condition, the maximum shear stress achievable at the centre of the plate (0.043 dyn/cm^2 at x=0 and 0.039 dyn/cm^2 at x=0.29 L) was very similar to that of the 11° 25 rpm condition (**Figure 3.1**), but the shear stress profile (**Figure 3.2**) and the profile of the time derivative of shear stress (**Figure 3.3**) were drastically different compared to the 11° 50 rpm and 11° 25 rpm conditions.

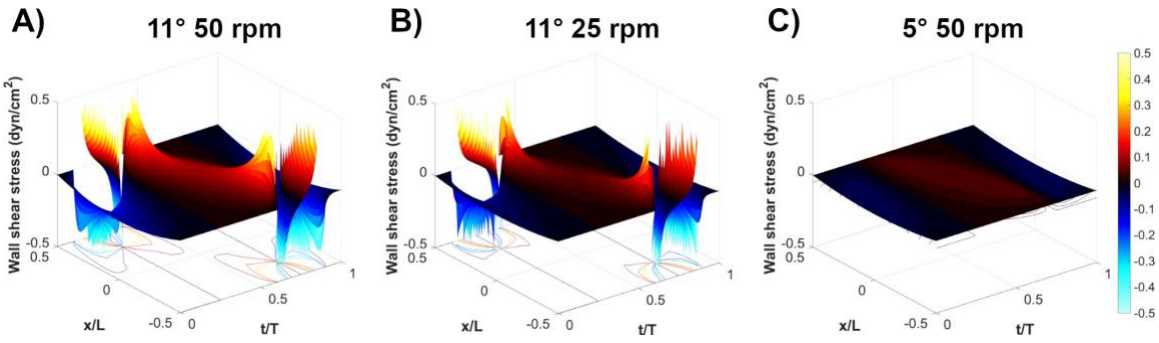

Figure 3.2 Fluid shear stress under the three selected rocking conditions. A) 11° 50 rpm, B) 11° 25 rpm, C) 5° 50 rpm. X axis: relative location (x) along the length of the well (L), Y: relative time (t) over a single rocking cycle (T), Z axis: wall shear stress in dyn/cm^2.

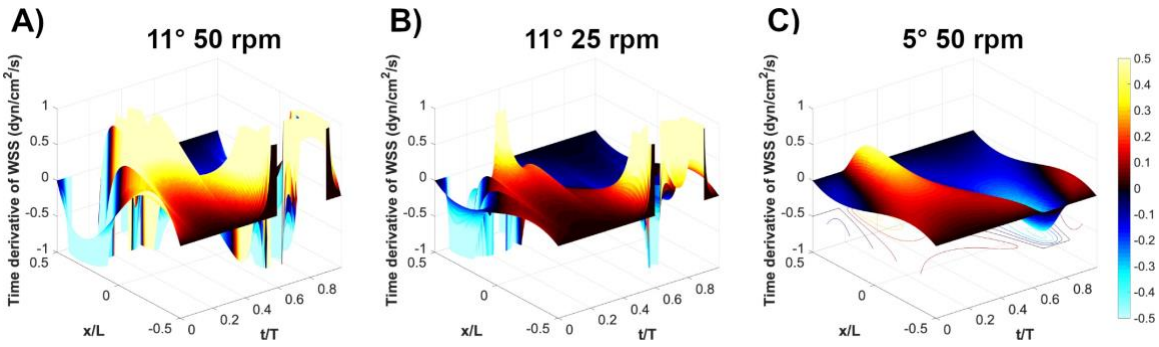

Figure 3.3 Time derivative of fluid shear stress under the three selected rocking conditions. A) 11° 50 rpm, B) 11° 25 rpm, C) 5° 50 rpm. X axis: relative location (x) along the length of the well (L), Y axis: relative time (t) over a single rocking cycle (T), Z axis: time derivative of wall shear stress in dyn/cm^2/s.

3.2 Culturing on the DAT coatings and under dynamic conditions did not substantially alter ASC growth

To investigate the effects of the culture microenvironment on ASC growth, ASCs were cultured for 7 days under different culture conditions, followed by immunohistochemical analysis and cell nuclei quantification using ImageJ. In both the 11° 50 rpm and 11° 25 rpm studies, the density of ASCs was significantly higher at 7 days as compared to 3 days for all groups (11° 50 rpm: $p<0.01$; 11° 25 rpm: $p<0.05$), suggesting that cell growth was supported in the system under all conditions. In both studies, the cell density at day 3 was not significantly different between the culture conditions (**Supplementary Figure 3.1**, **Supplementary Figure 3.2**). However, at day 7, culturing under 20% O_2 resulted in a significantly higher cell density as compared to under 2% O_2 in both studies ($p<0.05$). In the 11° 50 rpm study, culturing on the DAT coatings under 20% O_2 resulted in a significantly higher cell density at day 7 as compared to the uncoated group ($p<0.01$) (**Figure 3.4B**). In contrast, in the 11° 25 rpm study, the cell density was not affected by culturing on DAT coatings (**Figure 3.5**). Preliminary analysis of the two donors analyzed in the 5° 50 rpm study showed similar trends to the 11° 25 rpm study (**Supplementary Figure 3.3**, **Supplementary Figure 3.4**).

While traditionally regarded as a “classically-activated” M1-like or pro-inflammatory macrophage marker [194], [195], iNOS expression in MSCs has been shown to play a critical role in inducing MSC-mediated immunosuppression [196], [197]. Previous work by Dr. Tim Han in the Flynn lab also suggested a possible link between dynamic culture under shear stress and enhanced iNOS and immunomodulatory protein expression in ASCs cultured in 3D DAT scaffolds within a perfusion bioreactor system [189]. In all three of the rocking conditions studied (11° 50 rpm, 11° 25 rpm, and 5° 50 rpm), qualitative analysis of iNOS expression through immunofluorescence (IF) staining showed no obvious differences between the culture conditions after 3 and 7 days of culture. Moreover, staining of F-actin showed no obvious differences in ASC morphology induced by dynamic culture or culturing on the DAT coatings, as shown in **Figure 3.4** (11° 50 rpm), **Figure 3.5** (11° 25 rpm), and **Supplementary Figure 4** (5° 50 rpm).

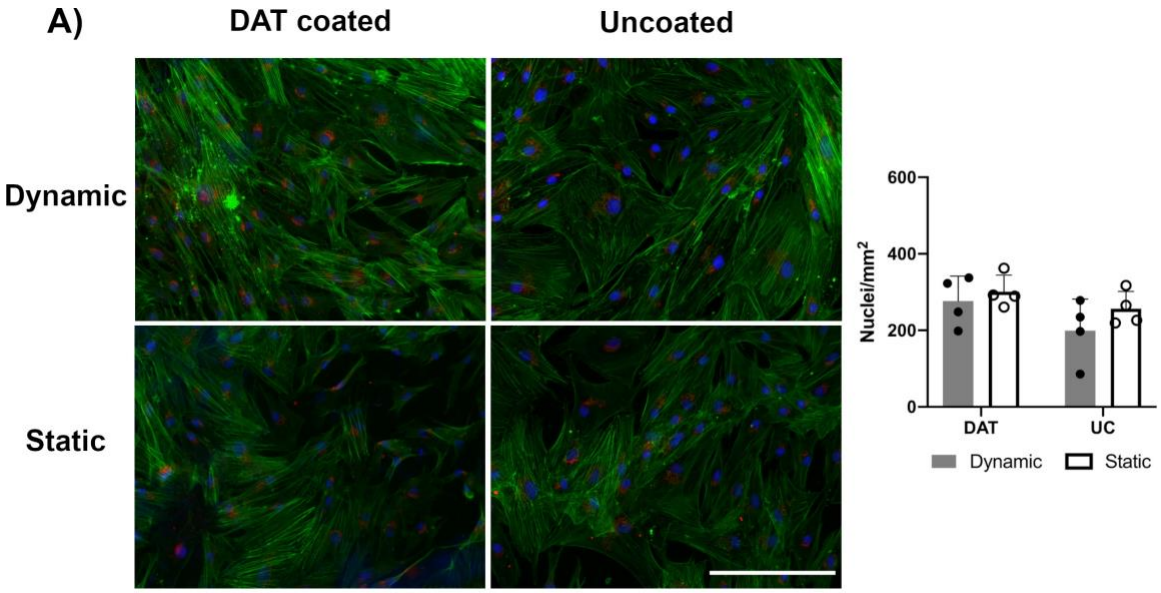
A)
DAT coated
Uncoated
Dynamic
Static
600
400
200
0
Nuclei/mm²
DAT
UC
Dynamic
Static

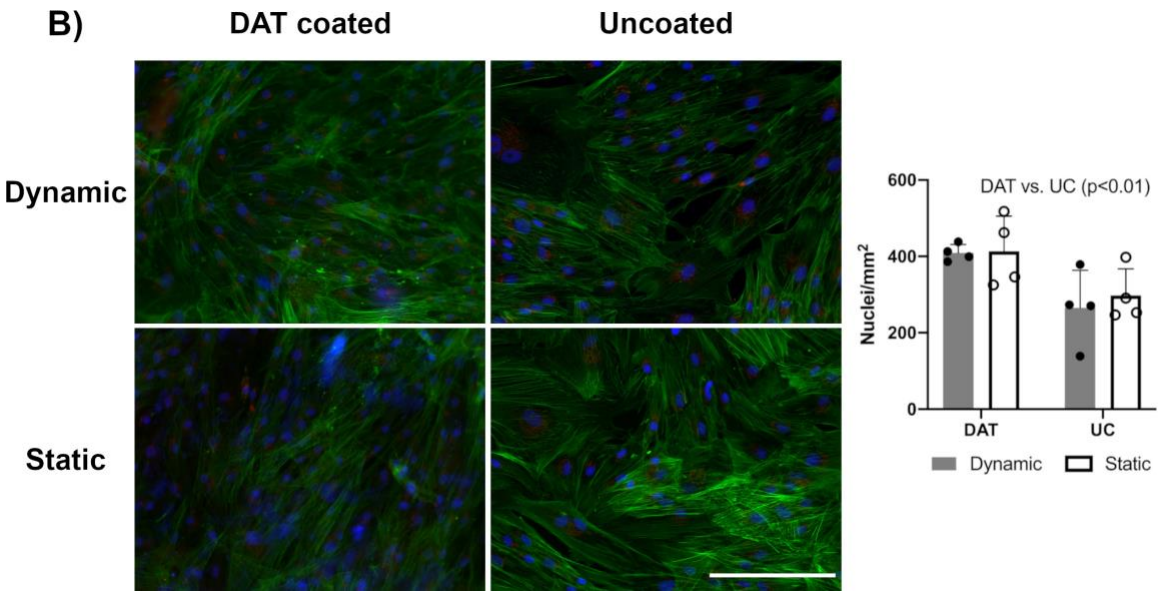
B)
DAT coated
Uncoated
Dynamic
Static
DAT vs. UC (p<0.01)
600
400
200
0
Nuclei/mm²
DAT
UC
Dynamic
Static

Figure 3.4 Dynamic culture under the highest shear conditions (11°, 50 rpm) did not substantially alter the ASC density at 7 days. Representative images of iNOS expression (red) with staining for F-actin (green) and nuclei (blue), along with quantification of nuclei, after 7 days of culture under A) 2% O_2 or B) 20% O_2. Main effects analysis showed that cell density in the 20% O_2 group was significantly higher than the 2% O_2 group ($p<0.05$). Cell density in the DAT coated group was significantly higher than the uncoated group under 20% O_2 ($p<0.01$). Qualitatively, no difference in iNOS expression was observed between any of the groups. Data was analyzed using two-way ANOVA with a Tukey's multiple comparisons test. ** $p < 0.01$. Error bars represent standard deviation (n=2 replicate wells/trial, N=4 trials with different ASC donors). Scale bars represent 200 μm. No primary antibody control: Supplementary Figure 3.6. Abbreviations: DAT, DAT coated; UC, uncoated TCPS.

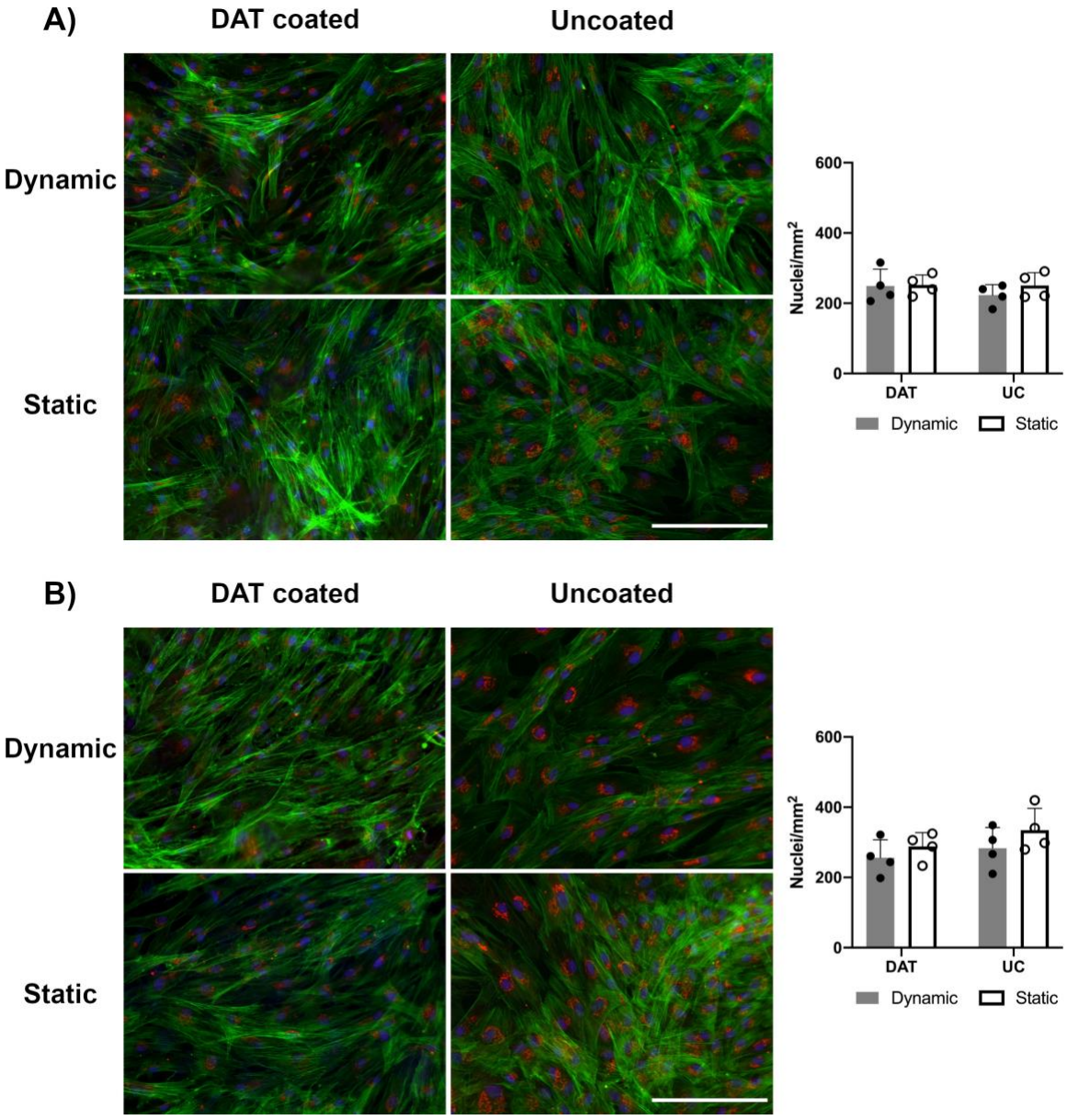
A)
DAT coated
Uncoated
Dynamic
Static
Nuclei/mm²
600
400
200
0
DAT
UC
Dynamic
Static
B)
DAT coated
Uncoated
Dynamic
Static
Nuclei/mm²
600
400
200
0
DAT
UC
Dynamic
Static

Figure 3.5 Culturing on the DAT coatings or under shear stress in the 11° 25 rpm condition did not alter the ASC density at 7 days. Representative images of iNOS expression (red) with staining for F-actin (green) and nuclei (blue), along with quantification of nuclei, after 7 days of culture under A) 2% O_2 or B) 20% O_2. Main effects analysis showed that cell density in the 20% O_2 group was significantly higher than the 2% O_2 group ($p<0.05$). Qualitatively, no difference in iNOS expression was observed between any of the groups. Data was analyzed using two-way ANOVA with a Tukey's multiple comparisons test. Error bars represent standard deviation (n=2 replicate wells/trial, N=4 trials with different ASC donors). Scale bars represent 200 μm. No primary antibody control: Supplementary Figure 3.6. Abbreviations: DAT, DAT coated; UC, uncoated TCPS.

3.3 Pro-angiogenic and immunomodulatory paracrine factor secretion was modulated by the oxygen tension, dynamic culture, and DAT coatings

To quantitatively evaluate how culturing in the varying microenvironments altered the levels of pro-angiogenic and immunomodulatory proteins secreted by ASCs, Luminex® assays were performed to measure the levels of angiogenin, VEGF, HGF, MCP-1, and IL-8, and ELISAs were performed to measure the levels of IL-6 in conditioned media samples collected after a 7-day culture period, with media conditioning for the final 48 h. A heatmap of the results is shown in **Figure 3.6**, with red corresponding to a higher level and blue corresponding to a lower level detected within the conditioned media samples.

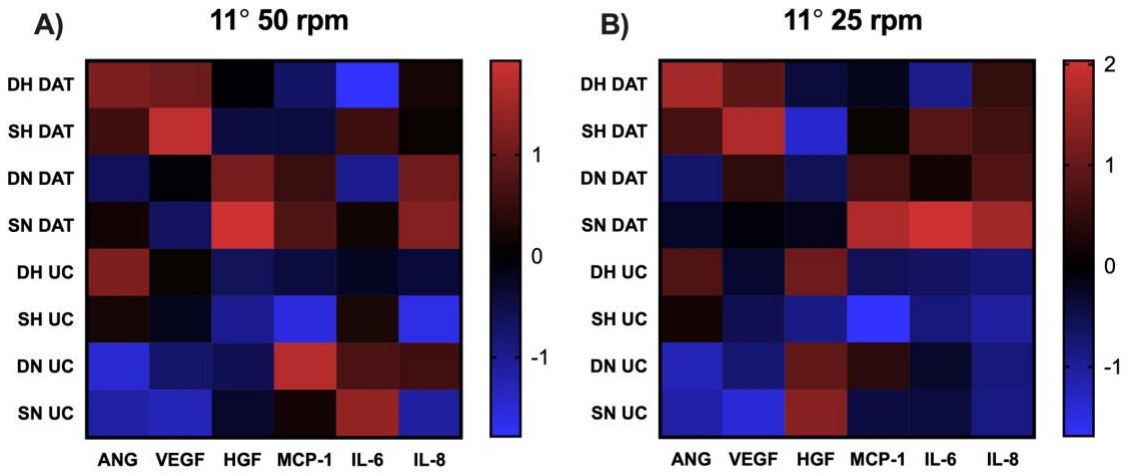

Figure 3.6 ASC paracrine factor secretion was modulated by the varying microenvironmental factors. Summary of the levels of secreted angiogenin, VEGF, HGF, MCP-1, IL-6 and IL-8 detected in the conditioned media samples from A) the 11° 50 rpm study and B) the 11° 25 rpm study. Coloured heatmap showing red as the highest value and blue as the lowest value. The colours represent z-score normalized average concentrations (normalized to total dsDNA content). n=2 replicate wells/trial, N=4 trials with different ASC donors, except IL-6 from the 11° 50 rpm experimental group: n=2 replicate wells/trial, N=5 trials with different ASC donors). Abbreviations: ANG, angiogenin; D, dynamic; S, static; H, hypoxia; N, normoxia; DAT, DAT coated; UC, uncoated TCPS.

The effects of the culture microenvironment on ASC paracrine factor secretion were analyzed in two ways: 1) based on two-way ANOVA analysis treating the three culture variables (i.e., culture substrate, dynamic culture, and oxygen tension) as main effects, and 2) based on the post-hoc analysis evaluating the effects of individual culture conditions. Overall, the expression of all evaluated paracrine factors were modulated by the different microenvironmental factors.

In terms of the main effects of the culture substrate, in the 11° 50 rpm study, culturing on the DAT coatings was shown to significantly enhance the expression of VEGF (2% O_2: $p<0.0001$, 20% O_2: $p<0.05$, **Figure 3.7B**, **Figure 3.8B**) and HGF ($p<0.01$, **Figure 3.7C**, **Figure 3.8C**) under both oxygen tensions, as well as the expression of angiogenin under 20% O_2 ($p<0.05$, **Figure 3.8A**). Similarly in the 11° 25 rpm study, the DAT coatings were shown to enhance the expression of VEGF under both oxygen tensions (2% O_2: $p<0.001$, 20% O_2: $p<0.0001$, **Figure 3.7B**, **Figure 3.8B**) and angiogenin under 20% O_2 ($p<0.001$, **Figure 3.8A**).

In terms of the main effects of dynamic culture, in the 11° 50 rpm study, culturing under dynamic conditions was shown to significantly enhance the expression of VEGF under 20% O_2 ($p<0.05$, **Figure 3.8B**) and the expression of HGF under 2% O_2 ($p<0.05$, **Figure 3.7C**). Similarly in the 11° 25 rpm study, culturing under dynamic conditions was shown to enhance the expression of VEGF under 20% O_2 ($p<0.001$, **Figure 3.8B**).

In terms of the main effects of oxygen tension, in the 11° 50 rpm study, culturing under 2% O_2 was shown to significantly enhance the expression of VEGF ($p<0.05$) and reduce the expression of HGF ($p<0.05$) as compared to culturing under 20% O_2. In the 11° 25 rpm study, culturing under 2% O_2 was shown to significantly enhance the expression of VEGF ($p<0.05$) and angiogenin ($p<0.01$) as compared to culturing under 20% O_2.

Consistent with the main effects analysis, the individual culture condition analysis also indicated that the secretion of VEGF and HGF were modulated by the culture microenvironment. Regarding VEGF secretion, in the 11° 50 rpm study, regardless of the oxygen level, VEGF secretion was significantly higher in samples cultured dynamically

on DAT coatings as compared to those cultured statically on TCPS ($p<0.05$). Further, under 2% O_2, VEGF secretion was significantly higher in samples cultured statically on DAT coatings as compared to those cultured either statically or dynamically on TCPS ($p<0.01$, **Figure 3.7B**). Similarly in the 11° 25 rpm study, regardless of the oxygen level, VEGF secretion was also higher in samples cultured statically on DAT coatings as compared to those cultured either statically or dynamically on TCPS ($p<0.01$). Additionally, under 20% O_2, VEGF secretion in samples cultured dynamically on TCPS was higher than those cultured statically on TCPS ($p<0.01$, **Figure 3.8B**). Furthermore, VEGF secretion in samples cultured dynamically on DAT coatings was significantly higher than all other groups ($p<0.05$).

HGF secretion was only significantly modulated by the cultured conditions in the 11° 50 rpm study. Under 2% O_2, HGF secretion was significantly higher in samples cultured dynamically on DAT coatings as compared to those cultured statically on TCPS ($p<0.01$, **Figure 3.7C**). Whereas under 20% O_2, HGF secretion was significantly higher in samples cultured statically on DAT coatings as compared to those cultured dynamically on TCPS ($p<0.05$, **Figure 3.8C**).

Angiogenin secretion was only significantly modulated by the cultured conditions in the 11° 25 rpm study under 20% O_2. More specifically, the samples cultured statically on DAT coatings had significantly higher levels as compared to those cultured statically on TCPS ($p<0.05$, **Figure 3.8A**).

Preliminary analysis of IL-6 secretion of ASCs from the two donors in the 5° 50 rpm study showed similar trends to the 11° 25 rpm study (**Supplementary Figure *5***). Based on the similarity of the findings (ASC growth and IL-6 secretion) to the other rocking conditions, it was decided that it would be more impactful to instead explore the effects of cytokine priming within the rocking bioreactor with a more focused set of culture conditions (11° 50 rpm).

In summary, the results demonstrated that varying microenvironmental factors can have combined effects on ASC paracrine factor secretion, with modulation of VEGF, HGF,

and angiogenin secretion observed under the conditions in the current study. The data suggests there may be interacting effects between the DAT coatings, dynamic culture, and oxygen tension, which contribute to the observed cellular response.

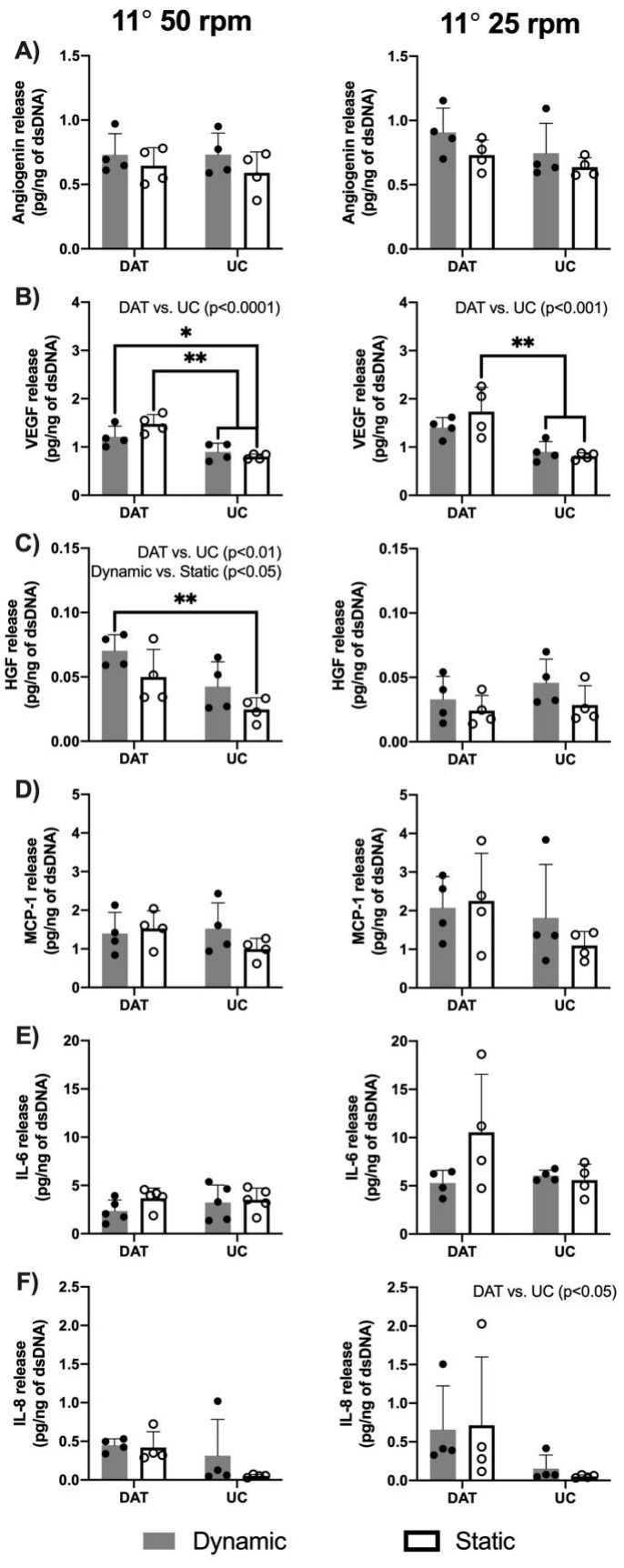
11° 50 rpm
11° 25 rpm
A)
Angiogenin release (pg/ng of dsDNA)
B)
VEGF release (pg/ng of dsDNA)
DAT vs. UC (p<0.0001)
DAT vs. UC (p<0.001)
C)
HGF release (pg/ng of dsDNA)
DAT vs. UC (p<0.01)
Dynamic vs. Static (p<0.05)
D)
MCP-1 release (pg/ng of dsDNA)
E)
IL-6 release (pg/ng of dsDNA)
F)
IL-8 release (pg/ng of dsDNA)
DAT vs. UC (p<0.05)
DAT
UC
Dynamic
Static

Figure 3.7 Under 2% O_2, culturing human ASCs for 7 days under dynamic conditions and/or on the DAT coatings altered VEGF and HGF secretion. Expression of A) Angiogenin, B) VEGF, C) HGF, D) MCP-1, E) IL-6 and F) IL-8, normalized to total dsDNA content. In the 11° 50 rpm study, culturing on the DAT coatings either dynamically or statically was shown to enhance VEGF secretion ($p<0.0001$). In addition, HGF secretion was significantly higher in the DAT coated group as compared to the uncoated group ($p<0.01$), as well as in the dynamic group as compared to the static group ($p<0.05$). In the 11° 25 rpm study, VEGF secretion was significantly higher in the samples cultured statically on the DAT coatings as compared to both uncoated groups ($p<0.001$). Further, main effects analysis showed that culturing on the DAT coatings significantly enhance the expression of IL-8 ($p<0.05$). Data analyzed using 2-way ANOVA and Tukey's multiple comparisons test. Error bars represent standard deviation (post-hoc test: *$p < 0.05$, **$p < 0.01$; n=2 replicate wells/trial, N=4 trials with different ASC donors, except IL-6 from the 11° 50 rpm experimental group: n=2 replicate wells/trial, N=5 trials with different ASC donors). Abbreviations: DAT, DAT coated; UC, uncoated TCPS.

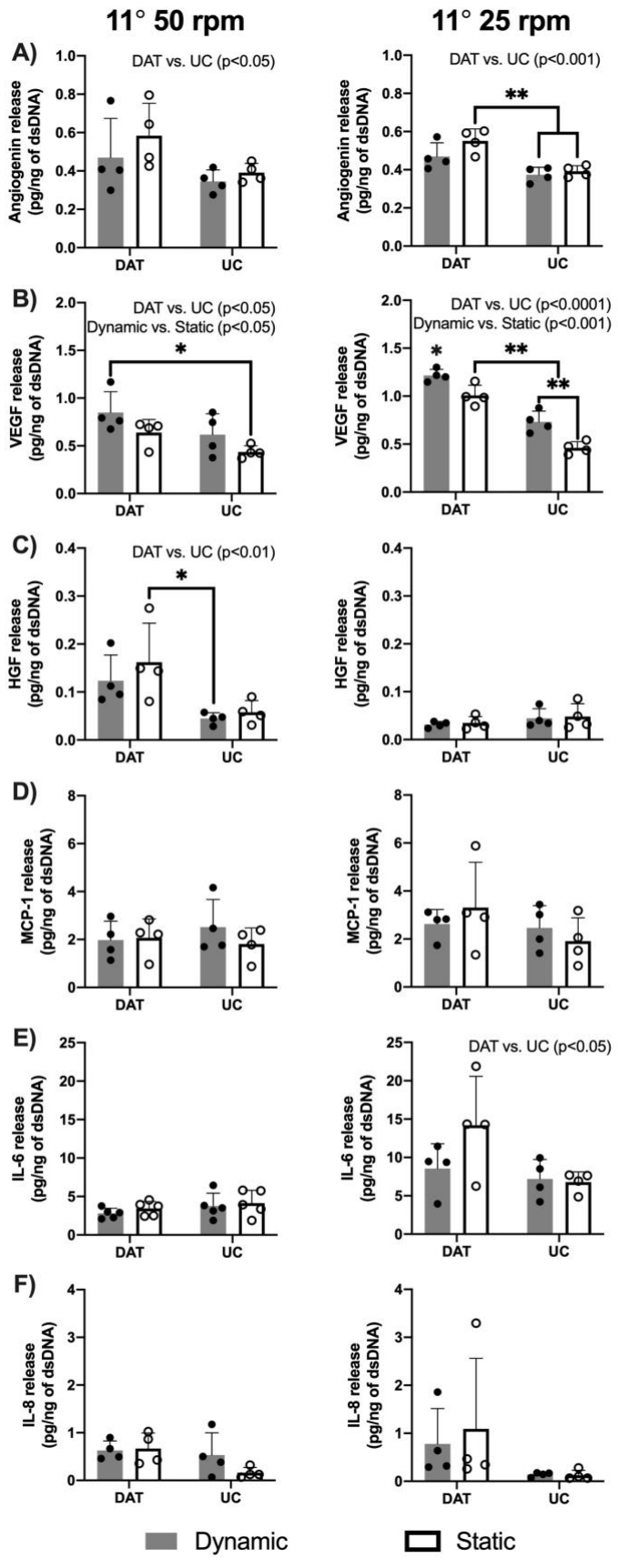
11° 50 rpm
11° 25 rpm
A)
DAT vs. UC (p<0.05)
DAT vs. UC (p<0.001)
Angiogenin release (pg/ng of dsDNA)
B)
DAT vs. UC (p<0.05)
Dynamic vs. Static (p<0.05)
DAT vs. UC (p<0.0001)
Dynamic vs. Static (p<0.001)
VEGF release (pg/ng of dsDNA)
C)
DAT vs. UC (p<0.01)
HGF release (pg/ng of dsDNA)
D)
MCP-1 release (pg/ng of dsDNA)
E)
DAT vs. UC (p<0.05)
IL-6 release (pg/ng of dsDNA)
F)
IL-8 release (pg/ng of dsDNA)
DAT
UC
Dynamic
Static

Figure 3.8 Under 20% O_2, culturing human ASCs for 7 days under dynamic conditions and/or on the DAT coatings altered angiogenin, VEGF and HGF secretion. Expression of A) Angiogenin, B) VEGF, C) HGF, D) MCP-1, E) IL-6 and F) IL-8, normalized to total dsDNA content. In the 11° 50 rpm study, culturing on the DAT coatings either dynamically or statically was shown to enhance angiogenin ($p<0.05$) and HGF secretion ($p<0.01$). In addition, VEGF secretion was significantly higher in the DAT coated group as compared to the uncoated group ($p<0.05$), as well as in the dynamic group as compared to the static group ($p<0.05$). In the 11° 25 rpm study, angiogenin secretion was significantly higher in the samples cultured statically on the DAT coatings as compared to both uncoated groups ($p<0.01$). VEGF secretion was significantly higher in the DAT coated group as compared to the uncoated TCPS group ($p<0.0001$), as well as in the dynamic group as compared to the static group ($p<0.001$). Further, main effects analysis showed that culturing on the DAT coatings significantly enhanced the expression of IL-6 ($p<0.05$). Data analyzed using 2-way ANOVA and Tukey's multiple comparisons test. Error bars represent standard deviation (post-hoc test: *$p < 0.05$, **$p < 0.01$; n=2 replicate wells/trial, N=4 trials with different ASC donors, except IL-6 from the 11° 50 rpm experimental group: n=2 replicate wells/trial, N=5 trials with different ASC donors). Abbreviations: DAT, DAT coated; UC, uncoated TCPS.

3.4 IDO expression was induced by TNF-α and IFN-γ priming

Immunostaining was performed to qualitatively assess whether priming with TNF-α and IFN-γ induced IDO expression, as expected based on previous literature reports [193] (**Figure 3.9**). With priming, uniform expression of IDO was observed in the ASCs regardless of the culture conditions. In contrast, IDO expression was not detected in any of the non-primed controls.

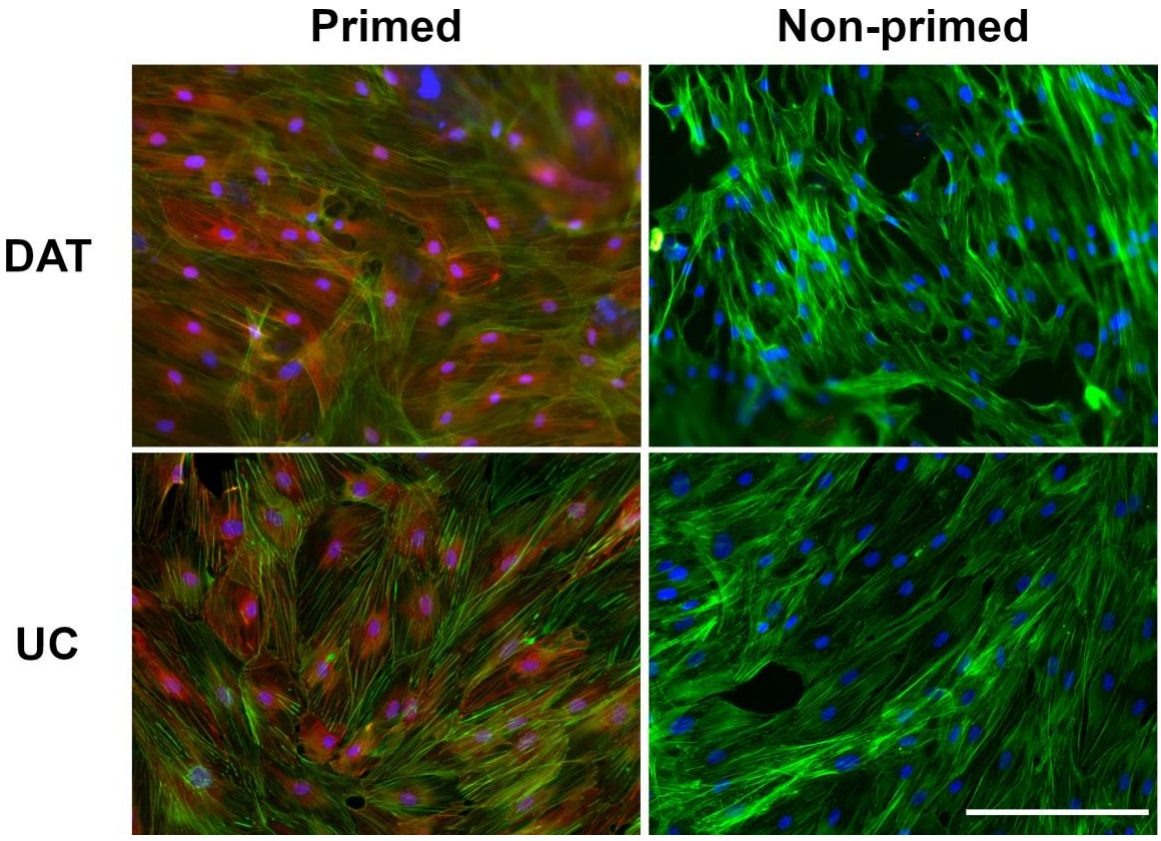

Figure 3.9 IDO expression was upregulated in human ASCs after 48 h of priming with the pro-inflammatory cytokines TNF-α and IFN-γ. Representative images shown of the ASCs cultured under dynamic 20% O_2 conditions showing IDO (red), F-actin (green) and nuclei (blue), at the end of the 7-day total culture period, with priming for the final 48 h. Expression of IDO was observed in all primed samples (n=1 replicate well/trial, N=2 trials with different ASC donors). Scale bar represents 200 μm. No primary antibody control: Supplementary Figure 3.7.

ELISA was then performed to quantitatively evaluate the effects of cytokine priming under the various culture conditions on the levels of secreted IDO present in conditioned media samples. IDO was not detected in the media of any of the non-primed samples. Under 20% O_2, significantly higher levels of IDO were detected in the media when the cells were cultured on TCPS as compared to those cultured on the DAT coatings ($p<0.05$) (**Figure 3.10**).

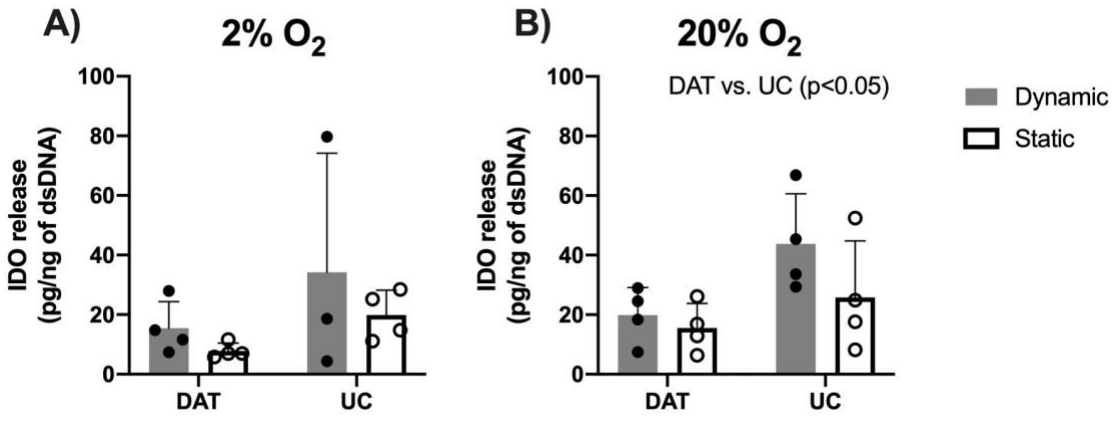

Figure 3.10 Priming with TNF-α and IFN-γ on the DAT coatings altered IDO secretion under 20% O_2. Expression of IDO measured by ELISA in samples cultured under A) 2% O_2 or B) 20% O_2 with result normalized to total dsDNA content. Main effects analysis showed that under 20% O_2, culturing on the DAT coatings significantly altered IDO secretion ($p<0.05$). Expression of IDO in the non-primed samples was not detectable. Data analyzed using two-way ANOVA and Tukey's multiple comparisons test. Error bars represent standard deviation (n=2 replicate wells/trial, N=3-4 trials with different ASC donors).

3.5 Priming with TNF-α and IFN-γ and dynamic culture significantly enhanced IL-6 and IL-8 secretion in the human ASCs

To quantitatively evaluate the combined effects of cytokine priming and the other microenvironmental factors on the expression levels of a range of pro-angiogenic and immunomodulatory proteins in the ASC-conditioned media, Luminex® assays were performed to compare the protein secretion levels of angiogenin, VEGF, HGF, MCP-1, and IL-8, and ELISAs were performed to compare the protein secretion levels of IDO and IL-6 in cell culture supernatant after 7 days of culture with or without the addition of 10 ng/mL TNF-α and 100 ng/mL IFN-γ for the final 48 h of culture. A heatmap of the results is shown in **Figure 3.11**, with red corresponding to a higher level and blue corresponding to a lower level detected within the conditioned media samples.

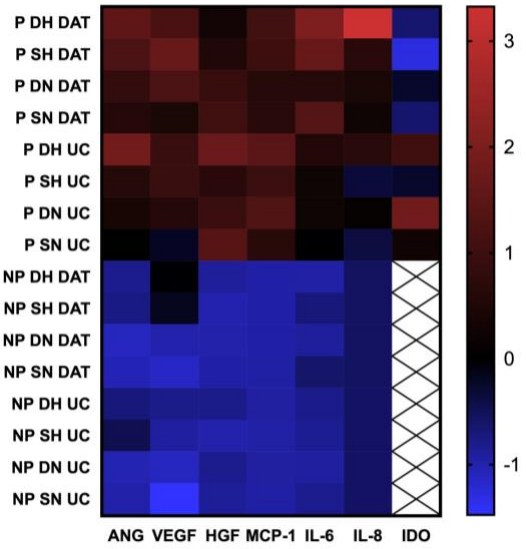

Figure 3.11 ASC paracrine factor secretion was modulated by the varying microenvironmental factors, with higher levels of the factors generally detected with cytokine priming. Levels of secreted angiogenin, VEGF, HGF, MCP-1, IL-6, IL-8, and IDO detected in conditioned media samples shown on a coloured heatmap with red as the highest value and blue as the lowest value. The colours represent z-score normalized average concentrations (normalized to total dsDNA content). n=2 replicate wells/trial, N=3-4 trials with different ASC donors. Abbreviations: ANG, angiogenin; P, primed; NP, non-primed; D, dynamic; S, static; H, hypoxia; N, normoxia; DAT, DAT coated; UC, uncoated TCPS.

Based on main effects analysis by repeated measures 2-way ANOVA, the expression levels of angiogenin, VEGF, HGF, MCP-1, IL-6, and IL-8 were significantly higher in the primed samples as compared to the non-primed samples under both oxygen levels (**Figure 3.12**, **Figure 3.13**). Under 2% O_2 with cytokine priming (**Figure 3.12**), culturing dynamically on the DAT coatings was shown to significantly enhance the expression of IL-6 as compared to the uncoated groups ($p<0.05$, **Figure 3.12E**). Similarly, culturing statically on the DAT coatings was shown to significantly enhance the expression of IL-6 as compared to the statically-cultured uncoated group ($p<0.01$). Further, culturing dynamically on the DAT coatings was shown to significantly augment the expression of IL-8 as compared to all other groups ($p<0.01$, **Figure 3.12F**). Under 20% O_2 with cytokine priming, culturing on the DAT coatings statically ($p<0.01$) or dynamically ($p<0.001$) was shown to significantly increase the expression of IL-8 as compared to the statically cultured uncoated group (**Figure 3.13F**).

In summary, the results demonstrated a significant upregulation of all analyzed factors following TNF-α and IFN-γ priming. Under priming, the varying microenvironmental factors can again have combined effects on ASC paracrine factor secretion, in particular on IL-6 and IL-8 secretion. Interestingly, compared to the initial study of the microenvironmental factors, oxygen tension had less of an effect in the primed samples.

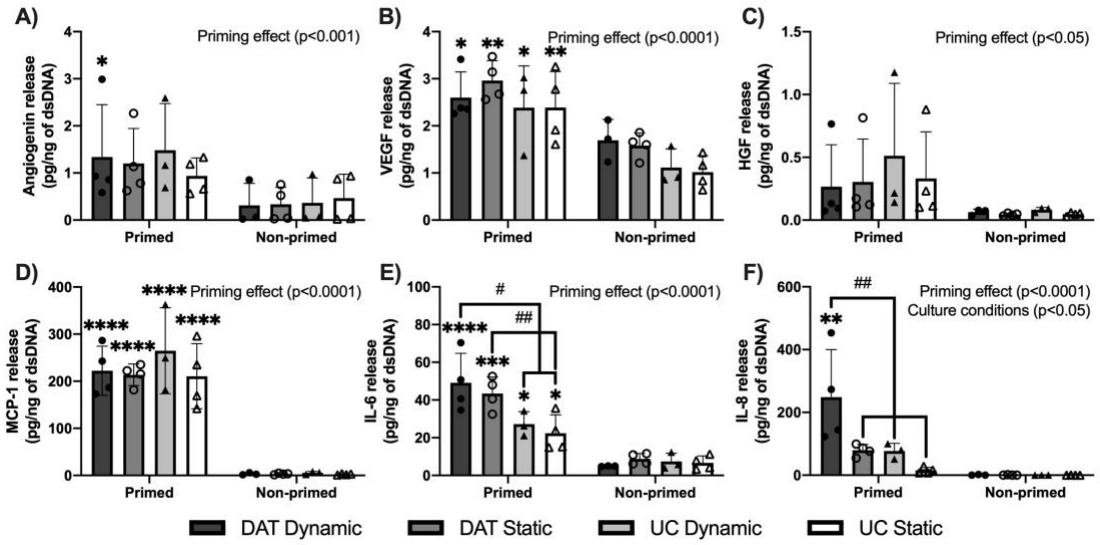

Figure 3.12 Priming with TNF-α and IFN-γ significantly enhanced the secretion of all tested paracrine factors in the human ASCs cultured under 2% O_2. Expression of A) Angiogenin, B) VEGF, C) HGF, D) MCP-1, E) IL-6 and F) IL-8, normalized to total dsDNA content. Cytokine priming, as a main effect, significantly enhanced the expression of angiogenin ($p<0.001$), VEGF ($p<0.0001$), HGF ($p<0.05$), MCP-1 ($p<0.0001$), IL-8 ($p<0.0001$), and IL-6 ($p<0.0001$). IL-6 secretion was significantly higher in the samples cultured dynamically on the DAT coatings as compared to both uncoated groups ($p<0.05$). IL-8 secretion was significantly higher in the samples cultured dynamically on the DAT coatings as compared to all other conditions ($p<0.01$). The effects of the four different culture conditions on IL-8 secretion were significantly different ($p<0.05$). Sidak's multiple comparisons: *$p<0.05$, **$p<0.01$, ***$p<0.001$, ****$p<0.0001$ = significant difference between the primed and the non-primed sample under the same culture condition. Tukey's multiple comparisons: #$p<0.05$, ##$p<0.01$ = significant difference between the primed samples under different culture conditions. Data analyzed using repeated measures 2-way ANOVA model, Tukey's and Sidak's multiple comparisons test. Error bars represent standard deviation (n=2 replicate wells/trial, N=3-4 trials with different ASC donors). Abbreviations: DAT, DAT coated; UC, uncoated TCPS; P, primed; NP, non-primed.

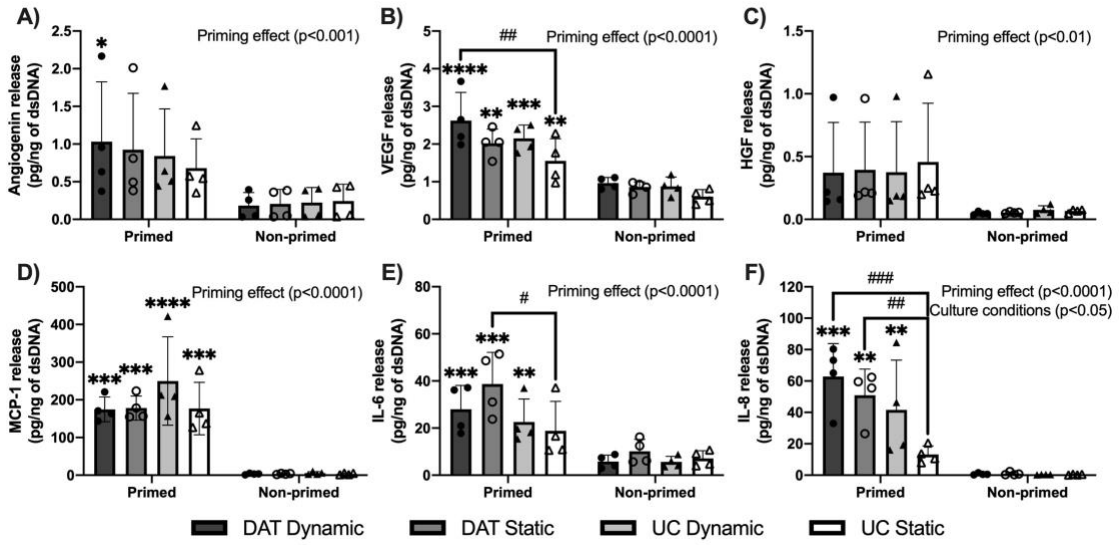

Figure 3.13 Priming with TNF-α and IFN-γ significantly enhanced the secretion of all tested paracrine factors in the human ASCs cultured under 20% O_2. Expression of A) Angiogenin, B) VEGF, C) HGF, D) MCP-1, E) IL-6 and F) IL-8, normalized to total dsDNA content. Cytokine priming, as a main effect, significantly enhanced the expression of angiogenin ($p<0.001$), VEGF ($p<0.0001$), HGF ($p<0.01$), MCP-1 ($p<0.0001$), IL-8 ($p<0.0001$), and IL-6 ($p<0.0001$). IL-8 secretion was significantly higher in the samples cultured on the DAT coatings as compared to the uncoated groups ($p<0.05$). The effects of the four different culture conditions on IL-8 secretion were significantly different ($p<0.05$). Sidak's multiple comparisons: *$p<0.05$, **$p<0.01$, ***$p<0.001$, ****$p<0.0001$ = significant difference between the primed and the non-primed sample under the same culture condition. Tukey's multiple comparisons: #$p<0.05$, ##$p<0.01$, ###$p<0.001$ = significant difference between the primed samples under different culture conditions. Data analyzed using repeated measures 2-way ANOVA model, Tukey's and Sidak's multiple comparisons test. Error bars represent standard deviation (n=2 replicate wells/trial, N=3-4 trials with different ASC donors). Abbreviations: DAT, DAT coated; UC, uncoated TCPS; P, primed; NP, non-primed.

Chapter 4

4 Discussion

The therapeutic potential of adipose-derived stromal cells (ASCs) has been studied extensively and proven in many disease models and early phase clinical studies. It is well established that ASCs are capable of differentiating into various cell types and more importantly, secreting a variety of pro-regenerative paracrine factors that can stimulate angiogenesis, modulate the immune response, and control inflammation [198]. Despite demonstrating promising therapeutic effects, several limitations may hinder the use of ASCs in clinical applications, including the need for large numbers of cells and the subsequent problems that come with long-term *in vitro* expansion, such as loss of phenotype and differentiation capacities [199]. In addition, loss of therapeutic potentials due to aging, chronic disease, and obesity may also reduce the efficacy of autologous ASC therapy [29].

In search of more effective *in vitro* expansion methods that can augment the regenerative capacity of ASCs, many preconditioning strategies have been proposed, including decellularized adipose tissue (DAT) culture substrates [141], [142], [200], hypoxia [96], [201], mechanical stimulation or dynamic culture [95], [144], and pro-inflammatory cytokine priming [118], [119], [202]. Further, bioreactors represent a promising *in vitro* cell expansion platform that can incorporate one or more preconditioning strategies. To explore the potential of combining dynamic culture, hypoxia, and DAT scaffolds as a strategy to enhance human ASC expansion and pro-regenerative function, Dr. Tim Han from the Flynn Lab developed a DAT scaffold-based perfusion bioreactor [188], [189]. Dynamic culturing of human ASCs in the perfusion bioreactor system under hypoxia was shown to be effective at increasing the density of ASCs on the DAT scaffolds, with improved capacity to support blood vessel formation and adipose tissue remodeling *in vivo* [188]. In addition, shear stress introduced by perfusion was shown to alter the ASC phenotype and paracrine profile, with *in vivo* findings demonstrating a more pro-regenerative host macrophage response in the dynamically cultured ASC-seeded DAT implants [189].

Overall, the perfusion bioreactor studies demonstrated promising preconditioning effects of dynamic culture on enhancing ASC expansion and modulating ASC phenotype and paracrine factor secretion. However, limitations of the system, such as complexity of the setup and the non-uniform distribution of ASCs in the scaffold, were also evident [188], [189]. These issues suggested the need for a more scalable bioreactor system capable of introducing a more uniform preconditioning effect on ASCs. In particular, a rocking bioreactor system was considered a suitable alternative as it has been successfully implemented in *in vitro* culture and expansion of human pluripotent stem cells [203], human bone marrow-derived mesenchymal stromal cells (BM-MSCs) [204], chondrocytes [205], lymphocytes [206], and chimeric antigen receptor (CAR)-T cells [207].

Mechanical stimulation is a culture strategy that has been mainly used to enhance the proliferation and differentiation capacities of MSCs towards the osteogenic [166], [168], [169] and chondrogenic lineages [162]–[164]. Recently, the effects of shear stress and tensile strain on MSC paracrine functions have also been explored. In particular, shear stress has been shown to enhance pro-angiogenic factor secretion by human ASCs [172], [173], as well as modulating the ability of human BM-MSCs to suppress tumor necrosis factor-alpha (TNF-α) secretion by activated immune cells [174], [175]. The magnitude and pattern of the shear stress, as well as the duration of exposure used in these studies, were quite diverse, and little is known about how these factors can affect the cell response.

The magnitude of shear stress studied in the literature ranges from hemodynamic fluid flow shear (e.g. 10 dyn/cm^2 [172], [173], 15 dyn/cm^2 [174], [175]) to low level or interstitial fluid flow shear (0.5 dyn/cm^2 [146], [176], 0.018-0.024 dyn/cm^2 [208]), with different shear patterns such as laminar, pulsatile, or oscillatory. Overall, the duration of exposure to shear stress used in the literature was typically short, ranging from a few hours [175] to up to 4 days [173], or even as short as 10 minutes [172]. The selection of a short culture period could be due to the high magnitude of shear stress used in these studies, as long-term exposure to high magnitude of shear stress may affect cell attachment.

The current thesis is one of the first to explore how longer-term exposure (up to 7 days) of lower-level fluid shear stress (0.04-0.3 dyn/cm^2) influences ASC proliferation and paracrine factor secretion. It is important to acknowledge that the rocking bioreactor introduces non-uniform and oscillatory shear stress, unlike many studies in the literature that have explored the effects of laminar and unidirectional flow [172], [173], [175], [176], [208]. While unidirectional flow would be more relevant when trying to mimic the physiological shear stresses experienced by cell types within the body, it is unclear what type of shear stress stimulation would be most effective for preconditioning strategies targeting paracrine functionality. Further investigation of the cell response under different shear stress patterns and magnitudes is warranted to identify the bioreactor conditions that will be most effective for promoting a pro-regenerative ASC phenotype.

Hypoxia is a well-established preconditioning strategy for culturing MSCs mainly due to its ability to modulate pro-angiogenic paracrine activity of MSCs through hypoxia inducible factor-1α (HIF-1α) mediated vascular endothelial growth factor (VEGF) secretion [110]. In addition to being demonstrated to promote ASC expansion and modulate ASC phenotype within DAT scaffolds in our lab's previous perfusion bioreactor studies [188], hypoxia has also been shown to promote MSC-mediated endothelial cell proliferation and tube formation [57], [114], [209]. Although a wide range of oxygen concentrations have been used in hypoxia studies, the physiologically relevant level of oxygen concentration in adipose tissue normally ranges from 2–8%, with 2% simulating poorly-vascularized fat [107]. To simulate the pathological or post-surgery cell environment in *in vitro* expansion, 2% O_2 was selected as the hypoxic environment for the current study.

In an effort to characterize the effects of the culture microenvironment on ASC growth in the rocking bioreactor, nuclear and F-actin staining was performed to quantify the cell density and assess cell morphology after 3 days or 7 days of culture. Overall, the results demonstrated that the growth and expansion of ASCs were well supported in the bioreactor under all culture conditions. Interestingly, the study also revealed that the normoxic environment (20% O_2) better supported ASC expansion as indicated by the higher cell density at day 7. Hypoxia is generally thought to enhance ASC or MSC

proliferation [102], [210]–[212]. However, there are conflicting reports in the literature. For example, Frazier *et al.* reported no significant effects of a 72 h exposure to 5% O_2 on human ASC viability and proliferation [213]. Similarly, Jiang *et al.* also reported no effects of hypoxia (1% O_2) on ASC proliferation over 7 days [214]. Other studies have also suggested an inhibitory effect of hypoxia on ASC or MSC proliferation [215]–[217]. Holzwarth *et al.* reported that human BM-MSCs cultured under 1%, 3%, or 5% O_2 showed reduced proliferation after a 7-day culture period in platelet lysate supplemented media relative to those cultured under 21% O_2 [217]. From these studies, it appears that there are several factors that could affect cell proliferation under hypoxia, including the cell type, oxygen concentration, the duration of exposure, and the culture media composition. An additional limitation to note in the current study was that more extensive media evaporation was observed in the hypoxic station due to the regular injection of dry gases to maintain the 2% O_2 level, which may have impacted cell growth to some extent.

The 11° 50 rpm cell density study also indicated that the DAT coatings resulted in a significantly higher cell density at day 7 under 20% O_2. Similarly, previous studies from the Flynn Lab have also demonstrated that DAT substrates can improve ASC proliferation [140], [141]. In particular, Shridhar *et al.* suggested that the fibrous tissue-like structure and extracellular matrix (ECM) composition of the DAT coatings can contribute to enhanced ASC proliferation [140]. In the current study, it is worth noting that the effects of DAT were not observed in the 11° 25 rpm study, which may be due to variability in the coatings coming from the differences in the donors used for the source materials.

The effect of shear stress on ASC proliferation is not well studied. Although shear stress was found to not significantly affect ASC density at day 7 in the current study, others have demonstrated differences in proliferation patterns between shear stress-stimulated ASCs and statically-cultured ASCs. For example, Elashry *et al.* showed that a 10-day exposure of fluid shear stress (oscillatory, 0.77 dyn/cm^2) increased proliferation of equine ASCs compared to static conditions [218]. Interestingly, another study by Kim *et al.* reported that the ASC proliferation rate was related to the level of shear stress [208]. By comparing three regions in a microfluidic device with a shear stress gradient, the group

revealed that human ASCs cultured in the lower shear stress region (0.018 dyn/cm^2) exhibited a higher proliferation rate compared to those in the higher shear stress region (0.024 dyn/cm^2). In addition, they also revealed a morphological change in the ASCs in relation to the level of shear stress, with a long and thin cell shape observed in the lower shear stress region and stronger staining for actin structures observed in the higher shear stress region. On the topic of cell morphology, a study by Kuo *et al.* reported a directional reorganization of F-actin in human BM-MSCs after being exposed to 1-hour of unidirectional flow with oscillatory shear (0.5 ± 4 dyn/cm^2) [146]. In the current study, the lack of obvious morphological changes in the ASCs cannot be well explained, but the difference in the type of shear stress applied (oscillatory or unidirectional) may have contributed to the different results. In addition, there may have been greater differences in the regions outside of the coverslip that was analyzed, where the cells would have been subjected to higher levels of shear stress.

In order to evaluate the effects of the culture microenvironment on ASC phenotype in the rocking bioreactor, immunostaining of inducible nitric oxide synthase (iNOS) was performed after 3 days or 7 days of culture. Although iNOS is commonly regarded as a classically activated M1 pro-inflammatory macrophage marker [195], its expression in MSCs has recently been shown to play a critical role in mediating MSC immunosuppression [196], [197]. Previous work by Dr. Tim Han with the perfusion bioreactor also suggested a possible link between dynamic culture under shear stress and enhanced iNOS in ASCs cultured in 3-dimentional (3D) DAT scaffolds [189]. In the current study, no notable difference in iNOS expression was observed between any of the groups. This may be due to the different level of shear stress introduced in the system, as well as structural differences in the DAT based on the different scaffold formats applied.

Several studies have suggested that human MSCs and mouse MSCs utilize different mediators in their immunosuppression, with indoleamine 2,3-dioxygenase (IDO) being used in human and iNOS used in mouse [67], [197], [219]. For example, significantly upregulated IDO levels were reported in human MSCs upon inflammatory cytokine stimulation with interferon gamma (IFN-γ) and tumor necrosis factor alpha (TNF-α), while iNOS levels remained low [219]. However, a research group led by Manochantr *et*

al. reported that iNOS is indeed involved in the immunosuppressive capacity of human MSCs and argued that IFN-γ may not be a key stimulator of iNOS in human MSCs [220], [221]. They also demonstrated an impaired T-cell immunosuppression effect of human MSCs when iNOS activity was inhibited by N-nitro-L-arginine methyl ester (L-NAME) [221]. Overall, these studies support the use of iNOS as a potential indicator of human ASCs with a more pro-regenerative secretory phenotype. However, further characterization is needed to more fully understand the role of iNOS in human MSC immunomodulatory activities.

To further assess how culturing in the varying microenvironments altered the paracrine profile of ASCs, Luminex assays and enzyme-linked immunosorbent assays (ELISA) were performed to evaluate the secretion levels of angiogenin, vascular endothelial growth factor (VEGF), hepatocyte growth factor (HGF), monocyte chemoattractant protein-1 (MCP-1), interleukin 6 (IL-6), and interleukin 8 (IL-8) in conditioned media samples collected after a 7-day culture period, with media conditioning for the final 48 h. Comparing between the DAT coated group and the uncoated tissue culture polystyrene (TCPS) group, the pro-angiogenic factors VEGF, HGF (11° 50 rpm only), and angiogenin (20% O_2 only) were detected at significantly higher levels in the DAT coated groups. This result is in line with the enhanced angiogenic factor secretion of human fibroblasts when cultured in DAT bioscaffolds as compared to collagen scaffolds, as demonstrated by Dr. Pascal Morissette Martin from the Flynn lab [143]. Similarly, as demonstrated by another research group, the addition of DAT powder to human ASC cultures increased their secretion of a range of growth factors including VEGF and HGF, with the expression levels gradually increasing over 48 h [222].

Regarding dynamic culture and shear stress stimulation, the current study demonstrated that the secretion of VEGF (20% O_2) and HGF (11° 50 rpm, 2% O_2) were upregulated in the dynamically cultured groups. Similarly, Bassaneze *et al.* also demonstrated a shear stress induced nitric oxide (NO)-dependent VEGF accumulation in human ASC conditioned media with an increasing production rate over a 96-h shear stress exposure (unidirectional, 10 dyn/cm^2) [173]. In addition, Bravo *et al.* also reported increased secretion of VEGF and HGF along with other pro-angiogenic factors by ASCs that were

exposed to 10 min of shear stress (unidirectional and intermittent, 10 dyn/cm^2) compared to statically cultured controls [172]. Regarding the pro-angiogenic functionalities of shear stress-stimulated ASCs (unidirectional, 0.5 dyn/cm^2, 30 min), Chen *et al.* reported improved viability of human endothelial cells from oxidative damage when cultured with shear stress-stimulated ASC conditioned media as compared to statically cultured ASC conditioned media controls [176].

In the current study, considering the combined effects of shear stress and hypoxia, an interesting secretion pattern of VEGF can be observed that is somewhat aligned with the Bravo *et al.* study, which revealed that shear stress and hypoxia had opposite effects on human ASC pro-angiogenic factor secretion [172]. More specifically, it was reported that shear stress and hypoxia each independently enhanced ASC pro-angiogenic capacities via cyclooxygenase-2 (COX-2)-dependent mechanism. However, when shear stress and hypoxia were combined, VEGF secretion was significantly reduced compared to introducing hypoxia alone. This result may partially explain why dynamic culture only significnatly enhanced VEGF secretion under 20% O_2 in the current study.

Pro-inflammatory cytokine priming is another widely investigated preconditioning strategy to enhance the immunomodulatory functionalities of MSCs. As mentioned above, IDO is a key factor in MSC-mediated immunosuppression, and its expression is induced through inflammatory stimulations [223]. In addition to being able to suppress T-cell proliferation, IDO enzymatic activity is capable of inhibiting natural killer (NK) cell proliferation and supporting monocyte differentiation into alternatively-activated M2 anti-inflammatory macrophages [69]. In the current study, no IDO expression was observed in the non-primed group as expected, but there was strong expression observed in all primed samples. Follow-up ELISA characterization of secreted IDO indicated that expression was significantly lower in the DAT coated groups compared to the uncoated groups under 20% O_2. In contrast to our findings, studies that utilized collagen or collagen composites as MSC culture substrate have demonstrated enhanced IDO secretion, as well as intracellular IDO enzymatic activity [224], [225]. This discrepancy warrants further investigation of the intracellular IDO level of ASCs cultured in the rocking bioreactor system under priming.

Under IFN-γ and TNF-α priming, elevated MSC secretion of VEGF, HGF, IL-6, and IL-8 have been reported [226]–[228]. Although little is known about the effect of IFN-γ and TNF-α priming on MSC secretion of angiogenin and MCP-1, they are also expected to be upregulated due to the autocrine ability of VEGF to regulate angiogenin and MCP-1 synthesis [227]. In the current study, the expression levels of all tested cytokines were significantly upregulated in the primed groups as expected based on main effects analysis. Interestingly, the immunomodulatory factors MCP-1, IL-6 and IL-8 were upregulated far more by priming than the angiogenic factors angiogenin, VEGF, and HGF. This phenomenon has not been explicitly reported in the literature, which warrants further investigation of the mechanism behind the upregulation of these paracrine factors under the effect of priming.

To the best of our knowledge, this is the first study to evaluate ASC paracrine activities under different culture conditions in combination with IFN-γ and TNF-α priming. Under both oxygen tensions, the immunomodulatory factors IL-6 and IL-8 were secreted at significantly different levels under the varying culture conditions. Interestingly, in contrast, the pro-angiogenic factors VEGF, HGF, and angiogenin were the most affected by the different culture conditions in the original study without priming. Although generally regarded as a pro-inflammatory cytokine, IL-6 is involved in many aspects of the immunoregulatory activities of MSCs, including promoting the polarization of macrophages towards an alternatively-activated M2-like phenotype [229], [230], inhibiting monocyte differentiation towards dendritic cells [231], and supporting the production of prostaglandin E2 (PGE2) and NO [72]. IL-8 on the other hand plays a key role in MSC-mediated endothelial progenitor cell homing and angiogenesis [232].

Overall, the results from the current study suggest that the culture microenvironment can be tuned to mediate ASC immunomodulatory factor secretion within an inflammatory culture environment. In particular, culturing dynamically on the DAT coatings was associated with higher expression levels of IL-6 and IL-8. Building from these findings, functional assays should be performed to more fully understand the roles of IL-6 and IL-8 in ASC-mediated immunomodulation and angiogenesis.

Chapter 5

5 Conclusions and future directions

5.1 Summary and significance

The present study investigated the effects of the culture microenvironment on adipose-derived stromal cell (ASC) proliferation and pro-angiogenic and immunomodulatory paracrine factor secretion in the context of a novel rocking bioreactor system. The specific microenvironmental factors investigated were oxygen tension, decellularized adipose tissue (DAT) culture substrates, dynamic culture as a form of shear stress stimulation, and pro-inflammatory cytokine priming.

In the first aim, the rocking bioreactor system was developed based on a preliminary design by Dr. Tim Han of the Flynn lab, with modifications to the culture vessel and rocking platform. A computational model of the fluid shear stress introduced in the system was developed to aid the selection of rocking conditions for subsequent studies. Overall, the system is capable of introducing low-level oscillatory fluid shear stress (~0.04-0.3 dyn/cm^2), along with enabling culture on the DAT coatings and within a hypoxic culture environment (2% O_2). To evaluate how different culture conditions could affect ASC growth and regenerative phenotype, immunostaining of the cell nucleus and inducible nitric oxide synthase (iNOS) was performed after 3 and 7 days of culture. Overall, the results suggested that ASC growth was supported by the system under all culture conditions, with no obvious differences in phenotype based on similar levels of iNOS expression and cell morphology across all groups.

In the second aim, to further assess how culturing in the varying microenvironments altered the paracrine profile of ASCs, Luminex assays and enzyme-linked immunosorbent assays (ELISA) were performed to evaluate the secretion levels of angiogenin, vascular endothelial growth factor (VEGF), hepatocyte growth factor (HGF), monocyte chemoattractant protein-1 (MCP-1), interleukin 6 (IL-6), and interleukin 8 (IL-8) in ASC conditioned media. The effects of the three microenvironmental factors, namely culture substrate, dynamic culture, and oxygen tension, were analyzed

individually. Culturing on DAT coatings was found to enhance the secretion VEGF, HGF (11° 50 rpm only), and angiogenin (20% O_2 only). Next, dynamic culture was found to enhance the secretion VEGF (20% O_2 only) and HGF (11° 50 rpm, 2% O_2 only). Finally, hypoxia enhanced the secretion of VEGF and angiogenin (11° 25 rpm only) and reduced the secretion of HGF (11° 50 rpm only). Interestingly, similar to what was reported by Bravo *et al.* [172], the enhancing effect of dynamic culture on VEGF secretion seems to be abolished or even reversed under the effect of hypoxia. Similar trends may be found in the secretion levels of other pro-angiogenic factors, but analysis of additional donors would be needed to assess whether there are statistically significant differences between any of the groups. Overall, the results from the second aim demonstrated that culturing in the varying microenvironments affected the secretion of the pro-angiogenic paracrine factors VEGF, HGF, and angiogenin.

In the third aim, pro-inflammatory cytokine priming with interferon gamma (IFN-γ) and tumor necrosis factor alpha (TNF-α) was incorporated as an additional culture microenvironmental factor. To confirm the effects of cytokine priming, immunostaining and ELISA were performed to assess the intracellular expression and secretion of indolamine 2, 3 dioxygenases (IDO), respectively. As expected, no expression of IDO was detected in the non-primed samples. Notably, the secretion level of IDO was significantly higher in the uncoated groups compared to the DAT coated group. Again, to evaluate how cytokine priming and the other three microenvironmental factors altered the paracrine profile of ASCs, Luminex assays and ELISA were performed to evaluate the secretion levels of angiogenin, VEGF, HGF, MCP-1, IL-6, and IL-8 in ASC conditioned media. Overall, the results demonstrated a significant upregulation of all analyzed factors following TNF-α and IFN-γ priming. Interestingly, the addition of the priming effect resulted in a different pattern of paracrine secretion as compared to the results from the second aim, with the immunomodulatory factors IL-6 and IL-8 being most affected by culturing in the varying microenvironments.

Taken together, the present study contributed to better understanding the roles of the cell microenvironment, including extracellular matrix (ECM) composition, oxygen tension, mechanical stimulation, and cytokine priming, in modulating paracrine factor secretion

by human ASCs. As there is a very limited number of studies in the literature that have investigated the combined effects of various cell microenvironmental factors, this study provides a valuable starting point for future exploration of this interesting research topic. Through further testing and development, the proposed culture system could potentially serve as an effective, easily translatable, and scalable platform for preconditioning human ASCs to enhance their pro-regenerative functionality for potential clinical usage.

5.2 Limitations and future directions

The studies discussed in this thesis provided important insights into how the proposed rocking bioreactor system can be used for human ASC expansion while providing a platform for learning about the roles of ECM composition, dynamic culture and mechanical stimulation, oxygen tension, and pro-inflammatory cytokine priming. Based on the findings from these studies, future work should focus on exploring the functionalities and biological relevance of the effects identified.

While the rocking bioreactor system showed promising results, there are some inherent limitations in the design that must be acknowledged. As found in the literature, various magnitudes and types of shear stress have been applied for MSC preconditioning, most of which are magnitudes higher than what was used in the current study. Therefore, exploring higher levels of shear stress (e.g., 10 dyn/cm^2 [174], [175]) may be an interesting future direction to consider, as well as comparing the biological effects of unidirectional versus oscillatory flow. Based on the results of the computational model, the cells in the centre of the well were expected to only experience a mild change in the magnitude of shear stress, while the cells near the edge of the plate experienced a much more drastic change. With the current setup analyzing the square coverslip within central region of the wells, the results from the immunohistochemical studies may only be representative of cells experiencing mild changes in shear stress, which may have contributed to the lack of differences in cell density, morphology, and iNOS expression between the groups. In the future, it would be worthwhile to assess whether the non-uniform oscillatory shear stresses applied lead to variability in the cell density and/or phenotype across the entire plate, particularly at the edges of the wells where the cells were subjected to the highest shear forces.

Based on the findings from the second aim, where pro-angiogenic paracrine factors were predominantly modulated by the varying microenvironmental factors, future studies should include pro-angiogenic secretome functional assays to verify that the preconditioning has biological effects on ASC-mediated angiogenesis. *In vitro* assays, such as human microvascular endothelial cell (HMVEC) tubule formation and proliferation assays, would be recommended as a starting point to further understand the effects of the different microenvironmental factors on the pro-angiogenic capacity of the ASC secretome [233].

Based on the findings from the third aim, where immunomodulatory paracrine factors were predominantly modulated by the varying microenvironmental factors, future studies could include immunomodulatory secretome functional assays, such as a peripheral blood mononuclear cell (PBMC)-derived macrophage polarization assay [234] or T-cell immunosuppression assay [235], to evaluate the biological relevance of the observed changes in the paracrine secretion profile. In addition, to further characterize the effects of priming on intracellular IDO expression, future studies should include Western blot to quantitatively evaluate the intracellular expression level of IDO or the l-kynurenine assay to measure the enzymatic activity of IDO [116].

Overall, considering human ASC heterogeneity [91] and the number of variables explored, the sample size of the current studies was relatively small, which may introduce variation in the data and limit the statistical power. In particular, exploring a more focused set of variables in studies from the third aim with a higher number of cell donors would be recommended.

For future work, the functionality of the elevated angiogenin, VEGF, IL-6, and IL-8 observed in the dynamically cultured and primed ASCs on DAT coatings under 2% O_2 would be worth further investigation. To study the functionality, an *in vivo* hindlimb ischemia model could be utilized. Following femoral artery ligation (FAL), systemic inflammation triggers infiltration of inflammatory cells to the site [236], which may be differentially modulated by the ASCs that were primed with IFN-γ and TNF-α. Analysis of angiogenesis following FAL through assessment of limb perfusion and through

immunostaining for vascular markers would provide indications on whether the elevated levels of the pro-angiogenic paracrine factors observed in some of the culture groups were indicative that the corresponding ASC population had enhanced pro-angiogenic functionality [236]. The mouse hindlimb ischemia model has previously been utilized to analyze the effects of human ASC-derived extracellular vesicles (EVs) on muscle damage prevention following femoral artery ligation [237].

In the context of the current study, preconditioned ASCs could be delivered to the site using a DAT-based hydrogel, as previously demonstrated in a subcutaneous Wistar rat model [238]. The subsets of ASC culture conditions that would be recommended to be included would be 1) primed dynamically cultured ASCs on DAT coatings under hypoxia and 2) non-primed dynamically cultured ASCs on DAT coatings under hypoxia, with 3) primed statically cultured ASCs on TCPS under hypoxia and 4) non-primed statically cultured ASCs on TCPS under hypoxia as controls. This design would allow the direct comparison between experimental groups 1) and 4) as two extreme conditions based on the observed results in the paracrine secretion study. Furthermore, the effects of cytokine priming could be evaluated under two representative culture conditions. Finally, this design would allow investigation of the combined effects of dynamic culture and DAT coatings.

References

[1] S. S. Choe, J. Y. Huh, I. J. Hwang, J. I. Kim, and J. B. Kim, "Adipose tissue remodeling: Its role in energy metabolism and metabolic disorders," *Front. Endocrinol. (Lausanne).*, vol. 7, no. APR, 2016.

[2] M. Coelho, T. Oliveira, and R. Fernandes, "Biochemistry of adipose tissue: An endocrine organ," *Arch. Med. Sci.*, vol. 9, no. 2, pp. 191–200, 2013.

[3] J. L. M. Carrillo, J. O. M. Del Campo, O. G. Coronado, P. T. V. Gutiérrez, J. F. C. Cordero, and J. V. Juárez, "Adipose Tissue and Inflammation," in *Adipose Tissue*, InTech, 2018, pp. 93–121.

[4] R. K. Zwick, C. F. Guerrero-Juarez, V. Horsley, and M. V. Plikus, "Anatomical, Physiological, and Functional Diversity of Adipose Tissue," *Cell Metabolism*, vol. 27, no. 1. Cell Press, pp. 68–83, 09-Jan-2018.

[5] C. W. Patrick, "Tissue engineering strategies for adipose tissue repair," *Anat. Rec.*, vol. 263, no. 4, pp. 361–366, Aug. 2001.

[6] M. G. Scioli, V. Cervelli, P. Gentile, A. Bielli, R. Bellini, and A. Orlandi, "Human adipose tissue-derived stem cells in breast reconstruction following surgery for cancer: A controversial issue," *Stem Cell Discov.*, vol. 03, no. 03, pp. 164–166, 2013.

[7] H. Panchal and E. Matros, "Current trends in postmastectomy breast reconstruction," *Plast. Reconstr. Surg.*, vol. 140, no. 5S, pp. 7S-13S, 2017.

[8] K. Prasad, R. Zhou, R. Zhou, D. Schuessler, K. K. Ostrikov, and K. Bazaka, "Cosmetic reconstruction in breast cancer patients: Opportunities for nanocomposite materials," *Acta Biomater.*, vol. 86, pp. 41–65, Mar. 2019.

[9] N. A. O'Halloran, E. B. Dolan, M. J. Kerin, A. J. Lowery, and G. P. Duffy, "Hydrogels in adipose tissue engineering—Potential application in post-mastectomy breast regeneration," *J. Tissue Eng. Regen. Med.*, vol. 12, no. 12, pp. 2234–2247, 2018.

[10] M. Mempin, H. Hu, D. Chowdhury, A. Deva, and K. Vickery, "The A, B and C's of silicone breast implants: Anaplastic large cell lymphoma, biofilm and capsular contracture," *Materials (Basel).*, vol. 11, no. 12, Nov. 2018.

[11] R. D. Farhadieh and J. Farhadi, "Breast Augmentation," *Plast. Reconstr. Surg. Approaches Tech.*, pp. 486–498, Oct. 2015.

[12] A. E. Steiert, M. Boyce, and H. Sorg, "Capsular contracture by silicone breast implants: Possible causes, biocompatibility, and prophylactic strategies," *Med. Devices Evid. Res.*, vol. 6, no. 1, pp. 211–218, Dec. 2013.

[13] S. Gal, Y. Xue, and L. L. Q. Pu, "What Do We Know Now About Autologous Fat Grafting?," *Ann. Plast. Surg.*, vol. 83, no. 4S Suppl 1, pp. S17–S20, Oct. 2019.

[14] S. Wu, D. M. Coombs, and R. Gurunian, "Liposuction: Concepts, safety, and techniques in body-contouring surgery," *Cleve. Clin. J. Med.*, vol. 87, no. 6, pp.

367–375, Jun. 2020.

[15] P. Bourin *et al.*, “Stromal cells from the adipose tissue-derived stromal vascular fraction and culture expanded adipose tissue-derived stromal/stem cells: A joint statement of the International Federation for Adipose Therapeutics and Science (IFATS) and the International So,” *Cytotherapy*, vol. 15, no. 6, pp. 641–648, Jun. 2013.

[16] E. Oberbauer, C. Steffenhagen, C. Wurzer, C. Gabriel, H. Redl, and S. Wolbank, “Enzymatic and non-enzymatic isolation systems for adipose tissue-derived cells: Current state of the art,” *Cell Regen.*, vol. 4, no. 1, p. 4:7, Jan. 2015.

[17] C. Tremolada, G. Palmieri, and C. Ricordi, “Adipocyte transplantation and stem cells: Plastic surgery meets regenerative medicine,” *Cell Transplant.*, vol. 19, no. 10, pp. 1217–1223, 2010.

[18] C. Conci *et al.*, “Tissue engineering and regenerative medicine strategies for the female breast,” *J. Tissue Eng. Regen. Med.*, vol. 14, no. 2, pp. 369–387, 2020.

[19] F. Shahzad and B. J. Mehrara, “The Future of Fat Grafting,” *Aesthetic Surg. J.*, vol. 37, no. 3, pp. S59–S64, 2017.

[20] M. Merimi *et al.*, “The Therapeutic Potential of Mesenchymal Stromal Cells for Regenerative Medicine: Current Knowledge and Future Understandings,” *Front. Cell Dev. Biol.*, vol. 9, Aug. 2021.

[21] R. Schäfer, G. Spohn, and P. C. Baer, “Mesenchymal stem/stromal cells in regenerative medicine: Can preconditioning strategies improve therapeutic efficacy?,” *Transfusion Medicine and Hemotherapy*, vol. 43, no. 4. S. Karger AG, pp. 256–267, 01-Jul-2016.

[22] A. El-Badawy *et al.*, “Adipose stem cells display higher regenerative capacities and more adaptable electro-kinetic properties compared to bone marrow-derived mesenchymal stromal cells,” *Sci. Rep.*, vol. 6, no. 1, pp. 1–11, Nov. 2016.

[23] S. Mohamed-Ahmed *et al.*, “Adipose-derived and bone marrow mesenchymal stem cells: A donor-matched comparison,” *Stem Cell Res. Ther.*, vol. 9, no. 1, pp. 1–15, Jun. 2018.

[24] B. Puissant *et al.*, “Immunomodulatory effect of human adipose tissue-derived adult stem cells: Comparison with bone marrow mesenchymal stem cells,” *Br. J. Haematol.*, vol. 129, no. 1, pp. 118–129, Apr. 2005.

[25] S. M. Melief, J. J. Zwaginga, W. E. Fibbe, and H. Roelofs, “Adipose Tissue-Derived Multipotent Stromal Cells Have a Higher Immunomodulatory Capacity Than Their Bone Marrow-Derived Counterparts,” *Stem Cells Transl. Med.*, vol. 2, no. 6, pp. 455–463, Jun. 2013.

[26] A. Bajek, N. Gurtowska, J. Olkowska, L. Kazmierski, M. Maj, and T. Drewa, “Adipose-Derived Stem Cells as a Tool in Cell-Based Therapies,” *Archivum Immunologiae et Therapiae Experimentalis*, vol. 64, no. 6. Birkhauser Verlag AG, pp. 443–454, 01-Dec-2016.

[27] Y. An *et al.*, “Exosomes from adipose-derived stem cells and application to skin

wound healing," *Cell Prolif.*, vol. 54, no. 3, Mar. 2021.

[28] M. Deptuła, A. Brzezicka, A. Skoniecka, J. Zieliński, and M. Pikuła, "Adipose-derived stromal cells for nonhealing wounds: Emerging opportunities and challenges," *Med. Res. Rev.*, vol. 41, no. 4, pp. 2130–2171, Jul. 2021.

[29] L. Badimon, B. Oñate, and G. Vilahur, "Adipose-derived Mesenchymal Stem Cells and Their Reparative Potential in Ischemic Heart Disease," *Rev. Española Cardiol. (English Ed.*, vol. 68, no. 7, pp. 599–611, Jul. 2015.

[30] B. A. Naaijkens, A. van Dijk, O. Kamp, P. A. J. Krijnen, H. W. M. Niessen, and L. J. M. Juffermans, "Therapeutic Application of Adipose Derived Stem Cells in Acute Myocardial Infarction: Lessons from Animal Models," *Stem Cell Rev. Reports*, vol. 10, no. 3, pp. 389–398, 2014.

[31] D. Chang, T. Fan, S. Gao, Y. Jin, M. Zhang, and M. Ono, "Application of mesenchymal stem cell sheet to treatment of ischemic heart disease," *Stem Cell Res. Ther.*, vol. 12, no. 1, Dec. 2021.

[32] J. H. Choi *et al.*, "Adipose tissue engineering for soft tissue regeneration," *Tissue Engineering - Part B: Reviews*, vol. 16, no. 4. pp. 413–426, 01-Aug-2010.

[33] S. Khazaei, G. Keshavarz, A. Bozorgi, H. Nazari, and M. Khazaei, "Adipose tissue-derived stem cells: a comparative review on isolation, culture, and differentiation methods," *Cell Tissue Bank.*, 2021.

[34] D. Mushahary, A. Spittler, C. Kasper, V. Weber, and V. Charwat, "Isolation, cultivation, and characterization of human mesenchymal stem cells," *Cytom. Part A*, vol. 93, no. 1, pp. 19–31, Jan. 2018.

[35] T. Rada, R. L. Reis, and M. E. Gomes, "Novel method for the isolation of adipose stem cells (ASCs)," *J. Tissue Eng. Regen. Med.*, vol. 3, no. 2, pp. 158–159, 2009.

[36] S. Gottipamula, M. S. Muttigi, U. Kolkundkar, and R. N. Seetharam, "Serum-free media for the production of human mesenchymal stromal cells: A review," *Cell Prolif.*, vol. 46, no. 6, pp. 608–627, 2013.

[37] P. Van Pham and N. B. Vu, "In vitro expansion of mesenchymal stem cells for clinical use," *Prog. Stem Cell*, vol. 3, no. 02, p. 87, Jun. 2016.

[38] J. Czapla *et al.*, "The effect of culture media on large-scale expansion and characteristic of adipose tissue-derived mesenchymal stromal cells," *Stem Cell Res. Ther.*, vol. 10, no. 1, Aug. 2019.

[39] S. H. Al-Saqi *et al.*, "Defined serum-free media for in vitro expansion of adipose-derived mesenchymal stem cells," *Cytotherapy*, vol. 16, no. 7, pp. 915–926, 2014.

[40] S. Kandoi *et al.*, "Evaluation of platelet lysate as a substitute for FBS in explant and enzymatic isolation methods of human umbilical cord MSCs," *Sci. Rep.*, vol. 8, no. 1, Dec. 2018.

[41] A. Oikonomopoulos *et al.*, "Optimization of human mesenchymal stem cell manufacturing: The effects of animal/xeno-free media," *Sci. Rep.*, vol. 5, no. 1, pp. 1–11, Nov. 2015.

[42] B. Lindroos *et al.*, “Serum-free, xeno-free culture media maintain the proliferation rate and multipotentiality of adipose stem cells in vitro,” *Cytotherapy*, vol. 11, no. 7, pp. 958–972, 2009.

[43] P. T. M. Dam *et al.*, “Human Adipose-Derived Mesenchymal Stromal Cells Exhibit High HLA-DR Levels and Altered Cellular Characteristics under a Xeno-free and Serum-free Condition,” *Stem Cell Rev. Reports*, vol. 17, no. 6, pp. 2291–2303, Dec. 2021.

[44] P. Zuk, “Adipose-Derived Stem Cells in Tissue Regeneration: A Review,” *ISRN Stem Cells*, vol. 2013, pp. 1–35, 2013.

[45] P. C. Baer, “Adipose-derived mesenchymal stromal/stem cells: An update on their phenotype in vivo and in vitro,” *World J. Stem Cells*, vol. 6, no. 3, p. 256, 2014.

[46] E. T. Camilleri *et al.*, “Identification and validation of multiple cell surface markers of clinical-grade adipose-derived mesenchymal stromal cells as novel release criteria for good manufacturing practice-compliant production,” *Stem Cell Res. Ther.*, vol. 7, no. 1, pp. 1–16, 2016.

[47] D. A. De Ugarte *et al.*, “Differential expression of stem cell mobilization-associated molecules on multi-lineage cells from adipose tissue and bone marrow,” *Immunol. Lett.*, vol. 89, no. 2–3, pp. 267–270, Oct. 2003.

[48] H. Suga *et al.*, “Functional implications of CD34 expression in human adipose-derived stem/progenitor cells,” *Stem Cells Dev.*, vol. 18, no. 8, pp. 1201–1209, Oct. 2009.

[49] A. J. Braga Osorio Gomes Salgado *et al.*, “Adipose Tissue Derived Stem Cells Secretome: Soluble Factors and Their Roles in Regenerative Medicine,” *Curr. Stem Cell Res. Ther.*, vol. 5, no. 2, pp. 103–110, 2010.

[50] G. J. Jimenez-Puerta, J. A. Marchal, E. López-Ruiz, and P. Gálvez-Martín, “Role of mesenchymal stromal cells as therapeutic agents: Potential mechanisms of action and implications in their clinical use,” *J. Clin. Med.*, vol. 9, no. 2, p. 445, 2020.

[51] N. K. Dubey, V. K. Mishra, R. Dubey, Y. H. Deng, F. C. Tsai, and W. P. Deng, “Revisiting the advances in isolation, characterization and secretome of adipose-derived stromal/stem cells,” *Int. J. Mol. Sci.*, vol. 19, no. 8, Aug. 2018.

[52] H. Qiu, S. Liu, K. Wu, R. Zhao, L. Cao, and H. Wang, “Prospective application of exosomes derived from adipose-derived stem cells in skin wound healing: A review,” *J. Cosmet. Dermatol.*, vol. 19, no. 3, pp. 574–581, Mar. 2020.

[53] M. Sandonà *et al.*, “Mesenchymal Stromal Cells and Their Secretome: New Therapeutic Perspectives for Skeletal Muscle Regeneration,” *Front. Bioeng. Biotechnol.*, vol. 9, May 2021.

[54] S. Rautiainen, T. Laaksonen, and R. Koivuniemi, “Angiogenic effects and crosstalk of adipose-derived mesenchymal stem/stromal cells and their extracellular vesicles with endothelial cells,” *Int. J. Mol. Sci.*, vol. 22, no. 19, p. 10890, Oct. 2021.

[55] D. S. Pinto, T. Ahsan, J. Serra, A. Fernandes-Platzgummer, J. M. S. Cabral, and C. L. da Silva, “Modulation of the in vitro angiogenic potential of human mesenchymal stromal cells from different tissue sources,” *J. Cell. Physiol.*, 2020.

[56] X. Li *et al.*, “Harnessing the secretome of adipose-derived stem cells in the treatment of ischemic heart diseases,” *Stem Cell Research and Therapy*, vol. 10, no. 1. BioMed Central Ltd., p. 196, 27-Jun-2019.

[57] J. Rehman *et al.*, “Secretion of Angiogenic and Antiapoptotic Factors by Human Adipose Stromal Cells,” *Circulation*, vol. 109, no. 10, pp. 1292–1298, Mar. 2004.

[58] H. Nakagami *et al.*, “Novel autologous cell therapy in ischemic limb disease through growth factor secretion by cultured adipose tissue-derived stromal cells,” *Arterioscler. Thromb. Vasc. Biol.*, vol. 25, no. 12, pp. 2542–2547, Dec. 2005.

[59] A. Elfenbein and M. Simons, “Overview of Angiogenesis,” *Cardiovasc. Mol. Imaging*, pp. 225–232, 2007.

[60] M. Presta, P. Dell’Era, S. Mitola, E. Moroni, R. Ronca, and M. Rusnati, “Fibroblast growth factor/fibroblast growth factor receptor system in angiogenesis,” *Cytokine Growth Factor Rev.*, vol. 16, no. 2 SPEC. ISS., pp. 159–178, Apr. 2005.

[61] E. J. Battegay, J. Rupp, L. Iruela-Arispe, E. H. Sage, and M. Pech, “PDGF-BB modulates endothelial proliferation and angiogenesis in vitro via PDGF β-receptors,” *J. Cell Biol.*, vol. 125, no. 4, pp. 917–928, May 1994.

[62] P. A. Guerrero and J. H. McCarty, “TGF-β Activation and Signaling in Angiogenesis,” *Physiol. Pathol. Angiogenes. - Signal. Mech. Target. Ther.*, Apr. 2017.

[63] E. Fagiani and G. Christofori, “Angiopoietins in angiogenesis,” *Cancer Lett.*, vol. 328, no. 1, pp. 18–26, Jan. 2013.

[64] X. Li *et al.*, “Harnessing the secretome of adipose-derived stem cells in the treatment of ischemic heart diseases,” *Stem Cell Res. Ther.*, vol. 10, no. 1, pp. 1–13, Jun. 2019.

[65] T. Kang *et al.*, “Adipose-Derived Stem Cells Induce Angiogenesis via Microvesicle Transport of miRNA-31,” *Stem Cells Transl. Med.*, vol. 5, no. 4, pp. 440–450, Apr. 2016.

[66] Y. Yang, Y. Cai, Y. Zhang, J. Liu, and Z. Xu, “Exosomes Secreted by Adipose-Derived Stem Cells Contribute to Angiogenesis of Brain Microvascular Endothelial Cells Following Oxygen–Glucose Deprivation In Vitro Through MicroRNA-181b/TRPM7 Axis,” *J. Mol. Neurosci.*, vol. 65, no. 1, pp. 74–83, May 2018.

[67] J. Su *et al.*, “Phylogenetic distinction of iNOS and IDO function in mesenchymal stem cell-mediated immunosuppression in mammalian species,” *Cell Death Differ.*, vol. 21, no. 3, pp. 388–396, Mar. 2014.

[68] E. Soleymaninejadian, K. Pramanik, and E. Samadian, “Immunomodulatory properties of mesenchymal stem cells: Cytokines and factors,” *Am. J. Reprod.*

Immunol., vol. 67, no. 1, pp. 1–8, Jan. 2012.

[69] M. François, R. Romieu-Mourez, M. Li, and J. Galipeau, "Human MSC suppression correlates with cytokine induction of indoleamine 2,3-dioxygenase and bystander M2 macrophage differentiation," *Mol. Ther.*, vol. 20, no. 1, pp. 187–195, 2012.

[70] A. B. Vasandan, S. Jahnavi, C. Shashank, P. Prasad, A. Kumar, and S. Jyothi Prasanna, "Human Mesenchymal stem cells program macrophage plasticity by altering their metabolic status via a PGE 2 -dependent mechanism," *Sci. Rep.*, vol. 6, no. 1, pp. 1–17, Dec. 2016.

[71] H. Yagi *et al.*, "Mesenchymal stem cells: Mechanisms of immunomodulation and homing," *Cell Transplant.*, vol. 19, no. 6–7, pp. 667–679, Jun. 2010.

[72] H. L.R. Rilo, J. Cagliani, D. Grande, E. P Molmenti, and E. J. Miller, "Immunomodulation by Mesenchymal Stromal Cells and Their Clinical Applications," *J. Stem Cell Regen. Biol.*, vol. 3, no. 2, pp. 1–14, Apr. 2017.

[73] L. Mazini, L. Rochette, M. Amine, and G. Malka, "Regenerative capacity of adipose derived stem cells (ADSCs), comparison with mesenchymal stem cells (MSCs)," *Int. J. Mol. Sci.*, vol. 20, no. 10, May 2019.

[74] E. Ivanova-Todorova *et al.*, "Adipose tissue-derived mesenchymal stem cells are more potent suppressors of dendritic cells differentiation compared to bone marrow-derived mesenchymal stem cells," *Immunol. Lett.*, vol. 126, no. 1–2, pp. 37–42, Sep. 2009.

[75] N. Abu-Shahba *et al.*, "Immunomodulatory and Antioxidative potentials of adipose-derived Mesenchymal stem cells isolated from breast versus abdominal tissue: a comparative study," *Cell Regen.*, vol. 9, no. 1, pp. 1–14, Dec. 2020.

[76] S. Lendeckel *et al.*, "Autologous stem cells (adipose) and fibrin glue used to treat widespread traumatic calvarial defects: Case report," *J. Cranio-Maxillofacial Surg.*, vol. 32, no. 6, pp. 370–373, Dec. 2004.

[77] A. Bajek, N. Gurtowska, J. Olkowska, L. Kazmierski, M. Maj, and T. Drewa, "Adipose-Derived Stem Cells as a Tool in Cell-Based Therapies," *Arch. Immunol. Ther. Exp. (Warsz).*, vol. 64, no. 6, pp. 443–454, Dec. 2016.

[78] A. Hassanshahi *et al.*, "Adipose-derived stem cells for wound healing," *J. Cell. Physiol.*, vol. 234, no. 6, pp. 7903–7914, Jun. 2019.

[79] C. Nie, D. Yang, J. Xu, Z. Si, X. Jin, and J. Zhang, "Locally administered Adipose-derived stem cells accelerate wound healing through differentiation and vasculogenesis," *Cell Transplant.*, vol. 20, no. 2, pp. 205–216, Mar. 2011.

[80] W. S. Kim *et al.*, "Wound healing effect of adipose-derived stem cells: A critical role of secretory factors on human dermal fibroblasts," *J. Dermatol. Sci.*, vol. 48, no. 1, pp. 15–24, Oct. 2007.

[81] L. Mazini, L. Rochette, B. Admou, S. Amal, and G. Malka, "Hopes and limits of adipose-derived stem cells (ADSCs) and mesenchymal stem cells (MSCs) in wound healing," *Int. J. Mol. Sci.*, vol. 21, no. 4, Feb. 2020.

[82] K. C. Moon *et al.*, “Potential of allogeneic adipose-derived stem cell–hydrogel complex for treating diabetic foot ulcers,” *Diabetes*, vol. 68, no. 4, pp. 837–846, Apr. 2019.

[83] G. Rigotti *et al.*, “Clinical treatment of radiotherapy tissue damage by lipoaspirate transplant: A healing process mediated by adipose-derived adult stem cells,” *Plast. Reconstr. Surg.*, vol. 119, no. 5, pp. 1409–1422, Apr. 2007.

[84] M. A. Khan *et al.*, “Global Epidemiology of Ischemic Heart Disease: Results from the Global Burden of Disease Study,” *Cureus*, vol. 12, no. 7, Jul. 2020.

[85] V. Karantalis and J. M. Hare, “Use of mesenchymal stem cells for therapy of cardiac disease,” *Circ. Res.*, vol. 116, no. 8, pp. 1413–1430, Apr. 2015.

[86] M. Mazo *et al.*, “Adipose stromal vascular fraction improves cardiac function in chronic myocardial infarction through differentiation and paracrine activity,” *Cell Transplant.*, vol. 21, no. 5, pp. 1023–1037, 2012.

[87] J. H. Houtgraaf *et al.*, “First experience in humans using adipose tissue-derived regenerative cells in the treatment of patients with ST-segment elevation myocardial infarction,” *J. Am. Coll. Cardiol.*, vol. 59, no. 5, pp. 539–540, Jan. 2012.

[88] E. C. Perin *et al.*, “Adipose-derived regenerative cells in patients with ischemic cardiomyopathy: The PRECISE Trial,” *Am. Heart J.*, vol. 168, no. 1, 2014.

[89] Y. Seo, T. H. Shin, and H. S. Kim, “Current strategies to enhance adipose stem cell function: An update,” *International Journal of Molecular Sciences*, vol. 20, no. 15. MDPI AG, 2019.

[90] J. R. Ferreira, G. Q. Teixeira, S. G. Santos, M. A. Barbosa, G. Almeida-Porada, and R. M. Gonçalves, “Mesenchymal stromal cell secretome: Influencing therapeutic potential by cellular pre-conditioning,” *Front. Immunol.*, vol. 9, p. 2837, 2018.

[91] W. K. Ong, S. Chakraborty, and S. Sugii, “Adipose tissue: Understanding the heterogeneity of stem cells for regenerative medicine,” *Biomolecules*, vol. 11, no. 7, Jul. 2021.

[92] M. A. A. Harrison, R. M. Wise, B. P. Benjamin, E. M. Hochreiner, O. A. Mohiuddin, and B. A. Bunnell, “Adipose-derived stem cells from obese donors polarize macrophages and microglia toward a pro-inflammatory phenotype,” *Cells*, vol. 10, no. 1, pp. 1–15, Jan. 2021.

[93] P. Gibler *et al.*, “Human adipose-derived stromal/stem cell culture and analysis methods for adipose tissue modeling in vitro: A systematic review,” *Cells*, vol. 10, no. 6, p. 1378, Jun. 2021.

[94] S. Ceccarelli, P. Pontecorvi, E. Anastasiadou, C. Napoli, and C. Marchese, “Immunomodulatory Effect of Adipose-Derived Stem Cells: The Cutting Edge of Clinical Application,” *Frontiers in Cell and Developmental Biology*, vol. 8. Frontiers Media S.A., 17-Apr-2020.

[95] G. D. Kusuma, J. Carthew, R. Lim, and J. E. Frith, “Effect of the

Microenvironment on Mesenchymal Stem Cell Paracrine Signaling: Opportunities to Engineer the Therapeutic Effect," *Stem Cells and Development*, vol. 26, no. 9. Mary Ann Liebert Inc., pp. 617–631, 01-May-2017.

[96] S. Kang, S. M. Kim, and J. H. Sung, "Cellular and molecular stimulation of adipose-derived stem cells under hypoxia," *Cell Biol. Int.*, vol. 38, no. 5, pp. 553–562, May 2014.

[97] H. M. Chung, C. H. Won, and J. H. Sung, "Responses of adipose-derived stem cells during hypoxia: Enhanced skin-regenerative potential," *Expert Opin. Biol. Ther.*, vol. 9, no. 12, pp. 1499–1508, Dec. 2009.

[98] A. Mohyeldin, T. Garzón-Muvdi, and A. Quiñones-Hinojosa, "Oxygen in stem cell biology: A critical component of the stem cell niche," *Cell Stem Cell*, vol. 7, no. 2, pp. 150–161, Aug. 2010.

[99] C. Mas-Bargues *et al.*, "Relevance of oxygen concentration in stem cell culture for regenerative medicine," *Int. J. Mol. Sci.*, vol. 20, no. 5, Mar. 2019.

[100] J. R. Choi *et al.*, "Impact of low oxygen tension on stemness, proliferation and differentiation potential of human adipose-derived stem cells," *Biochem. Biophys. Res. Commun.*, vol. 448, no. 2, pp. 218–224, May 2014.

[101] Y. Yamamoto *et al.*, "Low oxygen tension enhances proliferation and maintains stemness of adipose tissue-derived stromal cells," *Biores. Open Access*, vol. 2, no. 3, pp. 199–205, Jun. 2013.

[102] C. Fotia, A. Massa, F. Boriani, N. Baldini, and D. Granchi, "Hypoxia enhances proliferation and stemness of human adipose-derived mesenchymal stem cells," *Cytotechnology*, vol. 67, no. 6, pp. 1073–1084, May 2015.

[103] E. M. Weijers, L. J. Van Den Broek, T. Waaijman, V. W. M. Van Hinsbergh, S. Gibbs, and P. Koolwijk, "The influence of hypoxia and fibrinogen variants on the expansion and differentiation of adipose tissue-derived mesenchymal stem cells," *Tissue Eng. - Part A*, vol. 17, no. 21–22, pp. 2675–2685, 2011.

[104] Y. H. K. Yang, C. R. Ogando, C. Wang See, T. Y. Chang, and G. A. Barabino, "Changes in phenotype and differentiation potential of human mesenchymal stem cells aging in vitro," *Stem Cell Res. Ther.*, vol. 9, no. 1, pp. 1–14, May 2018.

[105] T. Shang, S. Li, Y. Zhang, L. Lu, L. Cui, and F. F. Guo, "Hypoxia promotes differentiation of adipose-derived stem cells into endothelial cells through demethylation of ephrinB2," *Stem Cell Res. Ther.*, vol. 10, no. 1, May 2019.

[106] S. Portron *et al.*, "Effects of In Vitro Low Oxygen Tension Preconditioning of Adipose Stromal Cells on Their In Vivo Chondrogenic Potential: Application in Cartilage Tissue Repair," *PLoS One*, vol. 8, no. 4, p. e62368, Apr. 2013.

[107] F. Wang, V. Zachar, C. P. Pennisi, T. Fink, Y. Maeda, and J. Emmersen, "Hypoxia enhances differentiation of adipose tissue-derived stem cells toward the smooth muscle phenotype," *Int. J. Mol. Sci.*, vol. 19, no. 2, Feb. 2018.

[108] S. H. Wu *et al.*, "Adipose-Derived Mesenchymal Stem Cells From a Hypoxic Culture Improve Neuronal Differentiation and Nerve Repair," *Front. Cell Dev.*

Biol., vol. 9, Apr. 2021.

[109] H. Moriyama *et al.*, "Notch signaling enhances stemness by regulating metabolic pathways through modifying p53, nf-κb, and hif-1α," *Stem Cells Dev.*, vol. 27, no. 13, pp. 935–947, Jul. 2018.

[110] S. Y. Song, H. M. Chung, and J. H. Sung, "The pivotal role of VEGF in adipose-derived-stem-cell-mediated regeneration," *Expert Opin. Biol. Ther.*, vol. 10, no. 11, pp. 1529–1537, Nov. 2010.

[111] E. Y. Lee *et al.*, "Hypoxia-enhanced wound-healing function of adipose-derived stem cells: Increase in stem cell proliferation and up-regulation of VEGF and bFGF," *Wound Repair Regen.*, vol. 17, no. 4, pp. 540–547, Jul. 2009.

[112] S. T. Hsiao *et al.*, "Hypoxic conditioning enhances the angiogenic paracrine activity of human adipose-derived stem cells," *Stem Cells Dev.*, vol. 22, no. 10, pp. 1614–1623, May 2013.

[113] C. Xue *et al.*, "Exosomes Derived from Hypoxia-Treated Human Adipose Mesenchymal Stem Cells Enhance Angiogenesis Through the PKA Signaling Pathway," *Stem Cells Dev.*, vol. 27, no. 7, pp. 456–465, Apr. 2018.

[114] C. Almeria *et al.*, "Hypoxia Conditioned Mesenchymal Stem Cell-Derived Extracellular Vesicles Induce Increased Vascular Tube Formation in vitro," *Front. Bioeng. Biotechnol.*, vol. 7, Oct. 2019.

[115] A. N. Gornostaeva, P. I. Bobyleva, E. R. Andreeva, D. A. Yakubets, and L. B. Buravkova, "Adipose-derived stromal cell immunosuppression of T cells is enhanced under 'physiological' hypoxia," *Tissue Cell*, vol. 63, Apr. 2020.

[116] M. Roemeling-Van Rhijn *et al.*, "Effects of hypoxia on the immunomodulatory properties of adipose tissue-derived mesenchymal stem cells," *Front. Immunol.*, vol. 4, no. JUL, 2013.

[117] J. Liu *et al.*, "Allogeneic adipose-derived stem cells promote ischemic muscle repair by inducing M2 macrophage polarization via the HIF-1α/IL-10 pathway," *Stem Cells*, vol. 38, no. 10, pp. 1307–1320, Oct. 2020.

[118] N. D. C. Noronha Nc *et al.*, "Priming approaches to improve the efficacy of mesenchymal stromal cell-based therapies," *Stem Cell Res. Ther.*, vol. 10, no. 1, pp. 1–21, May 2019.

[119] H. Y. Cheng, M. R. Anggelia, C. H. Lin, and C. F. Lin, "Preconditioned mesenchymal stromal cells to improve allotransplantation outcome," *Cells*, vol. 10, no. 9, Sep. 2021.

[120] S. F. H. De Witte, M. Franquesa, C. C. Baan, and M. J. Hoogduijn, "Toward development of imesenchymal stem cells for immunomodulatory therapy," *Front. Immunol.*, vol. 6, no. JAN, p. 1, 2016.

[121] E. Ragni *et al.*, "Inflammatory priming enhances mesenchymal stromal cell secretome potential as a clinical product for regenerative medicine approaches through secreted factors and EV-miRNAs: The example of joint disease," *Stem Cell Res. Ther.*, vol. 11, no. 1, pp. 1–19, Apr. 2020.

[122] T. R. T. Serejo *et al.*, “Assessment of the Immunosuppressive Potential of INF-γ Licensed Adipose Mesenchymal Stem Cells, Their Secretome and Extracellular Vesicles,” *Cells*, vol. 8, no. 1, p. 22, Jan. 2019.

[123] M. Kim, D. Il Shin, B. H. Choi, and B. H. Min, “Exosomes from IL-1β-Primed Mesenchymal Stem Cells Inhibited IL-1β- and TNF-α-Mediated Inflammatory Responses in Osteoarthritic SW982 Cells,” *Tissue Eng. Regen. Med.*, vol. 18, no. 4, pp. 525–536, Aug. 2021.

[124] C. Aussel *et al.*, “IL-1β primed mesenchymal stromal cells moderate hemorrhagic shock-induced organ injuries,” *Stem Cell Res. Ther.*, vol. 12, no. 1, Dec. 2021.

[125] M. François, R. Romieu-Mourez, M. Li, and J. Galipeau, “Human MSC suppression correlates with cytokine induction of indoleamine 2,3-dioxygenase and bystander M2 macrophage differentiation,” *Mol. Ther.*, vol. 20, no. 1, pp. 187–195, 2012.

[126] A. Hackel, A. Aksamit, K. Bruderek, S. Lang, and S. Brandau, “TNF-α and IL-1β sensitize human MSC for IFN-γ signaling and enhance neutrophil recruitment,” *Eur. J. Immunol.*, vol. 51, no. 2, pp. 319–330, Feb. 2021.

[127] T. Hoshiba *et al.*, “Decellularized extracellular matrix as an in vitro model to study the comprehensive roles of the ECM in stem cell differentiation,” *Stem Cells International*, vol. 2016. Hindawi Publishing Corporation, 2016.

[128] J. K. Leach and J. Whitehead, “Materials-Directed Differentiation of Mesenchymal Stem Cells for Tissue Engineering and Regeneration,” *ACS Biomater. Sci. Eng.*, vol. 4, no. 4, pp. 1115–1127, Apr. 2018.

[129] Y. Chen, Z. Shu, K. Qian, J. Wang, and H. Zhu, “Harnessing the Properties of Biomaterial to Enhance the Immunomodulation of Mesenchymal Stem Cells,” *Tissue Engineering - Part B: Reviews*, vol. 25, no. 6. Mary Ann Liebert Inc., pp. 492–499, 01-Dec-2019.

[130] T. J. Bartosh *et al.*, “Aggregation of human mesenchymal stromal cells (MSCs) into 3D spheroids enhances their antiinflammatory properties,” *Proc. Natl. Acad. Sci. U. S. A.*, vol. 107, no. 31, pp. 13724–13729, Aug. 2010.

[131] V. Miceli, M. Pampalone, S. Vella, A. P. Carreca, G. Amico, and P. G. Conaldi, “Comparison of Immunosuppressive and Angiogenic Properties of Human Amnion-Derived Mesenchymal Stem Cells between 2D and 3D Culture Systems,” *Stem Cells Int.*, vol. 2019, 2019.

[132] A. J. Steward and D. J. Kelly, “Mechanical regulation of mesenchymal stem cell differentiation,” *Journal of Anatomy*, vol. 227, no. 6. Blackwell Publishing Ltd, pp. 717–731, 01-Dec-2015.

[133] N. Huebsch *et al.*, “Harnessing traction-mediated manipulation of the cell/matrix interface to control stem-cell fate,” *Nat. Mater.*, vol. 9, no. 6, pp. 518–526, 2010.

[134] A. A. Abdeen, J. B. Weiss, J. Lee, and K. A. Kilian, “Matrix composition and mechanics direct proangiogenic signaling from mesenchymal stem cells,” *Tissue Eng. - Part A*, vol. 20, no. 19–20, pp. 2737–2745, 2014.

[135] P. Sawadkar *et al.*, “Three dimensional porous scaffolds derived from collagen, elastin and fibrin proteins orchestrate adipose tissue regeneration,” *J. Tissue Eng.*, vol. 12, 2021.

[136] R. R. Rao, A. W. Peterson, J. Ceccarelli, A. J. Putnam, and J. P. Stegemann, “Matrix composition regulates three-dimensional network formation by endothelial cells and mesenchymal stem cells in collagen/fibrin materials,” *Angiogenesis*, vol. 15, no. 2, pp. 253–264, Jun. 2012.

[137] M. Lazarini *et al.*, “Natural Type II Collagen Hydrogel, Fibrin Sealant, and Adipose-Derived Stem Cells as a Promising Combination for Articular Cartilage Repair,” *Cartilage*, vol. 8, no. 4, pp. 439–443, Oct. 2017.

[138] L. E. Flynn, “The use of decellularized adipose tissue to provide an inductive microenvironment for the adipogenic differentiation of human adipose-derived stem cells,” *Biomaterials*, vol. 31, no. 17, pp. 4715–4724, Jun. 2010.

[139] P. M. Martin, A. Shridhar, C. Yu, C. Brown, and L. E. Flynn, “Decellularized adipose tissue scaffolds for soft tissue regeneration and adipose-derived stem/stromal cell delivery,” in *Methods in Molecular Biology*, vol. 1773, Humana Press Inc., 2018, pp. 53–71.

[140] A. Shridhar, A. Y. L. Lam, Y. Sun, C. A. Simmons, E. R. Gillies, and L. E. Flynn, “Culture on Tissue-Specific Coatings Derived from α-Amylase-Digested Decellularized Adipose Tissue Enhances the Proliferation and Adipogenic Differentiation of Human Adipose-Derived Stromal Cells,” *Biotechnol. J.*, vol. 15, no. 3, p. 1900118, Nov. 2020.

[141] C. Yu, A. Kornmuller, C. Brown, T. Hoare, and L. E. Flynn, “Decellularized adipose tissue microcarriers as a dynamic culture platform for human adipose-derived stem/stromal cell expansion,” *Biomaterials*, vol. 120, pp. 66–80, Mar. 2017.

[142] T. T. Y. Han, S. Toutounji, B. G. Amsden, and L. E. Flynn, “Adipose-derived stromal cells mediate in vivo adipogenesis, angiogenesis and inflammation in decellularized adipose tissue bioscaffolds,” *Biomaterials*, vol. 72, pp. 125–137, Dec. 2015.

[143] P. Morissette Martin, A. Grant, D. W. Hamilton, and L. E. Flynn, “Matrix composition in 3-D collagenous bioscaffolds modulates the survival and angiogenic phenotype of human chronic wound dermal fibroblasts,” *Acta Biomater.*, vol. 83, pp. 199–210, 2019.

[144] K. H. Vining and D. J. Mooney, “Mechanical forces direct stem cell behaviour in development and regeneration,” *Nature Reviews Molecular Cell Biology*, vol. 18, no. 12. Nature Publishing Group, pp. 728–742, 01-Dec-2017.

[145] F. Y. Wei *et al.*, “Low-magnitude high-frequency vibration enhanced mesenchymal stem cell recruitment in osteoporotic fracture healing through the SDF-1/CXCR4 pathway,” *Eur. Cells Mater.*, vol. 31, pp. 341–354, Jan. 2016.

[146] Y. C. Kuo *et al.*, “Oscillatory shear stress mediates directional reorganization of actin cytoskeleton and alters differentiation propensity of mesenchymal stem

cells," *Stem Cells*, vol. 33, no. 2, pp. 429–442, 2015.

[147] L. He, M. Ahmad, and N. Perrimon, "Mechanosensitive channels and their functions in stem cell differentiation," *Exp. Cell Res.*, vol. 374, no. 2, pp. 259–265, Jan. 2019.

[148] M. A. Corrigan, G. P. Johnson, E. Stavenschi, M. Riffault, M. N. Labour, and D. A. Hoey, "TRPV4-mediates oscillatory fluid shear mechanotransduction in mesenchymal stem cells in part via the primary cilium," *Sci. Rep.*, vol. 8, no. 1, Dec. 2018.

[149] G. P. Johnson, E. Stavenschi, K. F. Eichholz, M. A. Corrigan, S. Fair, and D. A. Hoey, "Mesenchymal stem cell mechanotransduction is cAMP dependent and regulated by adenylyl cyclase 6 and the primary cilium," *J. Cell Sci.*, vol. 131, no. 21, 2018.

[150] A. Charoenpanich *et al.*, "Cyclic tensile strain enhances osteogenesis and angiogenesis in mesenchymal stem cells from osteoporotic donors," *Tissue Eng. - Part A*, vol. 20, no. 1–2, pp. 67–78, Jan. 2014.

[151] G. Subramanian, A. Stasuk, M. Elsaadany, and E. Yildirim-Ayan, "Effect of uniaxial tensile cyclic loading regimes on matrix organization and tenogenic differentiation of adipose-derived stem cells encapsulated within 3D collagen scaffolds," *Stem Cells Int.*, vol. 2017, 2017.

[152] A. Charoenpanich, J. Bodle, and E. Loboa, "The role of cyclic tensile strain on osteogenesis and angiogenesis in human mesenchymal stem/stromal cells," in *The Biology and Therapeutic Application of Mesenchymal Cells*, Hoboken, NJ, USA: John Wiley & Sons, Inc., 2016, pp. 208–221.

[153] A. J. Steward, J. H. Cole, F. S. Ligler, and E. G. Loboa, "Mechanical and Vascular Cues Synergistically Enhance Osteogenesis in Human Mesenchymal Stem Cells," *Tissue Eng. - Part A*, vol. 22, no. 15–16, pp. 997–1005, Aug. 2016.

[154] W. Wang *et al.*, "Effect of cyclic compression on bone marrow mesenchymal stromal cells in tissue engineered cartilage scaffold," *J. Biomed. Mater. Res. - Part A*, vol. 107, no. 6, pp. 1294–1302, Jun. 2019.

[155] A. Ode *et al.*, "CD73/5'-ecto-nucleotidase acts as a regulatory factor in osteo-/chondrogenic differentiation of mechanically stimulated mesenchymal stromal cells," *Eur. Cells Mater.*, vol. 25, pp. 37–47, Jan. 2013.

[156] G. Pattappa, J. Zellner, B. Johnstone, D. Docheva, and P. Angele, "Cells under pressure - the relationship between hydrostatic pressure and mesenchymal stem cell chondrogenesis," *Eur. Cell. Mater.*, vol. 37, pp. 360–381, 2019.

[157] M. S. Hosseini, M. Tafazzoli-Shadpour, N. Haghighipour, N. Aghdami, and A. Goodarzi, "The synergistic effects of shear stress and cyclic hydrostatic pressure modulate chondrogenic induction of human mesenchymal stem cells," *Int. J. Artif. Organs*, vol. 38, no. 10, pp. 557–564, 2015.

[158] A. S. Safavi, G. Rouhi, N. Haghighipour, F. Bagheri, M. B. Eslaminejad, and F. A. Sayahpour, "Efficacy of mechanical vibration in regulating mesenchymal stem

cells gene expression," *Vitr. Cell. Dev. Biol. - Anim.*, vol. 55, no. 5, pp. 387–394, 2019.

[159] J. Susanne, B. Lauren, S. Kathrin, H. Marcel, K. Johannes, and S. Sonja, "Mechanical Stimulation Increases the Proliferation and Differentiation Potential of Human Adipose-Derived Stromal Cells," *Int. J. Stem cell Res. Ther.*, vol. 5, no. 2, 2018.

[160] P. Dan, É. Velot, V. Decot, and P. Menu, "The role of mechanical stimuli in the vascular differentiation of mesenchymal stem cells," *J. Cell Sci.*, vol. 128, no. 14, pp. 2415–2422, Jul. 2015.

[161] T. M. Maul, D. W. Chew, A. Nieponice, and D. A. Vorp, "Mechanical stimuli differentially control stem cell behavior: Morphology, proliferation, and differentiation," *Biomech. Model. Mechanobiol.*, vol. 10, no. 6, pp. 939–953, Dec. 2011.

[162] Z. Li, L. Kupcsik, S. J. Yao, M. Alini, and M. J. Stoddart, "Mechanical load modulates chondrogenesis of human mesenchymal stem cells through the TGF-β pathway," *J. Cell. Mol. Med.*, vol. 14, no. 6 A, pp. 1338–1346, Jun. 2010.

[163] O. F. W. Gardner, N. Fahy, M. Alini, and M. J. Stoddart, "Joint mimicking mechanical load activates TGFβ1 in fibrin-poly(ester-urethane) scaffolds seeded with mesenchymal stem cells," *J. Tissue Eng. Regen. Med.*, vol. 11, no. 9, pp. 2663–2666, Sep. 2017.

[164] N. Fahy, M. Alini, and M. J. Stoddart, "Mechanical stimulation of mesenchymal stem cells: Implications for cartilage tissue engineering," *J. Orthop. Res.*, vol. 36, no. 1, pp. 52–63, Jan. 2018.

[165] A. Charoenpanich, M. E. Wall, C. J. Tucker, D. M. K. Andrews, D. S. Lalush, and E. G. Loboa, "Microarray analysis of human adipose-derived stem cells in three-dimensional collagen culture: Osteogenesis inhibits bone morphogenic protein and wnt signaling pathways, and cyclic tensile strain causes upregulation of proinflammatory cytokine regulators ," *Tissue Eng. - Part A*, vol. 17, no. 21–22, pp. 2615–2627, 2011.

[166] M. N. Kang, H. H. Yoon, Y. K. Seo, and J. K. Park, "Effect of mechanical stimulation on the differentiation of cord stem cells," *Connect. Tissue Res.*, vol. 53, no. 2, pp. 149–159, Apr. 2012.

[167] M. C. Qi, J. Hu, S. J. Zou, H. Q. Chen, H. X. Zhou, and L. C. Han, "Mechanical strain induces osteogenic differentiation: Cbfa1 and Ets-1 expression in stretched rat mesenchymal stem cells," *Int. J. Oral Maxillofac. Surg.*, vol. 37, no. 5, pp. 453–458, May 2008.

[168] X. Chen *et al.*, "Mechanical stretch induces antioxidant responses and osteogenic differentiation in human mesenchymal stem cells through activation of the AMPK-SIRT1 signaling pathway," *Free Radic. Biol. Med.*, vol. 126, pp. 187–201, Oct. 2018.

[169] R. Li *et al.*, "Mechanical strain regulates osteogenic and adipogenic differentiation of bone marrow mesenchymal stem cells," *Biomed Res. Int.*, vol. 2015, 2015.

[170] Z. Zhu, X. Gan, H. Fan, and H. Yu, “Mechanical stretch endows mesenchymal stem cells stronger angiogenic and anti-apoptotic capacities via NFκB activation,” *Biochem. Biophys. Res. Commun.*, vol. 468, no. 4, pp. 601–605, Dec. 2015.

[171] G. Kasper *et al.*, “Mesenchymal Stem Cells Regulate Angiogenesis According to Their Mechanical Environment,” *Stem Cells*, vol. 25, no. 4, pp. 903–910, 2007.

[172] B. Bravo *et al.*, “Opposite Effects of Mechanical Action of Fluid Flow on Proangiogenic Factor Secretion From Human Adipose-Derived Stem Cells With and Without Oxidative Stress,” *J. Cell. Physiol.*, vol. 232, no. 8, pp. 2158–2167, 2017.

[173] V. Bassaneze *et al.*, “Shear stress induces nitric oxide-mediated vascular endothelial growth factor production in Human adipose tissue mesenchymal stem cells,” *Stem Cells Dev.*, vol. 19, no. 3, pp. 371–378, Mar. 2010.

[174] H. J. Lee, M. F. Diaz, A. Ewere, S. D. Olson, C. S. Cox, and P. L. Wenzel, “Focal adhesion kinase signaling regulates anti-inflammatory function of bone marrow mesenchymal stromal cells induced by biomechanical force,” *Cell. Signal.*, vol. 38, no. November 2016, pp. 1–9, 2017.

[175] M. F. Diaz *et al.*, “Biomechanical Forces Promote Immune Regulatory Function of Bone Marrow Mesenchymal Stromal Cells,” *Stem Cells*, vol. 35, no. 5, pp. 1259–1272, May 2017.

[176] W. T. Chen *et al.*, “Alteration of mesenchymal stem cells polarity by laminar shear stimulation promoting β-catenin nuclear localization,” *Biomaterials*, vol. 190–191, pp. 1–10, 2019.

[177] A. Ravichandran, Y. Liu, and S. H. Teoh, “Review: bioreactor design towards generation of relevant engineered tissues: focus on clinical translation,” *J. Tissue Eng. Regen. Med.*, vol. 12, no. 1, pp. e7–e22, Jan. 2018.

[178] M. N. F. Bin Hassan *et al.*, “Large-Scale Expansion of Human Mesenchymal Stem Cells,” *Stem Cells Int.*, vol. 2020, 2020.

[179] J. Cao *et al.*, “Three-dimensional culture of MSCs produces exosomes with improved yield and enhanced therapeutic efficacy for cisplatin-induced acute kidney injury,” *Stem Cell Res. Ther.*, vol. 11, no. 1, May 2020.

[180] J. Gobin *et al.*, “Hollow-fiber bioreactor production of extracellular vesicles from human bone marrow mesenchymal stromal cells yields nanovesicles that mirrors the immuno-modulatory antigenic signature of the producer cell,” *Stem Cell Res. Ther.*, vol. 12, no. 1, 2021.

[181] A. Allen *et al.*, “Mesenchymal Stromal Cell Bioreactor for Ex Vivo Reprogramming of Human Immune Cells,” *Sci. Rep.*, vol. 10, no. 1, pp. 1–13, Jun. 2020.

[182] J. F. Alvarez-Barreto, B. Landy, S. Vangordon, L. Place, P. L. Deangelis, and V. I. Sikavitsas, “Enhanced osteoblastic differentiation of mesenchymal stem cells seeded in RGD-functionalized PLLA scaffolds and cultured in a flow perfusion bioreactor,” *J. Tissue Eng. Regen. Med.*, vol. 5, no. 6, pp. 464–475, Jun. 2011.

[183] A. K. L. Chen, S. Reuveny, and S. K. W. Oh, “Application of human mesenchymal and pluripotent stem cell microcarrier cultures in cellular therapy: Achievements and future direction,” *Biotechnol. Adv.*, vol. 31, no. 7, pp. 1032–1046, Nov. 2013.

[184] S. H. Kwon, S. H. Bhang, H. K. Jang, T. Rhim, and B. S. Kim, “Conditioned medium of adipose-derived stromal cell culture in three-dimensional bioreactors for enhanced wound healing,” *J. Surg. Res.*, vol. 194, no. 1, pp. 8–17, 2015.

[185] J. E. Frith, B. Thomson, and P. G. Genever, “Dynamic three-dimensional culture methods enhance mesenchymal stem cell properties and increase therapeutic potential,” *Tissue Eng. - Part C Methods*, vol. 16, no. 4, pp. 735–749, 2010.

[186] M. de Almeida Fuzeta *et al.*, “Scalable Production of Human Mesenchymal Stromal Cell-Derived Extracellular Vesicles Under Serum-/Xeno-Free Conditions in a Microcarrier-Based Bioreactor Culture System,” *Front. Cell Dev. Biol.*, vol. 8, p. 1197, Nov. 2020.

[187] J. Lembong *et al.*, “Bioreactor parameters for microcarrier-based human msc expansion under xeno-free conditions in a vertical-wheel system,” *Bioengineering*, vol. 7, no. 3, pp. 1–16, Sep. 2020.

[188] T. T. Y. Han and L. E. Flynn, “Perfusion bioreactor culture of human adipose-derived stromal cells on decellularized adipose tissue scaffolds enhances in vivo adipose tissue regeneration,” *J. Tissue Eng. Regen. Med.*, vol. 14, no. 12, pp. 1827–1840, 2020.

[189] T. T. Y. Han, J. T. Walker, A. Grant, G. A. Dekaban, and L. E. Flynn, “Preconditioning Human Adipose-Derived Stromal Cells on Decellularized Adipose Tissue Scaffolds Within a Perfusion Bioreactor Modulates Cell Phenotype and Promotes a Pro-regenerative Host Response,” *Front. Bioeng. Biotechnol.*, vol. 9, p. 131, Mar. 2021.

[190] X. Zhou, D. Liu, L. You, and L. Wang, “Quantifying fluid shear stress in a rocking culture dish,” *J. Biomech.*, vol. 43, no. 8, pp. 1598–1602, 2010.

[191] L. Flynn, J. L. Semple, and K. A. Woodhouse, “Decellularized placental matrices for adipose tissue engineering,” *J. Biomed. Mater. Res. - Part A*, vol. 79, no. 2, pp. 359–369, Nov. 2006.

[192] L. E. Flynn, “The use of decellularized adipose tissue to provide an inductive microenvironment for the adipogenic differentiation of human adipose-derived stem cells,” *Biomaterials*, vol. 31, no. 17, pp. 4715–4724, Jun. 2010.

[193] F. Mckinnirey, B. Herbert, G. Vesey, and S. McCracken, “Immune modulation via adipose derived Mesenchymal Stem cells is driven by donor sex in vitro,” *Sci. Rep.*, vol. 11, no. 1, pp. 1–14, Jun. 2021.

[194] U. Juhas, M. Ryba-Stanisławowska, P. Szargiej, and J. Myśliwska, “Different pathways of macrophage activation and polarization,” *Postepy Hig. Med. Dosw.*, vol. 69, pp. 496–502, 2015.

[195] Q. Xue, Y. Yan, R. Zhang, and H. Xiong, “Regulation of iNOS on immune cells

and its role in diseases," *International Journal of Molecular Sciences*, vol. 19, no. 12. MDPI AG, 01-Dec-2018.

[196] G. Ren *et al.*, "Mesenchymal Stem Cell-Mediated Immunosuppression Occurs via Concerted Action of Chemokines and Nitric Oxide," *Cell Stem Cell*, vol. 2, no. 2, pp. 141–150, Feb. 2008.

[197] W. Li *et al.*, "Mesenchymal stem cells: A double-edged sword in regulating immune responses," *Cell Death Differ.*, vol. 19, no. 9, pp. 1505–1513, Sep. 2012.

[198] F. J. Vizoso, N. Eiro, S. Cid, J. Schneider, and R. Perez-Fernandez, "Mesenchymal stem cell secretome: Toward cell-free therapeutic strategies in regenerative medicine," *Int. J. Mol. Sci.*, vol. 18, no. 9, Sep. 2017.

[199] W. K. Z. Wan Safwani, S. Makpol, S. Sathapan, and K. H. Chua, "The changes of stemness biomarkers expression in human adipose-derived stem cells during long-term manipulation," *Biotechnol. Appl. Biochem.*, vol. 58, no. 4, pp. 261–270, Jul. 2011.

[200] A. Shridhar, B. G. Amsden, E. R. Gillies, and L. E. Flynn, "Investigating the Effects of Tissue-Specific Extracellular Matrix on the Adipogenic and Osteogenic Differentiation of Human Adipose-Derived Stromal Cells Within Composite Hydrogel Scaffolds," *Front. Bioeng. Biotechnol.*, vol. 7, p. 402, Dec. 2019.

[201] Y. Yang, E. H. Lee, and Z. Yang, "Hypoxia conditioned mesenchymal stem cells in tissue regeneration application," *Tissue Eng. Part B Rev.*, Sep. 2021.

[202] A. Saparov, V. Ogay, T. Nurgozhin, M. Jumabay, and W. C. W. Chen, "Preconditioning of human mesenchymal stem cells to enhance their regulation of the immune response," *Stem Cells Int.*, vol. 2016, 2016.

[203] B. M. Davis, E. R. Loghin, K. R. Conway, and X. Zhang, "Automated Closed-System Expansion of Pluripotent Stem Cell Aggregates in a Rocking-Motion Bioreactor," *SLAS Technol.*, vol. 23, no. 4, pp. 364–373, Aug. 2018.

[204] A. C. Tsai, Y. Liu, X. Yuan, R. Chella, and T. Ma, "Aggregation kinetics of human mesenchymal stem cells under wave motion," *Biotechnol. J.*, vol. 12, no. 5, May 2017.

[205] K. Wierzchowski and M. Pilarek, "Microcarrier-Supported Culture of Chondrocytes in Continuously Rocked Disposable Bioreactor.," *Methods Mol. Biol.*, 2021.

[206] O. F. Garcia-Aponte, C. Herwig, and B. Kozma, "Lymphocyte expansion in bioreactors: upgrading adoptive cell therapy," *J. Biol. Eng.*, vol. 15, no. 1, Dec. 2021.

[207] A. Mizukami and K. Swiech, "Platforms for Clinical-Grade CAR-T Cell Expansion," *Methods Mol. Biol.*, vol. 2086, pp. 139–150, 2020.

[208] S. H. Kim, K. Ahn, and J. Y. Park, "Responses of human adipose-derived stem cells to interstitial level of extremely low shear flows regarding differentiation, morphology, and proliferation," *Lab Chip*, vol. 17, no. 12, pp. 2115–2124, 2017.

[209] J. Bachmann *et al.*, “Ischemia-Like Stress Conditions Stimulate Trophic Activities of Adipose-Derived Stromal/Stem Cells,” *Cells*, vol. 9, no. 9, p. 1935, 2020.

[210] C. Fotia, A. Massa, F. Boriani, N. Baldini, and D. Granchi, “Prolonged exposure to hypoxic milieu improves the osteogenic potential of adipose derived stem cells,” *J. Cell. Biochem.*, vol. 116, no. 7, pp. 1442–1453, Jul. 2015.

[211] J. R. Choi *et al.*, “In situ normoxia enhances survival and proliferation rate of human adipose tissue-derived stromal cells without increasing the risk of tumourigenesis,” *PLoS One*, vol. 10, no. 1, p. e0115034, Jan. 2015.

[212] C. Chen, Q. Tang, Y. Zhang, M. Yu, W. Jing, and W. Tian, “Physioxia: A more effective approach for culturing human adipose-derived stem cells for cell transplantation,” *Stem Cell Res. Ther.*, vol. 9, no. 1, pp. 1–12, May 2018.

[213] T. P. Frazier, J. M. Gimble, I. Kheterpal, and B. G. Rowan, “Impact of low oxygen on the secretome of human adipose-derived stromal/stem cell primary cultures,” *Biochimie*, vol. 95, no. 12, pp. 2286–2296, Dec. 2013.

[214] C. M. Jiang *et al.*, “Effects of hypoxia on the immunomodulatory properties of human gingiva-derived mesenchymal stem cells,” *J. Dent. Res.*, vol. 94, no. 1, pp. 69–77, 2015.

[215] D. W. Wang, B. Fermor, J. M. Gimble, H. A. Awad, and F. Guilak, “Influence of oxygen on the proliferation and metabolism of adipose derived adult stem cells,” *J. Cell. Physiol.*, vol. 204, no. 1, pp. 184–191, 2005.

[216] B. Antebi *et al.*, “Short-term physiological hypoxia potentiates the therapeutic function of mesenchymal stem cells,” *Stem Cell Res. Ther.*, vol. 9, no. 1, 2018.

[217] C. Holzwarth *et al.*, “Low physiologic oxygen tensions reduce proliferation and differentiation of human multipotent mesenchymal stromal cells,” *BMC Cell Biol.*, vol. 11, no. 1, pp. 1–11, Jan. 2010.

[218] M. I. Elashry, S. T. Gegnaw, M. C. Klymiuk, S. Wenisch, and S. Arnhold, “Influence of mechanical fluid shear stress on the osteogenic differentiation protocols for Equine adipose tissue-derived mesenchymal stem cells,” *Acta Histochem.*, vol. 121, no. 3, pp. 344–353, Apr. 2019.

[219] G. Ren *et al.*, “Species variation in the mechanisms of mesenchymal stem cell-mediated immunosuppression,” *Stem Cells*, vol. 27, no. 8, pp. 1954–1962, Aug. 2009.

[220] L. Meesuk, C. Tantrawatpan, P. Kheolamai, and S. Manochantr, “The immunosuppressive capacity of human mesenchymal stromal cells derived from amnion and bone marrow,” *Biochem. Biophys. Reports*, vol. 8, pp. 34–40, Dec. 2016.

[221] S. Thaweesapphithak, C. Tantrawatpan, P. Kheolamai, D. Tantikanlayaporn, S. Roytrakul, and S. Manochantr, “Human serum enhances the proliferative capacity and immunomodulatory property of MSCs derived from human placenta and umbilical cord,” *Stem Cell Res. Ther.*, vol. 10, no. 1, Mar. 2019.

[222] Z. Xia *et al.*, “The Application of Decellularized Adipose Tissue Promotes Wound

Healing," *Tissue Eng. Regen. Med.*, vol. 17, no. 6, pp. 863–874, Dec. 2020.

[223] D. S. Kim *et al.*, "Enhanced Immunosuppressive Properties of Human Mesenchymal Stem Cells Primed by Interferon-γ," *EBioMedicine*, vol. 28, pp. 261–273, Feb. 2018.

[224] J. Yang, X. Chen, T. Yuan, X. Yang, Y. Fan, and X. Zhang, "Regulation of the secretion of immunoregulatory factors of mesenchymal stem cells (MSCs) by collagen-based scaffolds during chondrogenesis," *Mater. Sci. Eng. C*, vol. 70, pp. 983–991, Jan. 2017.

[225] S. J. Cifuentes, P. Priyadarshani, D. A. Castilla-Casadiego, L. J. Mortensen, J. Almodóvar, and M. Domenech, "Heparin/collagen surface coatings modulate the growth, secretome, and morphology of human mesenchymal stromal cell response to interferon-gamma," *J. Biomed. Mater. Res. - Part A*, vol. 109, no. 6, pp. 951–965, Jun. 2021.

[226] A. Hackel, A. Aksamit, K. Bruderek, S. Lang, and S. Brandau, "TNF-α and IL-1β sensitize human MSC for IFN-γ signaling and enhance neutrophil recruitment," *Eur. J. Immunol.*, vol. 51, no. 2, pp. 319–330, Feb. 2021.

[227] Y. Liu *et al.*, "Effects of inflammatory factors on mesenchymal stem cells and their role in the promotion of tumor angiogenesis in colon cancer," *J. Biol. Chem.*, vol. 286, no. 28, pp. 25007–25015, Jul. 2011.

[228] C. Li, G. Li, M. Liu, T. Zhou, and H. Zhou, "Paracrine effect of inflammatory cytokine-activated bone marrow mesenchymal stem cells and its role in osteoblast function," *J. Biosci. Bioeng.*, vol. 121, no. 2, pp. 213–219, Feb. 2016.

[229] D. Philipp, L. Suhr, T. Wahlers, Y. H. Choi, and A. Paunel-Görgülü, "Preconditioning of bone marrow-derived mesenchymal stem cells highly strengthens their potential to promote IL-6-dependent M2b polarization," *Stem Cell Res. Ther.*, vol. 9, no. 1, pp. 1–17, Oct. 2018.

[230] M. R. Fernando, J. L. Reyes, J. Iannuzzi, G. Leung, and D. M. McKay, "The pro-inflammatory cytokine, interleukin-6, enhances the polarization of alternatively activated macrophages," *PLoS One*, vol. 9, no. 4, Apr. 2014.

[231] S. Ghannam, C. Bouffi, F. Djouad, C. Jorgensen, and D. Noël, "Immunosuppression by mesenchymal stem cells: Mechanisms and clinical applications," *Stem Cell Res. Ther.*, vol. 1, no. 1, p. 2, 2010.

[232] Y. W. Kwon *et al.*, "Tumor necrosis factor-α-activated mesenchymal stem cells promote endothelial progenitor cell homing and angiogenesis," *Biochim. Biophys. Acta - Mol. Basis Dis.*, vol. 1832, no. 12, pp. 2136–2144, Dec. 2013.

[233] S. E. Sherman, M. Kuljanin, T. T. Cooper, D. M. Putman, G. A. Lajoie, and D. A. Hess, "High Aldehyde Dehydrogenase Activity Identifies a Subset of Human Mesenchymal Stromal Cells with Vascular Regenerative Potential," *Stem Cells*, vol. 35, no. 6, pp. 1542–1553, Jun. 2017.

[234] S. Tokhanbigli, K. Baghaei, A. Asadirad, S. M. Hashemi, H. Asadzadeh-Aghdaei, and M. R. Zali, "Immunoregulatory impact of human mesenchymal-conditioned

media and mesenchymal derived exosomes on monocytes," *Mol. Biol. Res. Commun.*, vol. 8, no. 2, pp. 79–89, 2019.

[235] C. I. Marinescu, M. B. Preda, and A. Burlacu, "A procedure for in vitro evaluation of the immunosuppressive effect of mouse mesenchymal stem cells on activated T cell proliferation," *Stem Cell Res. Ther.*, vol. 12, no. 1, pp. 1–13, Dec. 2021.

[236] S. M. Krishna, S. M. Omer, J. Li, S. K. Morton, R. J. Jose, and J. Golledge, "Development of a two-stage limb ischemia model to better simulate human peripheral artery disease," *Sci. Rep.*, vol. 10, no. 1, pp. 1–16, Feb. 2020.

[237] F. Figliolini *et al.*, "Extracellular Vesicles From Adipose Stem Cells Prevent Muscle Damage and Inflammation in a Mouse Model of Hind Limb Ischemia: Role of Neuregulin-1," *Arterioscler. Thromb. Vasc. Biol.*, vol. 40, no. 1, pp. 239–254, Jan. 2020.

[238] H. K. Cheung, T. T. Y. Han, D. M. Marecak, J. F. Watkins, B. G. Amsden, and L. E. Flynn, "Composite hydrogel scaffolds incorporating decellularized adipose tissue for soft tissue engineering with adipose-derived stem cells," *Biomaterials*, vol. 35, no. 6, pp. 1914–1923, Feb. 2014.

Appendix A: Supplementary data

A.1 Supplementary data of Chapter 2

Appendix A Table 1. Summary of donor information and the experimental groups or studies they were included in

Donor ID	Sex	Age	BMI	Aim 1 & Aim 2			Aim 3	
				11° 50 rpm	11° 25 rpm	5° 50 rpm	IHC	CM assays
1 (200922)	F	52	22.8	√	√			√
2 (210121)	F	63	33.0	√*	√	√	√	√
3 (210201)	F	43	22.5	√	√	√	√	√
4 (210226)	F	60	26.5	√	√			√
5 (June12)	F	49	36.5	√				

* Only apply to IL-6 ELISA assay in Aim 2

Appendix A Table 2. Other paracrine factors investigated using Human Magnetic Luminex® Assay

Analytes	Experimental condition	Sample type	Number of donors	Result
Angiopoietin-1, IL-1β, IL-4, IL-10, TNF-α, EGF, FGF2	11° 50 rpm	Conditioned media	6	Not detectable (background adjusted)
			2*	
		Cell lysates	1	
	11° 50 rpm primed	Conditioned media	2	
Leptin, PDGF-AA, PIGF	11° 50 rpm	Conditioned media	2	
		Cell lysates	1	

* Samples concentrated 10 times using Amicon Ultra-0.5 Centrifugal Filter Unit (Millipore Sigma)

A.2 Supplementary data of Chapter 3

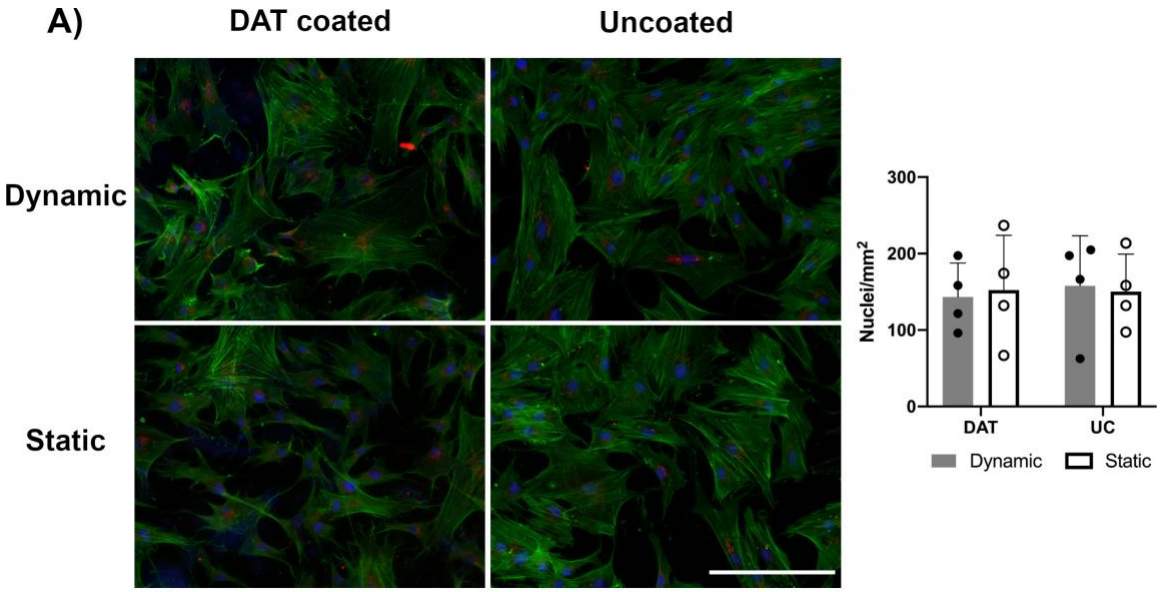

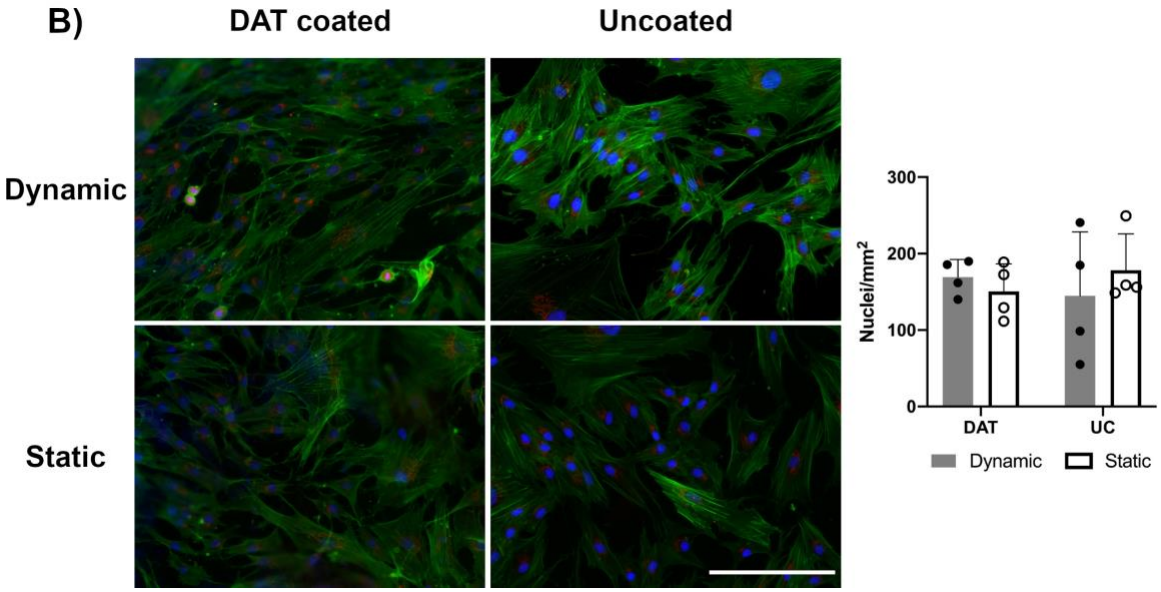

Supplementary Figure 3.1 Culturing on the DAT coatings or under shear stress in the 11° 50 rpm condition did not alter the ASC density at 3 days. Representative images of iNOS expression (red) with staining for F-actin (green) and nuclei (blue), along with quantification of nuclei, after 7 days of culture under A) 2% O_2 or B) 20% O_2. Qualitatively, no difference in iNOS expression was observed between any of the groups. Data was analyzed using 2-way ANOVA with a Tukey's multiple comparisons test. Error bars represent standard deviation (n=2 replicate wells/trial, N=4 trials with different ASC donors). Scale bars represent 200 μm. No primary antibody control: Supplementary Figure 3.6. Abbreviations: DAT, DAT coated; UC, uncoated.

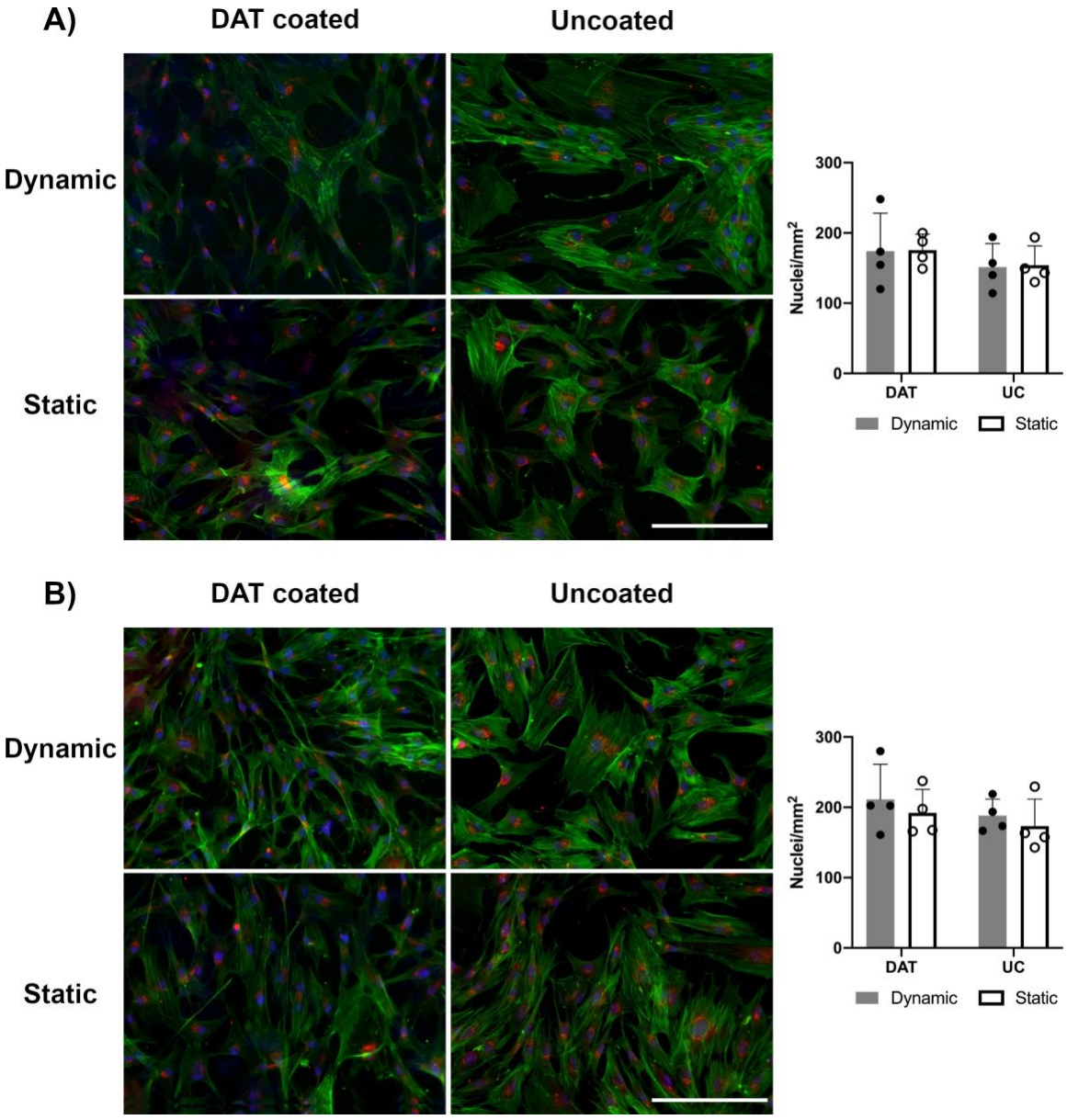
A)
DAT coated
Uncoated
Dynamic
Static
Nuclei/mm²
300
200
100
0
DAT
UC
Dynamic
Static
B)
DAT coated
Uncoated
Dynamic
Static
Nuclei/mm²
300
200
100
0
DAT
UC
Dynamic
Static

Supplementary Figure 3.2 Culturing on the DAT coatings or under shear stress in the 11° 25 rpm condition did not alter the ASC density at 3 days. Representative images of iNOS expression (red) with staining for F-actin (green) and nuclei (blue), along with quantification of nuclei, after 7 days of culture under A) 2% O_2 or B) 20% O_2. Qualitatively, no difference in iNOS expression was observed between any of the groups. Data was analyzed using 2-way ANOVA with a Tukey's multiple comparisons test. Error bars represent standard deviation (n=2 replicate wells/trial, N=4 trials with different ASC donors). Scale bars represent 200 μm. No primary antibody control: Supplementary Figure 3.6. Abbreviations: DAT, DAT coated; UC, uncoated.

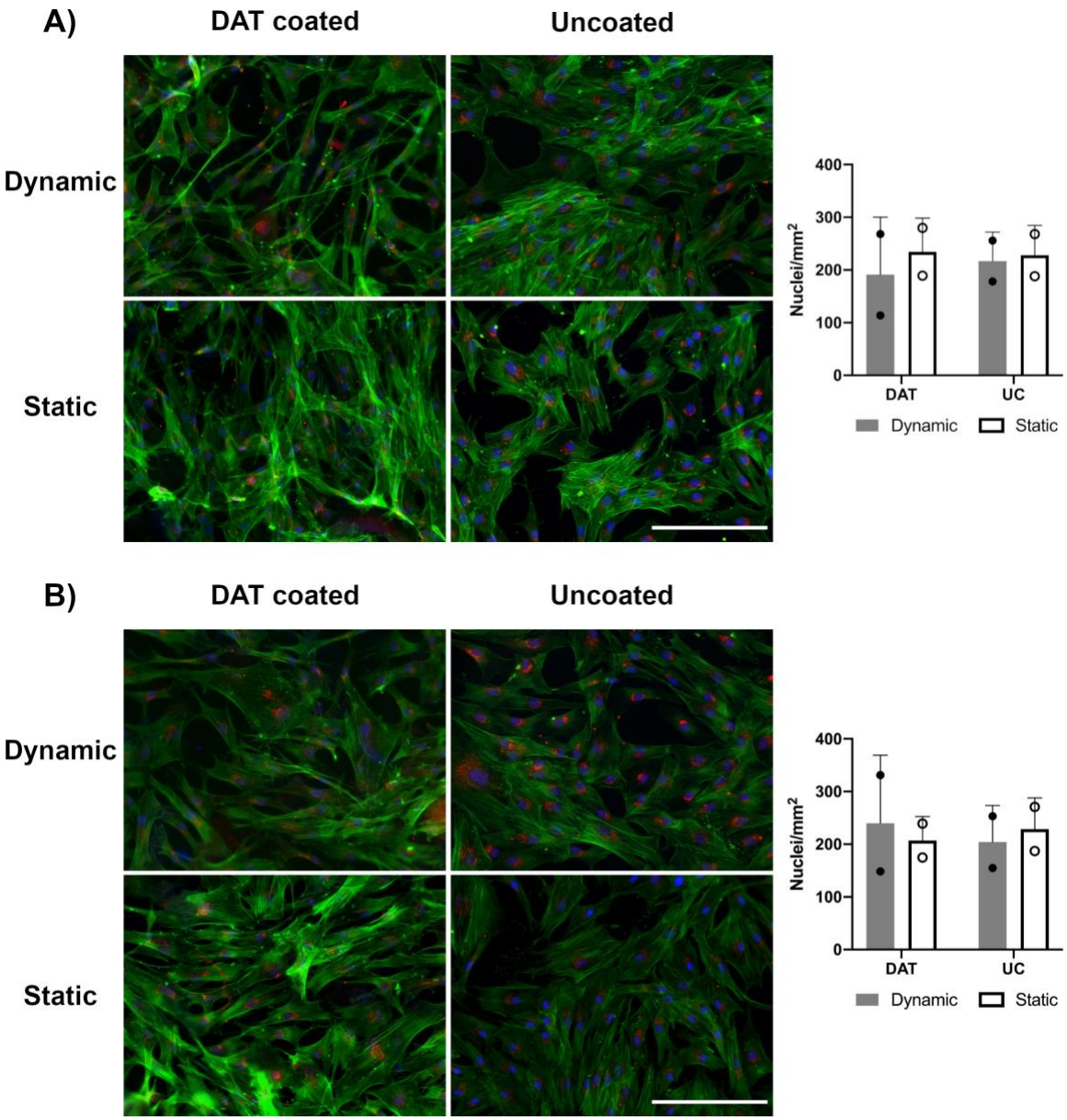

Supplementary Figure 3.3 Culturing on the DAT coatings or under shear stress in the 5° 50 rpm condition did not alter the ASC density at 3 days. Representative images of iNOS expression (red) with staining for F-actin (green) and nuclei (blue), along with quantification of nuclei, after 7 days of culture under A) 2% O_2 or B) 20% O_2. Qualitatively, no difference in iNOS expression was observed between any of the groups. Error bars represent standard deviation (n=2 replicate wells/trial, N=2 trials with different ASC donors). Scale bars represent 200 μm. No primary antibody control: Supplementary Figure 3.6. Abbreviations: DAT, DAT coated; UC, uncoated.

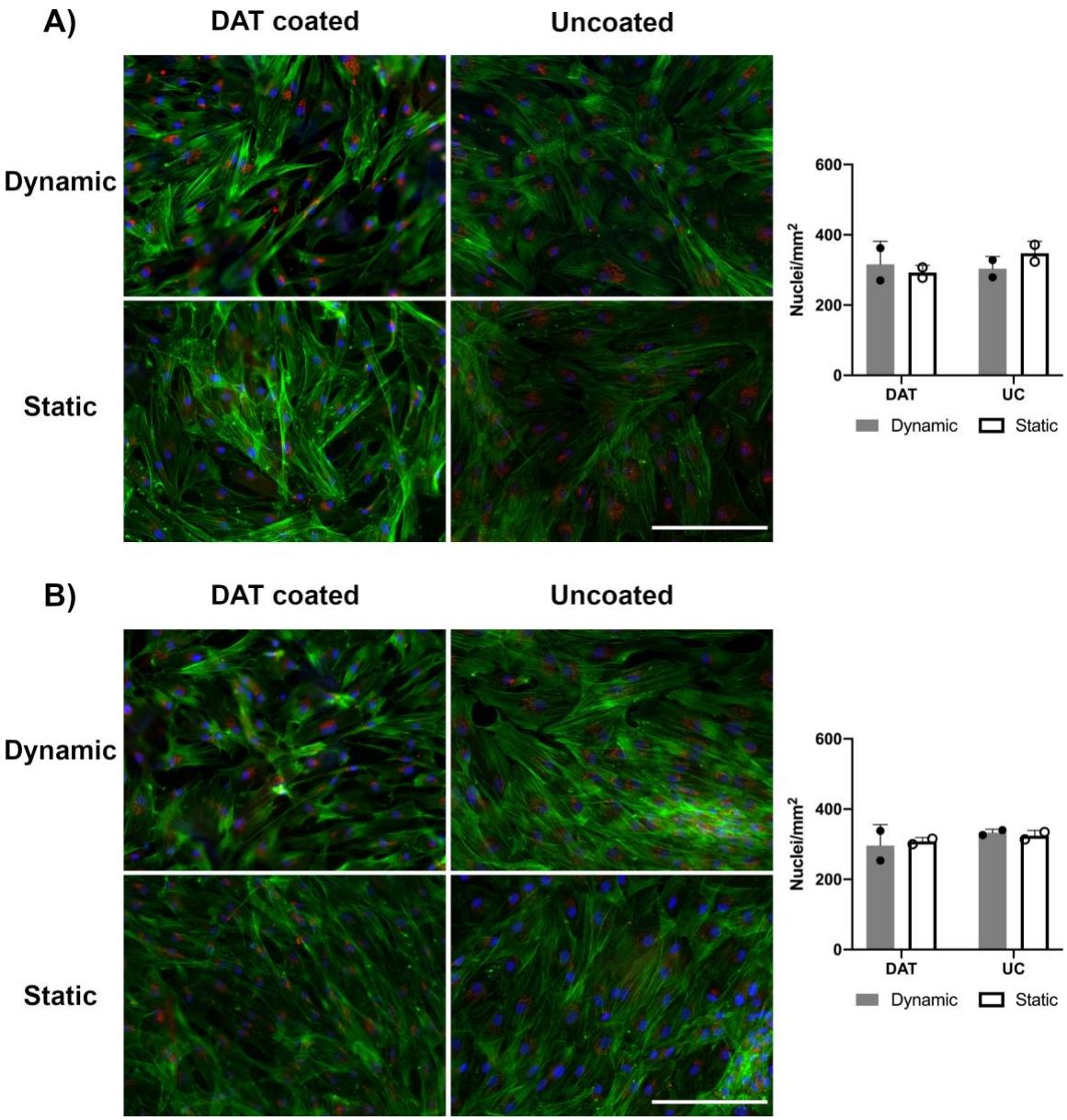

Supplementary Figure 3.4 Culturing on the DAT coatings or under shear stress in the 5° 50 rpm condition did not alter the ASC density at 7 days. Representative images of iNOS expression (red) with staining for F-actin (green) and nuclei (blue), along with quantification of nuclei, after 7 days of culture under A) 2% O_2 or B) 20% O_2. Qualitatively, no difference in iNOS expression was observed between any of the groups. Error bars represent standard deviation (n=2 replicate wells/trial, N=2 trials with different ASC donors). Scale bars represent 200 μm. No primary antibody control: Supplementary Figure 3.6. Abbreviations: DAT, DAT coated; UC, uncoated.

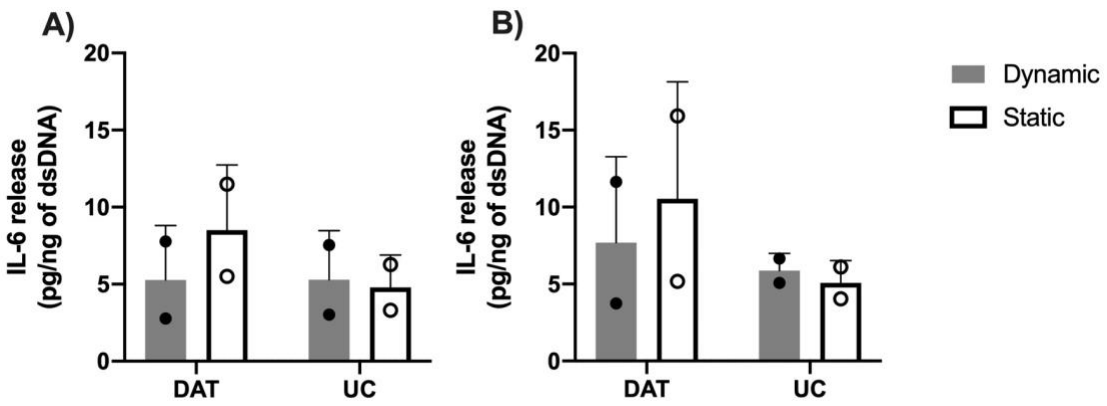

Supplementary Figure 3.5 Expression of IL-6 in human ASCs after 7 days of preconditioning from the 5° 50 rpm experimental group as measured by ELISA normalized to total dsDNA content. Expression of IL-6 measured by ELISA normalized to total dsDNA content. A) Samples cultured under 2% O_2; B) Samples cultured under 20% O_2. Statistical analysis not performed due to limited sample size. Error bars represent standard deviation (n=2 replicate wells/trial, N=2 trials with different ASC donors).

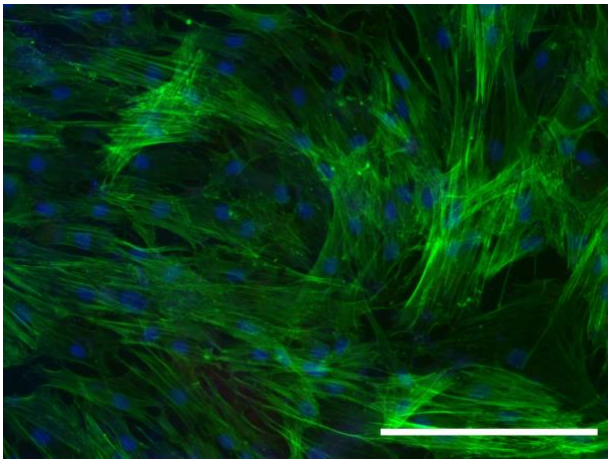

Supplementary Figure 3.6 No primary antibody control of iNOS immunohistochemical staining. Representative image with iNOS expression (red), F-actin (green), and nuclei (blue), Scale bars represent 200 μm.

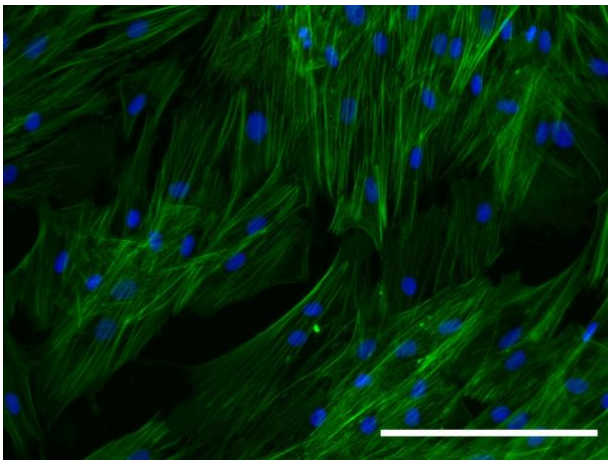

Supplementary Figure 3.7 No primary antibody control of IDO immunohistochemical staining. Representative image with IDO expression (red), F-actin (green), and nuclei (blue), Scale bars represent 200 μm.

Appendix B: Human Tissue/Cells Ethics Approval

Western Research

Date: 12 August 2021

To: Dr. Lauren Flynn

Project ID: 105426

Study Title: Tissue Engineering with Adipose-derived Stem Cells

Application Type: Continuing Ethics Review (CER) Form

Review Type: Delegated

REB Meeting Date: 24/Aug/2021

Date Approval Issued: 12/Aug/2021

REB Approval Expiry Date: 13/Aug/2022

Dear Dr. Lauren Flynn,

The Western University Research Ethics Board has reviewed the application. This study, including all currently approved documents, has been re-approved until the expiry date noted above.

REB members involved in the research project do not participate in the review, discussion or decision.

Western University REB operates in compliance with, and is constituted in accordance with, the requirements of the Tri-Council Policy Statement: Ethical Conduct for Research Involving Humans (TCPS 2); the International Conference on Harmonisation Good Clinical Practice Consolidated Guideline (ICH GCP); Part C, Division 5 of the Food and Drug Regulations; Part 4 of the Natural Health Products Regulations; Part 3 of the Medical Devices Regulations and the provisions of the Ontario Personal Health Information Protection Act (PHIPA 2004) and its applicable regulations. The REB is registered with the U.S. Department of Health & Human Services under the IRB registration number IRB 00000940.

Please do not hesitate to contact us if you have any questions.

Sincerely,

The Office of Human Research Ethics

Note: This correspondence includes an electronic signature (validation and approval via an online system that is compliant with all regulations).

Curriculum Vitae

Education

M.E.Sc. Biomedical Engineering (Collaborative specialization in Musculoskeletal Health Research) (September 2019-present)
Western University, London, ON, Canada

B.A.Sc. Engineering Science (Major in Biomedical Systems Engineering) (September 2015-April 2019)
University of Toronto, Toronto, ON, Canada

Experience

Thesis Student (September 2018-April 2019)
Translational Biology and Engineering Program, University of Toronto
Supervisor: Dr. Craig A. Simmons (simmons@mie.utoronto.ca)
Research topic: Validation and application of an *ex vivo* mouse heart bioreactor to study aortic valve mechanobiology

Summer Research Trainee (May 2, 2016–August 31, 2016)
Rehabilitation Engineering Lab, Toronto Rehab Institute-Lyndhurst Centre, UHN
Supervisor: Dr. Kei Masani (k.masani@utoronto.ca)

Coursework

MSK 9100B: Musculoskeletal Health Research B – Fundamental Concepts in Clinical and Health Services Research (Jan 2020 – Apr 2020)
Grade: 87

BME 9550B: Principles of Communication and Knowledge Translation for Biomedical Engineers (Jan 2020 – Apr 2020)
Grade: 89

MSK 9000A: Musculoskeletal Health Research A – Biomedical and Bioengineering Concepts (September 2019-December 2019)
Grade: 89

Awards

(M.E.Sc.) CMHR Transdisciplinary Bone & Joint Training Award ($9750/yr, Sept. 2019-Aug. 2021)
(B.A.Sc.) University of Toronto President's Entrance Scholarship ($2000, 2015)

Teaching Assistantship

(M.E.Sc) **CBE 4423B/BME 9526B:** Tissue Engineering (January 2021 – April 2021)
(M.E.Sc) **CBE 2290A:** Fundamentals of Biochemical and Environmental Engineering (September 2018 – December 2019)